

The scalar bi-spectrum in the Starobinsky model: The equilateral case

Jérôme Martin

Institut d'Astrophysique de Paris, UMR7095-CNRS, Université Pierre et Marie Curie, 98bis boulevard Arago, 75014 Paris, France.

E-mail: jmartin@iap.fr

L. Sriramkumar[‡]

Harish-Chandra Research Institute, Chhatnag Road, Jhansi, Allahabad 211019, India.

Abstract. While a featureless, nearly scale invariant, primordial scalar power spectrum fits the most recent Cosmic Microwave Background (CMB) data rather well, certain features in the spectrum are known to lead to a better fit to the data (although, the statistical significance of such results remains an open issue). In the inflationary scenario, one or more periods of deviations from slow roll are necessary in order to generate features in the scalar perturbation spectrum. Over the last couple of years, it has been recognized that such deviations from slow roll inflation can also result in reasonably large non-Gaussianities. The Starobinsky model involves the canonical scalar field and consists of a linear inflaton potential with a sudden change in the slope. The change in the slope causes a brief period of departure from slow roll which, in turn, results in a sharp rise in power, along with a burst of oscillations in the scalar spectrum for modes that leave the Hubble radius just before and during the period of fast roll. The hallmark of the Starobinsky model is that it allows the scalar power spectrum to be evaluated analytically in terms of the three parameters that describe the model, viz. the two slopes that describe the potential on either side of the discontinuity and the Hubble scale at the time when the field crosses the discontinuity. In this work, we evaluate the bi-spectrum of the scalar perturbations in the Starobinsky model in the equilateral limit. Remarkably, we find that, just as the power spectrum, all the different contributions to the bi-spectrum too can be evaluated completely analytically and expressed in terms of the three parameters that describe the model. We show that the quantity f_{NL} , which characterizes the extent of non-Gaussianity, can be expressed purely in terms of the ratio of the two slopes on either side of the discontinuity in the potential. Further, we find that, for certain values of the parameters, f_{NL} in the Starobinsky model can be as large as the mean value that has been arrived at from the analysis of the recent CMB data. We also demonstrate that the usual hierarchy of contributions to the bi-spectrum can be altered for certain values of the parameters. Altogether, we find that the Starobinsky model represents a unique scenario wherein, even when the slow roll conditions are violated, the background, the perturbations as well as the corresponding two and three point correlation functions can be evaluated

[‡] Current address: Department of Physics, Indian Institute of Technology Madras, Chennai 600036, India. E-mail: sriram@physics.iitm.ac.in

completely analytically. As a consequence, the Starobinsky model can also be used to calibrate numerical codes aimed at computing the non-Gaussianities.

PACS numbers: 98.80.Cq, 98.70.Vc, 98.80.Es

1. Introduction

A nearly scale invariant primordial scalar power spectrum, along with the assumption of the concordant, background cosmological model (i.e. the spatially flat, Λ CDM model), seems to be in remarkable agreement with the data from the Wilkinson Microwave Anisotropy Probe (WMAP) of the anisotropies in the Cosmic Microwave Background (CMB) (for the most recent observations, see Refs. [1]; for earlier results, see Refs. [2]; for constraints on different inflationary scenarios, see Refs. [3, 4, 5, 6]). But, specific features in the primordial spectrum seem to improve the fit to the data to a reasonable extent (for an inherently incomplete list, see Refs. [7, 8, 9, 10, 11, 12, 13]), although the statistical relevance of such results remains difficult to assess. Notably, while a sharp drop in power on scales corresponding to the Hubble scale today has been found to fit the low CMB quadrupole better [7, 8, 9, 10], a burst of oscillations of a suitable amplitude and over a certain range of scales seem to provide a considerably improved fit to the outliers in the CMB angular power spectrum near the multipoles of $l = 22$ and 40 [11]. Moreover, interestingly, oscillating inflaton potentials that generate small modulations over a wide range of scales in the perturbation spectrum have also been found to perform better against the data than the more conventional power law spectrum [13].

As is well known, a featureless, scale invariant perturbation spectrum can be produced by a suitably long epoch of slow roll inflation (see any of the following texts [14] or reviews [15]). However, generating features in the scalar power spectrum require one or more periods of deviation from slow roll inflation [16, 17, 18]. For instance, it is found that one needs a large deviation from slow roll in order to produce a sharp drop in power, say, so as to fit the low quadrupole [16]. The larger the deviation from slow roll, the sharper the drop is found to be and, in fact, a brief departure from inflation—which leads to a sharp rise in power *and* a couple of oscillations before the spectrum turns nearly scale invariant—has been found to provide a good fit to the data at the lower multipoles [10]. In contrast, a small and short burst of deviation from slow roll seems sufficient to generate the oscillations that result in a much better fit to the outliers near the multipoles of $l = 22$ and 40 [11]. While certain features indeed lead to a better fit to the data than the standard power law primordial spectrum, the improvement in the fit is often arrived at with the introduction of extra parameters. As we pointed out above, the statistical significance of features achieved at the cost of additional parameters, say, from the Bayesian point of view [19], remains to be investigated satisfactorily.

During the last few years, a variety of approaches have been developed to determine the extent of non-Gaussianities in the WMAP data (for an inexhaustive list, see Refs. [20]; in this context, also see the recent reviews [21]). Many of these analyses seem to indicate that the CMB may possibly possess reasonably large amount of non-Gaussianities. For instance, the WMAP seven year data constrains the parameter f_{NL} that is often introduced to characterize the extent of the non-Gaussianity to be $f_{\text{NL}} = 32 \pm 21$ in the local limit, at 68% confidence level (see Ref. [1]; also see the reviews [21]). While a Gaussian primordial spectrum (which corresponds to a

vanishing f_{NL}) lies within $2\text{-}\sigma$, evidently, the mean value seems to indicate a rather large amount of non-Gaussianity.

The ongoing Planck mission [22] is expected to reduce the above-mentioned uncertainty in the WMAP's determination of f_{NL} by a factor of about four or so. On the theoretical side, it has been realized that, if Planck indeed detects a reasonable amount of non-Gaussianity, then it can act as a powerful tool to substantially constrain the plethora of inflationary models that seem to be allowed by the currently available data [21]. For example, it has been established that the canonical scalar field models which lead to a nearly scale invariant primordial spectrum contain only a negligible amount of non-Gaussianity, with the magnitude of f_{NL} turning out to be much smaller than unity [23, 24]. Hence, these models will cease to be viable if non-Gaussianity turns out to be substantial. However, it is known that primordial spectra with features, generated due to one or more deviations from slow roll inflation, can lead to reasonably large non-Gaussianities [25]. (It should be mentioned that, initial states other than the Bunch-Davies vacuum can also lead to features and, possibly, relatively substantial non-Gaussianities [26]. But, we shall not consider such situations in this paper.) Therefore, if non-Gaussianity indeed proves to be large, then, either one has to reconcile with the fact that the primordial spectrum contains features or one has to pay more attention to non-canonical scalar field models such as, say, the D-brane inflation models [27, 28].

Often, the efforts in evaluating the non-Gaussianities when features arise in the primordial spectrum due to a departure from slow roll have involved numerical computations [25], and it is instructive to consider a model wherein it may be possible to evaluate them analytically. In this work, we shall consider the Starobinsky model [16], which involves the canonical scalar field and consists of a linear inflaton potential with an abrupt change in the slope at a given point. The change in the slope causes a brief period of fast roll, which leads to a sharp rise in power and oscillations in the scalar spectrum for modes that leave the Hubble radius just before and during the period of fast roll. The important aspect of the Starobinsky model is that the scalar power spectrum can be evaluated analytically and, under certain conditions on the parameters, the analytic spectrum matches the exact spectrum, computed numerically, extremely well. We shall focus on the equilateral limit and illustrate that, remarkably, under the same conditions, all the contributions to the scalar bi-spectrum too can be calculated completely analytically and expressed entirely in terms of the three parameters that describe the Starobinsky model. We shall also discuss the ranges of the parameters over which the non-Gaussianity in the model can be large.

At this point, we ought to mention that non-Gaussianities in the Starobinsky model have, in fact, been computed earlier [29]. But, since the formalism followed in the earlier work is rather different from the approach that we shall adopt, carrying out an exact comparison between the two efforts turns out to be difficult. While the non-Gaussianity parameter in the equilateral limit obtained in both the approaches lead to a sharp peak near the characteristic scale associated with the problem, we find the approach we have adopted here is able to capture the finer details as well. We believed that this

can be attributed to the δN formalism adopted in the earlier work, which is essentially applicable on super Hubble scales. Despite the additional efforts that were made to take into account the contributions due to the decaying mode—which become important when deviations from slow roll occur (in this context, see, for example, Refs. [30])—we find that the approach still proves to be insufficient to arrive at the exact form for the final result.

This paper is organized as follows. In the following section, we shall outline the essential aspects of the Starobinsky model. We shall first describe the background evolution in the model, and then go on to discuss the scalar power spectrum that arises in the model. In particular, we shall highlight the assumptions and approximations that are made in arriving at analytic expressions for the background evolution and the scalar power spectrum. In Sec. 3, we shall rapidly sketch the by-now standard procedure for evaluating the inflationary bi-spectrum of the scalar perturbations and the non-Gaussianity parameter f_{NL} . In Sec. 4, using the method outlined in Sec. 3, we shall evaluate the dominant contribution to the scalar bi-spectrum in the Starobinsky model in the equilateral limit. In Sec. 5, we shall evaluate all the other sub-dominant contributions as well. In Sec. 6, we shall discuss the range of values of the parameters over which the non-Gaussianity parameter f_{NL} can be as large as indicated by the currently observed mean values. We shall also touch upon an issue related to the hierarchy of the different contributions to the bi-spectrum. Finally, we shall close in Sec. 7 with a brief summary and outlook. We shall relegate some details concerning the evaluation of certain integrals to an appendix.

A few words on the conventions and notations that we shall adopt are in order at this stage of our discussion. We shall work in units such that $\hbar = c = 1$, and we shall set the Planck mass to be $M_{\text{Pl}} = (8\pi G)^{1/2}$. Also, while Greek indices shall refer to the spacetime coordinates, the Latin indices (barring the sub-script k which shall represent the wavenumber of the perturbations) shall denote the three spatial coordinates. Moreover, we shall work with the metric signature of $(-, +, +, +)$. We shall express the various quantities in terms of either the cosmic time t , the conformal time η (also, at times, denoted as τ), or the number of e-folds N , as is convenient. As usual, while an overdot shall denote differentiation with respect to the cosmic time, an overprime shall denote differentiation with respect to the conformal time coordinate. Lastly, a plus or a minus sign in the sub-script or the super-script of any quantity shall denote its value before and after the field crosses the discontinuity in the potential, respectively.

2. The Starobinsky model

In this section, we shall sketch the Starobinsky model [16] in some detail. We shall first describe the assumptions and the approximations that go into evaluating the background. We shall then go on to discuss the scalar modes and the resulting power spectrum that arise in the model.

2.1. The background evolution in the Starobinsky model

Consider a spatially flat Friedmann universe that is described by the scale factor a , which is driven by the canonical scalar field ϕ . If the scalar field is described by the potential $V(\phi)$, then the evolution of such a system is governed by the following Friedman and Klein-Gordon equations:

$$H^2 = \frac{1}{3 M_{\text{Pl}}^2} \left[\frac{\dot{\phi}^2}{2} + V(\phi) \right] \quad \text{and} \quad \ddot{\phi} + 3 H \dot{\phi} + V_\phi = 0, \quad (1)$$

where $H = \dot{a}/a$ is the Hubble parameter, and $V_\phi \equiv dV/d\phi$. As we had mentioned, the Starobinsky model consists of a linear potential with a sharp change in its slope at a given point. Let the value of the scalar field where the slope changes abruptly be ϕ_0 , and let the slope of the potential above and below ϕ_0 be A_+ and A_- , respectively. Also, let the value of the potential at $\phi = \phi_0$ be, say, V_0 . In other words, the potential $V(\phi)$ describing the canonical scalar field is given by

$$V(\phi) = \begin{cases} V_0 + A_+ (\phi - \phi_0) & \text{for } \phi > \phi_0, \\ V_0 + A_- (\phi - \phi_0) & \text{for } \phi < \phi_0. \end{cases} \quad (2)$$

This potential is displayed in the top left panel of Fig. 1. It is useful to note here that the quantities A_+ and A_- are of dimension three.

Now, consider the case wherein the field is rolling down the above potential from a value such that $\phi > \phi_0$. The exact trajectory of the field, computed numerically, is illustrated in Fig. 1 (top right panel, solid black line). In the slow roll approximation, the number of e-folds, $N \equiv \ln(a/a_i)$, is given by

$$N \simeq -\frac{1}{M_{\text{Pl}}^2} \int_{\phi_i}^{\phi} d\phi \frac{V}{V_\phi}, \quad (3)$$

where ϕ_i and a_i are the initial values (i.e. at $N = 0$) of the field and the scale factor, respectively. If the field begins to roll down slowly, the trajectory of the field until it reaches the discontinuity at ϕ_0 can be easily obtained by carrying out the above integral for N . One obtains that

$$\phi_+ = -\left(\frac{V_0}{A_+} - \phi_0\right) + \left[\left(\phi_i - \phi_0 + \frac{V_0}{A_+}\right)^2 - 2 M_{\text{Pl}}^2 N\right]^{1/2}, \quad (4)$$

and, as can be seen in Fig. 1 (top right panel, dotted blue line), this expression turns out to be an excellent approximation to the actual numerical solution (as one would expect, since the corresponding slow roll parameters are very small; see discussion below). This expression allows us to estimate the e-fold, say, N_0 , at which the field reaches the point where the slope of the potential changes, and it is given by

$$N_0 = \left(\frac{\phi_i - \phi_0}{2 M_{\text{Pl}}^2}\right) \left(\phi_i - \phi_0 + \frac{2 V_0}{A_+}\right). \quad (5)$$

The ‘velocity’ of the field before it reaches the discontinuity can be evaluated to be

$$\frac{d\phi_+}{dN} = -M_{\text{Pl}}^2 \left[\left(\phi_i - \phi_0 + \frac{V_0}{A_+}\right)^2 - 2 M_{\text{Pl}}^2 N\right]^{-1/2}. \quad (6)$$

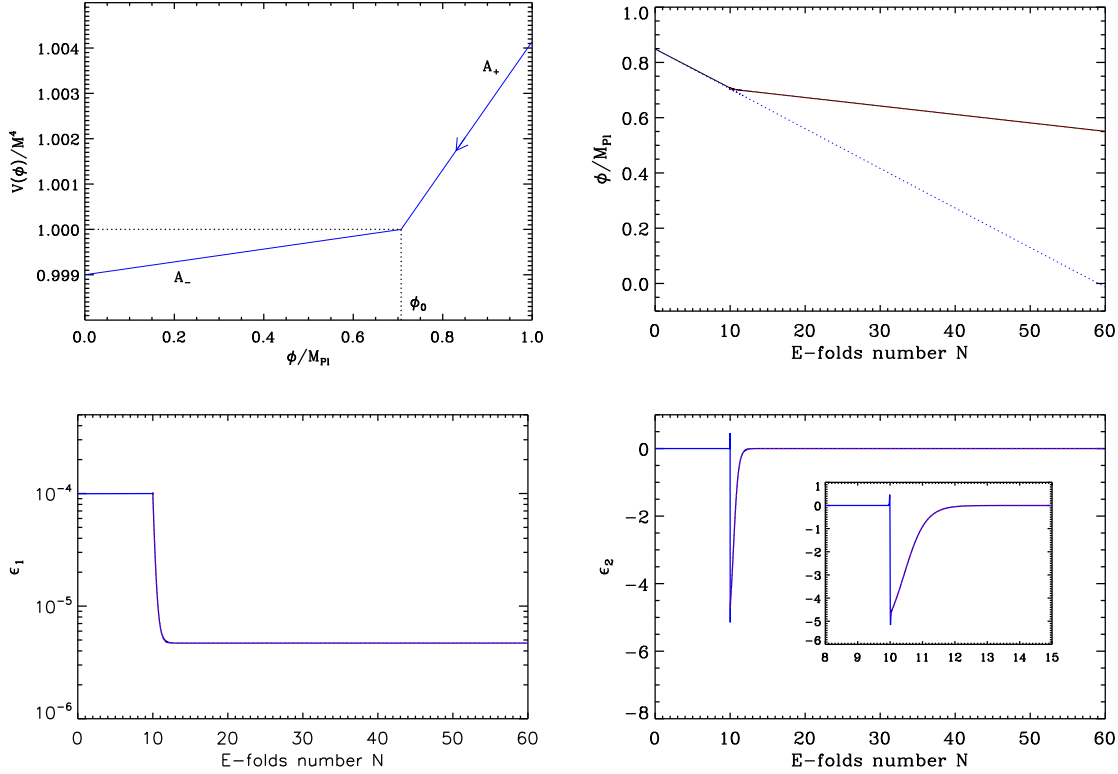


Figure 1. The potential, the evolution of the scalar field and the first two slow roll parameters in the Starobinsky model. **Top left panel:** The potential (2) with $\phi_0/M_{\text{Pl}} \simeq 0.707$, $V_0/M_{\text{Pl}}^4 = M^4/M_{\text{Pl}}^4 \simeq 2.37 \times 10^{-12}$, $A_+/M_{\text{Pl}}^3 \simeq 3.35 \times 10^{-14}$ and $A_-/M_{\text{Pl}}^3 \simeq 7.26 \times 10^{-15}$, which corresponds to $\Delta A/A_- = (A_- - A_+)/A_- \simeq -3.61$. The mass M has been chosen such that the model is COBE normalized. **Top right panel:** The exact, numerically computed, evolution of the field ϕ (for the above-mentioned values of the parameters) has been plotted as a function of the number of e-folds (the solid black line). The initial value of the field has been chosen to be $\phi_i/M_{\text{Pl}} \simeq 0.849$, and it corresponds to $N_0 = 10$, where N_0 is the e-fold at which the field crosses the discontinuity [cf. Eq. (5)]. The dotted blue line corresponds to the slow roll expression (4) for the evolution of the field. Clearly, the slow roll result is an excellent approximation to the actual result before the discontinuity. The dotted red line corresponds to Eq. (9), and it too accurately matches the exact solution after the discontinuity. **Bottom left panel:** The numerical result for the evolution of the first slow roll parameter ϵ_1 (the solid blue curve). The parameters that we work with lead to $\epsilon_{1+} \simeq 10^{-4}$ [cf. Eq. (13)], as is confirmed by the plot. The dotted red curve represents the approximate expression of ϵ_1 after the discontinuity, viz. Eq. (14). **Bottom right panel:** The solid blue curve represents the exact evolution of the second slow roll parameter ϵ_2 , obtained numerically. The dotted red curve represents the expression (17), which is valid after the field has crossed the discontinuity in the potential. The inset highlights the excellent agreement between the numerical and the analytical results.

Actually, the Starobinsky model assumes that the constant V_0 is the dominant term in the potential for a range of ϕ near ϕ_0 . This regime is very similar to the so-called vacuum dominated regime in hybrid inflation. In such a case, we can set $V \simeq V_0$ in the slow roll trajectory, and the expressions for ϕ_+ and $d\phi_+/dN$ above simplify to

$$\phi_+ \simeq \phi_i - \frac{A_+ M_{\text{Pl}}^2}{V_0} N \quad \text{and} \quad \frac{d\phi_+}{dN} \simeq -\frac{A_+ M_{\text{Pl}}^2}{V_0}. \quad (7)$$

The fact that, before the discontinuity, the slow roll trajectory can be well approximated by a straight line with a negative slope is also evident from Fig. 1 (top right panel). Further, in this limit, the above relation for N_0 reduces to $N_0 = [V_0 (\phi_i - \phi_0)/A_+ M_{\text{Pl}}^2]$.

When the field crosses ϕ_0 , the slow roll approximation ceases to be valid, and we must return to the exact Klein-Gordon equation to understand the evolution of the field. Upon treating the number of e-folds as the independent variable, the Klein-Gordon equation in (1) can be rewritten as

$$H^2 \frac{d^2\phi}{dN^2} + (3 - \epsilon_1) H^2 \frac{d\phi}{dN} + V_\phi = 0, \quad (8)$$

where $\epsilon_1 \equiv -\dot{H}/H^2$ is the first slow roll parameter. Since the constant term V_0 in the potential is dominant, as a first step, it is a good approximation to assume that the Hubble parameter H is constant. In other words, one always has $\epsilon_1 \ll 1$, even when the field passes over the discontinuity in the slope of the potential. This, in turn, implies that inflation does not end even though the slow roll approximation breaks down temporarily with the higher order slow roll parameters becoming large (see discussion below). In fact, this situation can be viewed as the very definition of inflation with a transition. The above Klein-Gordon equation can be easily solved under these conditions and, upon requiring the field and its derivative to be continuous at the transition, we obtain the following solution for the field when $\phi < \phi_0$:

$$\phi_- \simeq \phi_0 + \frac{\Delta A}{9 H_0^2} \left[1 - e^{-3(N-N_0)} \right] - \frac{A_-}{3 H_0^2} (N - N_0), \quad (9)$$

where

$$\Delta A \equiv A_- - A_+ \quad (10)$$

and we have set $H_0^2 \simeq V_0/(3 M_{\text{Pl}}^2)$. We have plotted this solution for the evolution of the field in Fig. 1 (top right panel, dotted red line). As can be noticed in the plot, the agreement with the exact, numerical, solution is very good.

Let us now evaluate the slow roll parameters on either side of the transition due to the discontinuity in the slope of the potential. We have already introduced the first slow roll parameter ϵ_1 . As is well-known, the second and the higher slow roll parameters are defined as [31, 32]

$$\epsilon_{n+1} = \frac{d \ln |\epsilon_n|}{dN} \quad \text{for} \quad n \geq 1. \quad (11)$$

When the slow roll approximation is valid, the first two slow roll parameters can be expressed in terms of the potential $V(\phi)$ and its derivatives as follows:

$$\epsilon_1 \simeq \frac{M_{\text{Pl}}^2}{2} \left(\frac{V_\phi}{V} \right)^2 \quad \text{and} \quad \epsilon_2 \simeq 2 M_{\text{Pl}}^2 \left[\left(\frac{V_\phi}{V} \right)^2 - \frac{V_{\phi\phi}}{V} \right], \quad (12)$$

where $V_{\phi\phi} = d^2V/d\phi^2$. Clearly, these relations can be used until the field reaches ϕ_0 and one obtains that

$$\epsilon_{1+} \simeq \frac{M_{\text{Pl}}^2}{2} \left[\frac{A_+}{V_0 + A_+(\phi - \phi_0)} \right]^2 \simeq \frac{A_+^2}{18 M_{\text{Pl}}^2 H_0^4}, \quad (13)$$

where the last expression has been arrived at upon assuming that V_0 is dominant. The fact that the first slow roll parameter is almost a constant before the transition can be easily seen in Fig. 1 (bottom left panel). Further, since the potential is linear in ϕ , we have $\epsilon_{2+} \simeq 4\epsilon_{1+}$, i.e. the second slow roll parameter is also a constant until the time the field reaches the discontinuity at ϕ_0 . Again, this behavior is confirmed by the corresponding numerical result plotted in Fig. 1 (bottom right panel).

Once the field has crossed the break in the potential, one has to use the exact expressions to arrive at the behavior of the slow roll parameters. Upon using the solution (9), we find that the first slow roll parameter can be obtained to be

$$\epsilon_{1-} = \frac{1}{2 M_{\text{Pl}}^2} \left(\frac{d\phi_-}{dN} \right)^2 = \frac{A_-^2}{18 M_{\text{Pl}}^2 H_0^4} \left[1 - \frac{\Delta A}{A_-} e^{-3(N-N_0)} \right]^2. \quad (14)$$

This expression proves to be an excellent approximation to the exact result, as can be checked in Fig. 1 (it is represented by the dotted red curve in the bottom left panel). Let us now turn to the evolution of the second slow roll parameter after the transition. It can be written as

$$\epsilon_2 = -6 + 2\epsilon_1 - \frac{2V_\phi}{H^2} \left(\frac{d\phi}{dN} \right)^{-1}, \quad (15)$$

which, we should emphasize, is an exact expression. In fact, we can arrive at the form of the second slow roll parameter after the transition, upon using the expression (14) for ϵ_{1-} in Eq. (11). We find that, ϵ_{2-} is given by

$$\epsilon_{2-} \simeq \frac{6\Delta A}{A_-} \frac{e^{-3(N-N_0)}}{1 - (\Delta A/A_-) e^{-3(N-N_0)}}. \quad (16)$$

However, at sufficiently late times after the transition, when the slow roll evolution has been restored, we expect that $\epsilon_{2-} \simeq 4\epsilon_{1-}$, as it was in the case before the transition to fast roll (since the potential continues to be linear). Careful analysis points to the fact that, in order to achieve this relation at late times, one needs to actually take into account the property that, strictly, the Hubble parameter is not a constant. In fact, this amounts to using the usual approximation that consists of replacing the potential V by M^4 while its derivative V_ϕ is still calculated exactly. Upon taking this fact into account, one actually obtains that

$$\epsilon_{2-} \simeq \frac{6\Delta A}{A_-} \frac{e^{-3(N-N_0)}}{1 - (\Delta A/A_-) e^{-3(N-N_0)}} + 4\epsilon_{1-}, \quad (17)$$

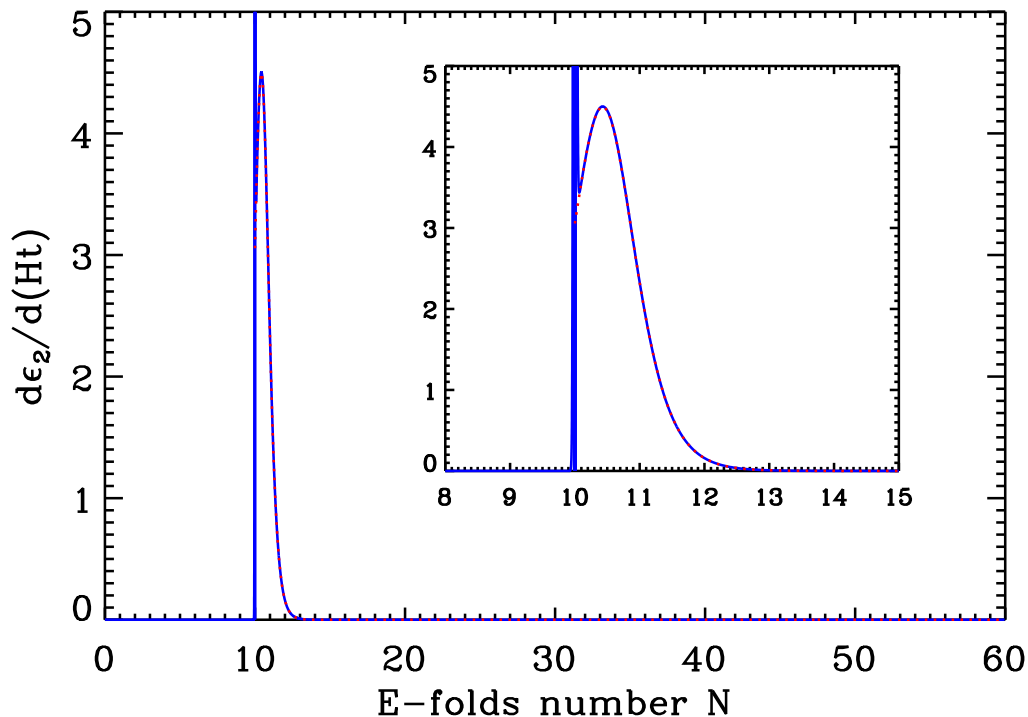


Figure 2. The solid blue curve denotes the evolution of the quantity $d\epsilon_2/d(Ht)$, computed numerically, and plotted as a function of the number of e-folds. Note that we have worked with the same set of parameters as in Fig. 1. The dotted red curve represents the analytical expression (19). As is clear from the inset, the analytical expression approximates the actual numerical result very well after the transition. The vertical blue line is just a numerical artifact of the parametrization used here and we have carefully checked that it plays no role in the following considerations.

with ϵ_{1-} in the second term being given by Eq. (14). Clearly, as the first term vanishes at late times (i.e. at large N), the above expression satisfies the required relation between the first two slow roll parameters when slow roll has been restored much after the transition. Yet again, we find that this relation almost exactly matches the exact numerical result for ϵ_2 , as is evident from Fig. 1 (see the bottom right panel). In particular, the above expressions point to the fact that the value of the second slow roll parameter soon after the transition is controlled by only one quantity, viz. $\Delta A/A_-$, and is given by $6(\Delta A/A_-)/(1 - \Delta A/A_-)$. Therefore, if $|\Delta A/A_-|$ is large, then ϵ_2 quickly approaches -6 immediately after the transition, as can also be checked in Fig. 1 (the figure actually corresponds to $|\Delta A/A_-| \simeq 3.61$).

As we shall discuss in the next section, in order to evaluate the dominant contribution to the scalar bi-spectrum in the Starobinsky model, we shall also require the quantity $\dot{\epsilon}_2$. One can show that, it can be written as

$$\frac{d\epsilon_2}{dt} = -\frac{2V_{\phi\phi}}{H} + 12H\epsilon_1 - 3H\epsilon_2 - 4H\epsilon_1^2 + 5H\epsilon_1\epsilon_2 - \frac{H}{2}\epsilon_2^2, \quad (18)$$

and, under the conditions of our interest, this relation reduces to

$$\begin{aligned} \frac{d\epsilon_{2-}}{dt} &\simeq -3H_0\epsilon_{2-} - \frac{H_0}{2}\epsilon_{2-}^2 \\ &\simeq -\frac{18H_0\Delta A}{A_-} \frac{e^{-3(N-N_0)}}{[1 - (\Delta A/A_-)e^{-3(N-N_0)}]^2}. \end{aligned} \quad (19)$$

We should mention here that, in arriving at the final equality, we have ignored the second term involving ϵ_{1-} in Eq. (17). The fact that this is a valid approximation is confirmed by the numerical analysis. As in the case of ϵ_{2-} , we find that, during the period soon after the transition, the value of $\dot{\epsilon}_{2-}$ is determined only by ratio $\Delta A/A_-$. In Fig. 2, we have plotted the above expression for $\dot{\epsilon}_2$ as well as the exact numerical result. It is clear from the figure that the expression (19) is an excellent approximation to the actual result.

Let us now briefly pause to summarize the results we have obtained. It is evident from the above expressions for the slow roll parameters that the change in the slope in the potential leads to a departure from slow roll for a short span of time, before slow roll is again recovered when the friction on the scalar field due to the expansion of the universe begins to dominate the force due to the potential. While the first slow roll parameter ϵ_1 remains small throughout the evolution (which essentially occurs due to V_0 being the dominant term in the potential around ϕ_0), the second slow roll parameter ϵ_2 and its time derivative $\dot{\epsilon}_2$ exhibit a sharp rise as the field crosses ϕ_0 , before falling off. We have been able to obtain simple analytical expressions for the various background quantities even in the regime where the conditions for slow roll are violated. This point turns out to be the key for our analysis. As we shall see, the simple expressions for the slow roll parameters permit us to evaluate the bi-spectrum in the equilateral limit completely analytically. However, before we turn to the evaluation of the scalar bi-spectrum, let us discuss the power spectrum that arises in the Starobinsky model.

2.2. The scalar power spectrum in the Starobinsky model

Let $\mathcal{R}(\eta, \mathbf{x})$ be the dimensionless curvature perturbation induced by the scalar field, and let $\mathcal{R}_{\mathbf{k}}(\eta)$ denote the associated Fourier modes defined through the relation

$$\mathcal{R}(\eta, \mathbf{x}) = \int \frac{d^3\mathbf{k}}{(2\pi)^{3/2}} \mathcal{R}_{\mathbf{k}} e^{i\mathbf{k}\cdot\mathbf{x}}. \quad (20)$$

On quantization, the operator corresponding to the curvature perturbation can be expressed as

$$\hat{\mathcal{R}}(\eta, \mathbf{x}) = \int \frac{d^3\mathbf{k}}{(2\pi)^{3/2}} \left[\hat{a}_{\mathbf{k}} f_k(\eta) e^{i\mathbf{k}\cdot\mathbf{x}} + \hat{a}_{\mathbf{k}}^\dagger f_k^*(\eta) e^{-i\mathbf{k}\cdot\mathbf{x}} \right], \quad (21)$$

where $\hat{a}_{\mathbf{k}}$ and $\hat{a}_{\mathbf{k}}^\dagger$ are the usual creation and annihilation operators which satisfy the following non-trivial commutation relation: $[\hat{a}_{\mathbf{k}}, \hat{a}_{\mathbf{p}}^\dagger] = \delta^{(3)}(\mathbf{k} - \mathbf{p})$. In the case of the canonical scalar field, the modes f_k are governed by the differential equation [14, 15]

$$f_k'' + 2\frac{z'}{z}f_k' + k^2 f_k = 0, \quad (22)$$

where $z \equiv a \dot{\phi}/H = a M_{\text{Pl}} \sqrt{2\epsilon_1}$. The quantity $\mathcal{R}_{\mathbf{k}}$ is of dimension -3 , f_k of dimension $-3/2$, while z is of dimension one. It is useful to note that, in terms of the Mukhanov-Sasaki variable $v_k = z f_k$ (which is of dimension $-1/2$), the above equation for f_k reduces to

$$v_k'' + \left(k^2 - \frac{z''}{z}\right) v_k = 0. \quad (23)$$

The dimensionless scalar power spectrum $\mathcal{P}_s(k)$ is defined in terms of the correlation function of the Fourier modes of the curvature perturbation as follows:

$$\langle 0 | \hat{\mathcal{R}}_{\mathbf{k}}(\eta) \hat{\mathcal{R}}_{\mathbf{p}}(\eta) | 0 \rangle = \frac{(2\pi)^2}{2k^3} \mathcal{P}_s(k) \delta^{(3)}(\mathbf{k} + \mathbf{p}), \quad (24)$$

where the vacuum state $|0\rangle$ is defined as $\hat{a}_{\mathbf{k}}|0\rangle = 0$, $\forall \mathbf{k}$. Since we can write, $\hat{\mathcal{R}}_{\mathbf{k}} = (\hat{a}_{\mathbf{k}} f_k + \hat{a}_{-\mathbf{k}}^\dagger f_k^*)$, one obtains that

$$\mathcal{P}_s(k) = \frac{k^3}{2\pi^2} |f_k|^2 = \frac{k^3}{2\pi^2} \left(\frac{|v_k|}{z}\right)^2 \quad (25)$$

with the right hand side (which depends on time) evaluated in the super Hubble limit [i.e. when $k/(aH) \rightarrow 0$] or, more generically, at the end of inflation. The curvature perturbation is usually assumed to be in the Bunch-Davies vacuum, which corresponds to choosing $v_k \rightarrow e^{ik\eta}/\sqrt{2k}$ in the sub Hubble limit, i.e. as $k/(aH) \rightarrow \infty$. It is clear from Eq. (23) that it is the ‘effective potential’ z''/z which determines the evolution of the scalar perturbations. It can be written in terms of the slow roll parameters as follows:

$$\frac{z''}{z} = \mathcal{H}^2 \left(2 - \epsilon_1 + \frac{3}{2}\epsilon_2 + \frac{1}{4}\epsilon_2^2 - \frac{1}{2}\epsilon_1\epsilon_2 + \frac{1}{2}\epsilon_2\epsilon_3\right), \quad (26)$$

where $\mathcal{H} \equiv a'/a = aH$ is the conformal Hubble parameter, and it should be emphasized that the above expression is an exact one.

Our aim now is to derive the scalar power spectrum for modes that leave the Hubble radius in the vicinity of the transition at ϕ_0 . Before the transition to a brief period of fast roll near ϕ_0 , all the slow roll parameters remain small, and the effective potential simplifies to $z''/z \simeq 2\mathcal{H}^2$. We should emphasize here that, for simplicity, we are neglecting terms involving the first order slow roll parameters that would lead to a non-vanishing spectral index for modes far from the characteristic scale, viz. the mode which leaves the Hubble radius when the scalar field crosses the break in the inflaton potential. Recall that, since the evolution is dominated by the constant term V_0 in the potential, the expansion is of the de Sitter form corresponding to the Hubble parameter H_0 . Therefore, around the transition, the scale factor can be expressed in terms of the conformal time as $a(\eta) = -(H_0\eta)^{-1}$, so that we have $z''/z \simeq 2/\eta^2$. In such a case, the solution to the Mukhanov-Sasaki variable v_k that satisfies the standard Bunch-Davies initial condition is given by

$$v_k^+(\eta) = \frac{1}{\sqrt{2k}} \left(1 - \frac{i}{k\eta}\right) e^{-ik\eta}. \quad (27)$$

During the transitory fast roll regime, as the field crosses ϕ_0 , the slow roll parameters are no longer small and, hence the solutions to the Mukhanov-Sasaki variable v_k can be expected to look different. In particular, we have seen that the second slow roll parameter ϵ_2 and its time derivative $\dot{\epsilon}_2$ can be large immediately after the transition. From Eq. (26), it is then clear that, a priori, one can no longer expect the effective potential to be just given by $z''/z \simeq 2\mathcal{H}^2$. However, remember that ϵ_1 remains small even during the transition. Further, one has $\dot{\epsilon}_2 = H \epsilon_2 \epsilon_3$. Upon using these facts and the result that $\dot{\epsilon}_2$ can be approximated using Eq. (18) (and, of course, the property that $V_{\phi\phi} = 0$), one finds that, after the transition

$$\begin{aligned} \frac{z''}{z} &\simeq \mathcal{H}^2 \left(2 + \frac{3}{2} \epsilon_{2-} + \frac{1}{4} \epsilon_{2-}^2 + \frac{1}{2} \epsilon_{2-} \epsilon_{3-} \right) \\ &\simeq \mathcal{H}^2 \left[2 + \frac{3}{2} \epsilon_{2-} + \frac{1}{4} \epsilon_{2-}^2 + \frac{1}{2} \left(-3 \epsilon_{2-} - \frac{1}{2} \epsilon_{2-}^2 \right) \right] \simeq 2 \mathcal{H}^2. \end{aligned} \quad (28)$$

This implies that certain cancellations occur so that the effective potential still retains the same form, i.e. $z''/z \simeq 2\mathcal{H}^2$, even after the field has crossed ϕ_0 . But, due to the fast roll, post-transition, the modes v_k do not remain in the Bunch-Davies vacuum and, as a result, the solution to v_k takes the general form

$$v_k^-(\eta) = \frac{\alpha_k}{\sqrt{2k}} \left(1 - \frac{i}{k\eta} \right) e^{-ik\eta} + \frac{\beta_k}{\sqrt{2k}} \left(1 + \frac{i}{k\eta} \right) e^{ik\eta}, \quad (29)$$

where α_k and β_k are the standard Bogoliubov coefficients.

The Bogoliubov coefficients α_k and β_k can now be determined by carefully matching the mode v_k and its derivative at the transition at ϕ_0 . In order to do so, we first need to understand the behavior of z and the effective potential z''/z across the transition. In terms of the conformal time coordinate, the transition occurs at $\eta_0 = -(a_0 H_0)^{-1}$, where a_0 is the scale factor at η_0 . Recalling that $z = a M_{\text{Pl}} \sqrt{2\epsilon_1}$, and upon using the expression of ϵ_1 before and after the transition, we arrive at

$$z(\eta) \simeq \begin{cases} -\frac{A_+}{3 H_0^3 \eta} & \text{for } \eta < \eta_0, \\ -\frac{A_-}{3 H_0^3 \eta} - \frac{a_0^3 \Delta A \eta^2}{3} & \text{for } \eta > \eta_0. \end{cases} \quad (30)$$

As a consequence, one obtains that

$$z'(\eta) \simeq \begin{cases} \frac{A_+}{3 H_0^3 \eta^2} & \text{for } \eta < \eta_0, \\ \frac{A_-}{3 H_0^3 \eta^2} - \frac{2 a_0^3 \Delta A \eta}{3} & \text{for } \eta > \eta_0, \end{cases} \quad (31)$$

and it is clear that z' jumps at the transition by the amount

$$[z'(\eta_0)]_{\pm} \equiv z'_-(\eta_0) - z'_+(\eta_0) = -\frac{a_0^2 \Delta A}{H_0}. \quad (32)$$

So, at the transition, that is to say when $\eta \simeq \eta_0$ (and only at the transition!), we can write

$$z' \simeq \frac{a_0^2 A_+}{3 H_0} - \frac{a_0^2 \Delta A}{H_0} \Theta(\eta - \eta_0), \quad (33)$$

where $\Theta(x)$ is the step function. This implies that the effective potential z''/z can be described as a Dirac delta function at the transition, and we have

$$\frac{z''}{z} \simeq \frac{3 a_0 H_0 \Delta A}{A_+} \delta^{(1)}(\eta - \eta_0). \quad (34)$$

The above expression for z''/z allows us to establish the matching conditions on the modes at the transition, which read as

$$[v_k(\eta_0)]_{\pm} = v_k^{-}(\eta_0) - v_k^{+}(\eta_0) = 0 \quad (35)$$

and

$$[v'_k(\eta_0)]_{\pm} = v_k^{-'}(\eta_0) - v_k^{+'}(\eta_0) = \frac{3 a_0 H_0 \Delta A}{A_+} v_k(\eta_0). \quad (36)$$

The modes (27) and (29), along with these two conditions, then lead to the following expressions for the Bogoliubov coefficients α_k and β_k :

$$\alpha_k = 1 + \frac{3 i \Delta A}{2 A_+} \frac{k_0}{k} \left(1 + \frac{k_0^2}{k^2}\right), \quad (37)$$

$$\beta_k = -\frac{3 i \Delta A}{2 A_+} \frac{k_0}{k} \left(1 + \frac{i k_0}{k}\right)^2 e^{2 i k/k_0}, \quad (38)$$

where $k_0 = -1/\eta_0 = a_0 H_0$ corresponds to the mode that leaves the Hubble radius at the transition. The ratio $k/k_0 = k/(a_0 H_0)$ can also be viewed as the ratio of the physical wavenumber at the transition, viz. k/a_0 , to the characteristic physical wave number $k_0^{\text{phys}} \equiv H_0$. Therefore, upon using the modes (29) post-transition, the resulting power spectrum, evaluated as $k \eta \rightarrow 0$, is found to be [16]

$$\begin{aligned} \mathcal{P}_s(k) &= \left(\frac{H_0}{2\pi}\right)^2 \left(\frac{3 H_0^2}{A_-}\right)^2 |\alpha_k - \beta_k|^2 \\ &= \left(\frac{H_0}{2\pi}\right)^2 \left(\frac{3 H_0^2}{A_-}\right)^2 \left\{ 1 - \frac{3 \Delta A}{A_+} \frac{k_0}{k} \left[\left(1 - \frac{k_0^2}{k^2}\right) \sin\left(\frac{2k}{k_0}\right) \right. \right. \\ &\quad \left. \left. + \frac{2k_0}{k} \cos\left(\frac{2k}{k_0}\right) \right] + \frac{9 \Delta A^2}{2 A_+^2} \frac{k_0^2}{k^2} \left(1 + \frac{k_0^2}{k^2}\right) \left[\left(1 + \frac{k_0^2}{k^2}\right) \right. \right. \\ &\quad \left. \left. - \frac{2k_0}{k} \sin\left(\frac{2k}{k_0}\right) + \left(1 - \frac{k_0^2}{k^2}\right) \cos\left(\frac{2k}{k_0}\right) \right] \right\}, \end{aligned} \quad (39)$$

and it should be emphasized that the spectrum depends on the wavenumber only through the ratio k/k_0 . Also, as one would expect, this power spectrum turns scale invariant far away from k_0 on either side. While, for $k/k_0 \rightarrow 0$, its scale invariant value is given by

$$\lim_{k/k_0 \rightarrow 0} \mathcal{P}_s(k) = \left(\frac{H_0}{2\pi}\right)^2 \left(\frac{3 H_0^2}{A_+}\right)^2, \quad (40)$$

for $k/k_0 \rightarrow \infty$, it simplifies to

$$\lim_{k/k_0 \rightarrow \infty} \mathcal{P}_s(k) = \left(\frac{H_0}{2\pi}\right)^2 \left(\frac{3 H_0^2}{A_-}\right)^2. \quad (41)$$

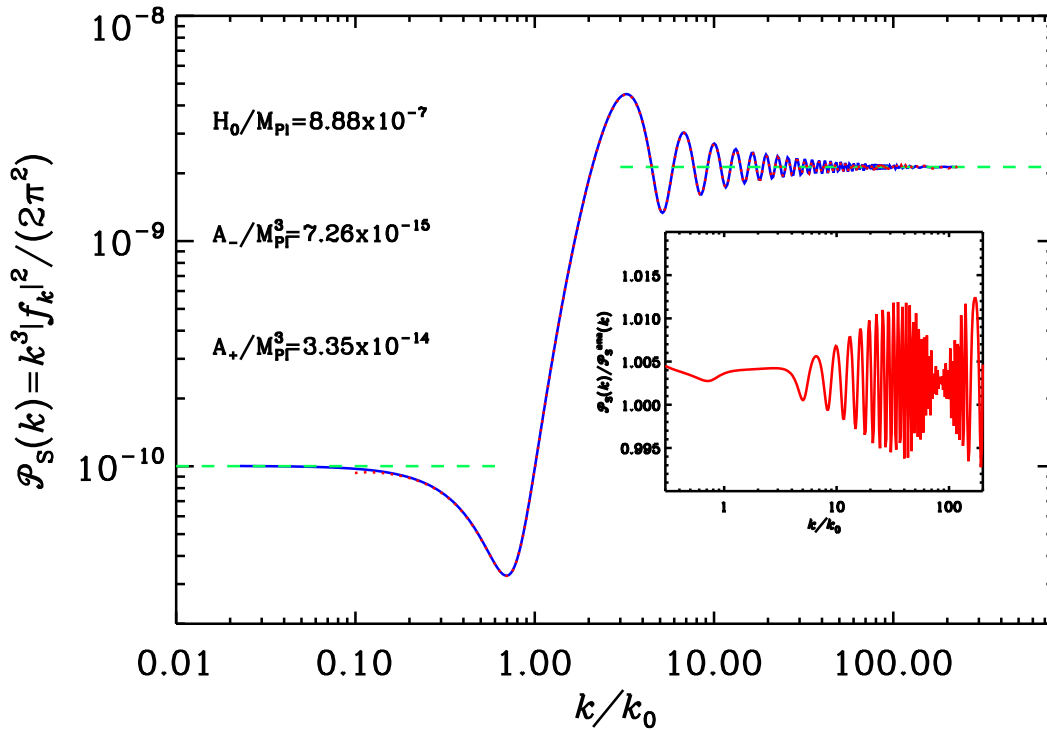


Figure 3. The scalar power spectrum in the Starobinsky model. While the blue solid curve denotes the analytic spectrum (39), the red dots represent the corresponding numerical scalar power spectrum that has been obtained through an exact numerical integration of the background as well as the perturbations. The green dashed lines indicate the asymptotic scale invariant values [cf. Eqs. (40) and (41)]. And, the inset highlights the small difference between the exact numerical spectrum and the analytic one over a certain window in the wavenumber. In plotting these spectra, we have worked with the same values of the parameters that we had mentioned in the first figure. The first scale (i.e. the largest one) for which the power spectrum has been numerically computed corresponds to the physical wavenumber given by $k/a_i = 500 H_i$ at the beginning of inflation, which is an arbitrary but convenient choice. In terms of this scale, k_0 is given by $k_0 = y k_i$, where $500 H_i y e^{-N_0} = H_0$. Given that $N_0 = 10$ and $H_i \simeq H_0$ (as can be easily checked in the slow roll approximation and as can be verified with great accuracy numerically), one obtains $k_0 \simeq 44 k_i$. Evidently, the analytically evaluated spectrum is in remarkable agreement with the numerical result. We should mention that an inaccurate determination of k_0 would have resulted in a ‘phase shift’ between the numerical and analytical spectra.

Given a H_0 , or equivalently, V_0 , COBE normalization (i.e. the amplitude of the power spectrum at suitably small scales) determines the value of A_- . In Fig. 3, we have plotted the above analytical power spectrum and the corresponding numerical result for certain values of the parameters for which COBE normalization is achieved and the assumptions of the Starobinsky model are valid. The two results are clearly in good agreement, which indicates the remarkable extent of validity of the assumptions and approximations that

are used to arrive at analytic forms for the background evolution, the modes as well as the power spectrum in the Starobinsky model.

3. A rapid outline of the procedure for evaluating the scalar bi-spectrum

In this section, we shall quickly sketch the by-now commonly used procedure for evaluating the scalar bi-spectrum generated during inflation (for the original discussion, see Ref. [24]; for further discussions, see Refs. [25, 27] and also the recent review [28]). Due to the constrained nature of the Einstein equations, the scalar perturbations during inflation can be basically described by a single function, say, the curvature perturbation \mathcal{R} . Just as the scalar power spectrum can be expressed in terms of the two point function of the curvature perturbation [using Eqs. (21) and (24)], the scalar bi-spectrum is related to the three point function through a suitable Fourier transform [cf. Eqs. (68) and (70)]. It is well known that, at the linear order in the perturbations, the curvature perturbation \mathcal{R} is governed by a quadratic action [15], which leads to the equation of motion (22) that we had considered in order arrive at the the power spectrum in the previous section. Evidently, in a linear and Gaussian theory, the three point function will be identically zero[§]. Therefore, in order to evaluate the bi-spectrum during inflation, the first step that needs to be taken is to arrive at the action describing the curvature perturbation at the next higher, i.e. the cubic, order. Then, based on the cubic order terms, one evaluates the corresponding three point function of the curvature perturbation (and, thence the bi-spectrum) using the standard techniques of perturbative quantum field theory. In what follows, we shall first describe as to how the cubic order action is arrived at, and then discuss the contributions to the scalar bi-spectrum due to the various terms in the cubic order action.

3.1. The cubic order action describing the curvature perturbation

The action that describes the curvature perturbation at the cubic order is usually arrived at using the Arnowitt-Deser-Misner (ADM) formalism [33]. Recall that, in the ADM formalism, the metric is expressed in terms of the lapse and the shift functions N and N^i as follows:

$$ds^2 = -N^2 d(x^0)^2 + h_{ij} (N^i dx^0 + dx^i) (N^j dx^0 + dx^j), \quad (42)$$

where x^0 and x^i denote the time and the spatial coordinates. As is common knowledge, the lapse and the shift functions N and N^i turn out to be Lagrangian multipliers in the action for the complete system, and the variation of the action with respect to them leads to the Hamiltonian and the momentum constraints. The remaining equations govern the dynamics of the spatial metric h_{ij} . These six equations (corresponding to the independent components of the spatial metric) and the four

[§] It may be useful to point out here that, even a linear theory can lead to non-Gaussian distributions, when one works with, say, non-vacuum initial states.

constraint equations essentially constitute the ten Einstein equations corresponding to the complete spacetime metric.

The system of our interest is gravity described by the Einstein-Hilbert action and a scalar field that is governed by the canonical action. For such a case, in terms of the metric (42), the action describing the complete system can be written as [24, 28]

$$\begin{aligned} \mathcal{S}[N, N_i, h_{ij}, \phi] = \int dx^0 \int d^3\mathbf{x} N \sqrt{h} \left\{ \frac{M_{\text{Pl}}^2}{2} \left[\frac{1}{N^2} (E_{ij} E^{ij} - E^2) + {}^{(3)}R \right] \right. \\ \left. + \left[\frac{1}{2 N^2} \left(\frac{\partial \phi}{\partial x^0} \right)^2 - \frac{N^i}{N^2} \frac{\partial \phi}{\partial x^0} \partial_i \phi - \frac{1}{2} h^{ij} \partial_i \phi \partial_j \phi \right. \right. \\ \left. \left. + \frac{N^i N^j}{2 N^2} \partial_i \phi \partial_j \phi - V(\phi) \right] \right\}, \end{aligned} \quad (43)$$

where $h \equiv \det(h_{ij})$, ${}^{(3)}R$ is the spatial curvature associated with the metric h_{ij} , and the scalar field is assumed to be, in general, dependent on time as well as space. The quantity E_{ij} is the rescaled second fundamental form and is given by

$$E_{ij} = N K_{ij} = \frac{1}{2} \left[\frac{\partial h_{ij}}{\partial x^0} - ({}^{(3)}\nabla_i N_j + {}^{(3)}\nabla_j N_i) \right], \quad (44)$$

while $E = h_{ij} E^{ij}$. Evidently, in the above action, the quantities within the first and the second square brackets correspond to the gravitational and the scalar field parts, respectively.

In the Hamiltonian formulation that we are working in, the conjugate momenta corresponding to the spatial metric h_{ij} and the scalar field ϕ , are given by

$$\pi^{ij} = \frac{M_{\text{Pl}}^2 \sqrt{h}}{2} (K^{ij} - h^{ij} K) \quad \text{and} \quad \pi_\phi = \frac{\sqrt{h}}{N} \left(\frac{\partial \phi}{\partial x^0} - N^i \partial_i \phi \right). \quad (45)$$

The Hamiltonian density, say, \mathcal{H} , of the entire system can be expressed in terms of the generalized coordinates h_{ij} and ϕ , and the corresponding conjugate momenta π_{ij} and π_ϕ as follows:

$$\begin{aligned} \mathcal{H} = \frac{2 N}{M_{\text{Pl}}^2 \sqrt{h}} \left(\pi^{ij} \pi_{ij} - \frac{\pi^2}{2} \right) - \frac{M_{\text{Pl}}^2 N \sqrt{h}}{2} {}^{(3)}R - 2 N_j {}^{(3)}\nabla_i \pi^{ij} \\ + N \left(\frac{\pi_\phi^2}{2 \sqrt{h}} + \frac{\sqrt{h}}{2} h^{ij} \partial_i \phi \partial_j \phi + \sqrt{h} V(\phi) \right) + \pi_\phi N^i \partial_i \phi, \end{aligned} \quad (46)$$

where, clearly, the first line corresponds to gravity, while the second line corresponds to that of the scalar field. Moreover, it is evident from the above Hamiltonian that the lapse and the shift functions indeed act as Lagrange multipliers, as we mentioned above. Varying with respect to N and N_i respectively leads to the following Hamiltonian and momentum constraints:

$$\begin{aligned} \frac{M_{\text{Pl}}^2}{2} [(K^{ij} - h^{ij} K) (K_{ij} - h_{ij} K) - 2 K^2 - {}^{(3)}R] \\ + \frac{1}{2 N^2} \left(\frac{\partial \phi}{\partial x^0} - N^i \partial_i \phi \right)^2 + \frac{1}{2} h^{ij} \partial_i \phi \partial_j \phi + V(\phi) = 0, \end{aligned} \quad (47)$$

and

$$-2 {}^{(3)}\nabla_i \pi^{ij} + \pi_\phi h^{ij} \partial_i \phi = 0. \quad (48)$$

Let us emphasize that, so far, the formalism has been general. Nothing has yet been said about the symmetries and the form of the metric tensor, nor has any approximation been made.

In the case of the Friedmann metric, based on the time coordinate that one works with, the lapse function N can either be set to unity if one chooses x^0 to be the cosmic time t or we can set $N = a$ when working with the conformal time $x^0 = \eta$. At this stage, it is instructive to briefly compare the ADM approach with the more common method of arriving at the equations governing the perturbations from the Einstein equations. In the latter approach, when the scalar perturbations are taken into account, the spatially flat, Friedmann metric in an arbitrary gauge is usually written as

$$ds^2 = - (1 + 2\varphi) dt^2 + 2a(t) \partial_i B dt dx^i + a^2(t) \left[(1 - 2\psi) \delta_{ij} dx^i dx^j + 2\partial_i \partial_j \mathcal{E} dx^i dx^j \right], \quad (49)$$

where φ , B , ψ and \mathcal{E} are the scalar functions that describe the perturbations. Upon comparing this line-element with Eq. (42), it is clear that, we have

$$\begin{aligned} N_i N^i - N^2 &= -(1 + 2\varphi), \quad N_i = a \partial_i B, \\ h_{ij} &= a^2 (1 - 2\psi) \delta_{ij} + 2a^2 \partial_i \partial_j \mathcal{E}. \end{aligned} \quad (50)$$

At the first order in perturbations, these equations reduce to

$$N \simeq 1 + \varphi, \quad N_i \simeq a \partial_i B, \quad h_{ij} \simeq a^2 (\delta_{ij} - 2\psi \delta_{ij} + 2\partial_i \partial_j \mathcal{E}), \quad (51)$$

and the lapse function N is just unity at the zeroth order because we have chosen to work in terms of the cosmic time coordinate.

From the above expressions for the different components of the metric tensor, one can evaluate the second fundamental force and the spatial curvature, and one obtains that

$$K_{ij} = \left(H - 2H\psi - \dot{\psi} - H\varphi \right) a^2 \delta_{ij} - a \partial_i \partial_j B + a^2 \partial_i \partial_j \left(\dot{\mathcal{E}} + 2H\mathcal{E} \right), \quad (52)$$

$${}^{(3)}R = \frac{4}{a^2} \partial_i \partial^i \psi. \quad (53)$$

For a consistent perturbation theory, we must, of course, perturb the scalar field as well. Let us write the scalar field as a homogeneous term plus a perturbative part, i.e. as $\phi + \delta\phi$. If we then use the above expressions for K_{ij} and ${}^{(3)}R$ in the constraint equations (47) and (48), we arrive at

$$\begin{aligned} & -3H \left(H\varphi + \dot{\psi} \right) + \frac{1}{a^2} \partial_i \partial^i \psi - \frac{H}{a} \partial_i \partial^i B + H \partial_i \partial^i \dot{\mathcal{E}} \\ & = \frac{1}{2M_{\text{Pl}}^2} \left(-\dot{\phi}^2 \varphi + \dot{\phi} \delta\dot{\phi} + V_\phi \delta\phi \right), \end{aligned} \quad (54)$$

$$\partial^i \dot{\psi} + H \partial^i \varphi = \frac{\dot{\varphi}}{2M_{\text{Pl}}^2} \partial^i \delta\phi. \quad (55)$$

These are nothing but the time-time and time-space perturbed Einstein equations.

Our main goal now is to evaluate the action (43) at the cubic order in the perturbed quantities. Ideally, one would have liked to work in an arbitrary gauge, as is done to arrive at the standard action that describes the curvature perturbations at the quadratic order [15]. However, as one can imagine, the calculation in an arbitrary gauge turns out to be rather complicated and, to the best of our knowledge, so far, the action at the cubic order seems to have been arrived at by working in a specific gauge. In fact, the gauge that proves to be the most convenient is the one wherein $\mathcal{E} = 0$ and $\delta\phi = 0$, i.e. the gauge wherein perturbations in the inflaton are assumed to vanish [24, 27, 28]. Then, using the perturbed equations derived above, it is easy to show that

$$\varphi = -\frac{\dot{\psi}}{H}, \quad a B = \frac{\psi}{H} - \frac{a^2 \dot{\phi}^2}{2 M_{\text{Pl}}^2 H^2} \partial^{-2} \dot{\psi}, \quad (56)$$

where the operator ∂^{-2} is defined by the relation $\partial^{-2} \partial_i \partial^i \psi \equiv \psi$. The first of these two equations can be obtained from the momentum constraint, while the second arises due to the Hamiltonian constraint. Let us now introduce the curvature perturbation \mathcal{R} , a quantity that is conserved at super Hubble scales, and is given by [34, 35]

$$\mathcal{R} = -\psi - \frac{H}{\dot{\phi}} \delta\phi, \quad (57)$$

In the gauge that we are working in, we have $\mathcal{R} = -\psi$, and the above equations simplify to

$$\varphi = \frac{\dot{\mathcal{R}}}{H}, \quad a B = -\frac{\mathcal{R}}{H} + \frac{a^2 \dot{\phi}^2}{2 M_{\text{Pl}}^2 H^2} \partial^{-2} \dot{\mathcal{R}}. \quad (58)$$

These expressions match Eqs. (28) and (29) in the first article of Refs. [27], if one notices that, in the case of a canonical scalar field, the quantity Σ introduced in the article is given by $\Sigma = \dot{\phi}^2/2$.

We shall assume that the spatial metric h_{ij} is given by

$$h_{ij} = a^2(t) e^{2\mathcal{R}(t, \mathbf{x})} \delta_{ij} \quad (59)$$

and, it is worth noting that, in the gauge that we are working in, the quantity \mathcal{R} that appears in the exponential above is essentially the curvature perturbation. One finds that, it suffices to solve the two constraint equations for the lapse and the shift functions at the linear order in perturbations. This is due to the fact that, at the cubic order in \mathcal{R} , two type of terms arise in the action which involve the lapse and shift functions at the second and the third orders. However, it is found that, the coefficient of the second order term contains a first order constraint, while the third order term proves to be proportional to the zeroth order constraint, both of which, evidently, vanish [24, 27, 28].

For the canonical scalar field of our interest, the action that governs the curvature perturbation \mathcal{R} at the quadratic and the cubic orders can be arrived at from the original action (43). After a considerable amount of manipulations, most of which involve using the solutions to the constraint equations, repeatedly integrating the action by parts and

systematically throwing away the surface terms, one can show that, at the quadratic order in \mathcal{R} , the action (43) simplifies to [24, 27, 28]

$$\mathcal{S}_2[\mathcal{R}] = \frac{1}{2} \int d\eta \int d^3\mathbf{x} \, z^2 \left[\mathcal{R}'^2 - (\partial\mathcal{R})^2 \right]. \quad (60)$$

It is straightforward to check that the variation of this action with respect to \mathcal{R} leads to the differential equation (22) that we had considered earlier.

The action at the cubic order in the curvature perturbation can be obtained in a similar fashion, and is found to be [24, 27, 28]

$$\begin{aligned} \mathcal{S}_3[\mathcal{R}] = M_{\text{Pl}}^2 \int d\eta \int d^3\mathbf{x} \left[a^2 \epsilon_1^2 \mathcal{R} \mathcal{R}'^2 + a^2 \epsilon_1^2 \mathcal{R} (\partial\mathcal{R})^2 \right. \\ \left. - 2 a \epsilon_1 \mathcal{R}' (\partial^i \mathcal{R}) (\partial_i \chi) + \frac{a^2}{2} \epsilon_1 \epsilon_2' \mathcal{R}^2 \mathcal{R}' + \frac{\epsilon_1}{2} (\partial^i \mathcal{R}) (\partial_i \chi) (\partial^2 \chi) \right. \\ \left. + \frac{\epsilon_1}{4} (\partial^2 \mathcal{R}) (\partial\chi)^2 + a \mathcal{F} \left(\frac{\delta\mathcal{L}_2}{\delta\mathcal{R}} \right) \right], \end{aligned} \quad (61)$$

where the quantity χ is defined through the relation

$$\chi \equiv \partial^{-2} \Lambda, \quad (62)$$

with Λ being given by

$$\Lambda \equiv \frac{a^2 \dot{\phi}^2}{2 M_{\text{Pl}}^2 H^2} \dot{\mathcal{R}} = a \epsilon_1 \mathcal{R}'. \quad (63)$$

Note that, while Λ is of dimension one, χ is of dimension -1 . The quantity $\delta\mathcal{L}_2/\delta\mathcal{R}$ denotes the variation of the Lagrangian density corresponding to the quadratic action (60), and can be written as

$$\frac{\delta\mathcal{L}_2}{\delta\mathcal{R}} = \dot{\Lambda} + H \Lambda - \epsilon_1 (\partial^2 \mathcal{R}). \quad (64)$$

The term $\mathcal{F}(\delta\mathcal{L}_2/\delta\mathcal{R})$ that has been introduced in the above cubic order action refers to the following expression:

$$\begin{aligned} \mathcal{F} \left(\frac{\delta\mathcal{L}_2}{\delta\mathcal{R}} \right) = \frac{1}{2aH} \left\{ \left[a^2 H \epsilon_2 \mathcal{R}^2 + 4 a \mathcal{R} \mathcal{R}' + (\partial^i \mathcal{R}) (\partial_i \chi) - \frac{1}{H} (\partial\mathcal{R})^2 \right] \frac{\delta\mathcal{L}_2}{\delta\mathcal{R}} \right. \\ \left. + [\Lambda (\partial_i \mathcal{R}) + (\partial^2 \mathcal{R}) (\partial_i \chi)] \delta^{ij} \partial_j \left[\partial^{-2} \left(\frac{\delta\mathcal{L}_2}{\delta\mathcal{R}} \right) \right] \right. \\ \left. + \frac{1}{H} \delta^{im} \delta^{jn} (\partial_i \mathcal{R}) (\partial_j \mathcal{R}) \partial_m \partial_n \left[\partial^{-2} \left(\frac{\delta\mathcal{L}_2}{\delta\mathcal{R}} \right) \right] \right\}. \end{aligned} \quad (65)$$

Before we proceed, four remarks are required to be made. Firstly, we should point out that, in the above expressions that constitute the action \mathcal{S}_3 , the spatial indices are to be raised or lowered with the Kröneckers symbol. Secondly, notice that, all the terms in the expression (65) for $\mathcal{F}(\delta\mathcal{L}_2/\delta\mathcal{R})$, barring the first one, contain a derivative of the curvature perturbation (either a time or a spatial derivatives or both). Since the quantities have to be evaluated at the end of inflation, the terms which involve the derivatives will not contribute to the final results. Thirdly, we have checked that our expression for \mathcal{S}_3 is consistent with the results obtained earlier (such as in the first three

articles of Refs. [27]). Lastly, it is useful to note that, because the speed of sound is unity for the canonical scalar field, no term involving $\dot{\mathcal{R}}^3$ arises, as it happens in cases involving non-canonical scalar fields.

3.2. The definition of the bi-spectrum and the different contributions

The goal now is to treat the third order action (61) as the interaction term and evaluate the three point function of the curvature perturbation using the standard techniques of perturbative quantum field theory. To begin with, it can be shown that the last term in the action (61) which involves $\delta\mathcal{L}_2/\delta\mathcal{R}$ can be removed by a field redefinition of \mathcal{R} of the following form:

$$\mathcal{R} \rightarrow \mathcal{R}_n + F(\mathcal{R}_n), \quad (66)$$

where $F = \epsilon_2 \mathcal{R}^2/4$ (for further details, see Refs. [24, 27, 28]). With such a redefinition, the interaction Hamiltonian corresponding the action $\mathcal{S}_3[\mathcal{R}]$ above can be written in terms of the conformal time coordinate as

$$\begin{aligned} H_{\text{int}}(\eta) = & -M_{\text{Pl}}^2 \int d^3\mathbf{x} \left[a^2 \epsilon_1^2 \mathcal{R} \mathcal{R}'^2 + a^2 \epsilon_1^2 \mathcal{R} (\partial \mathcal{R})^2 - 2a\epsilon_1 \mathcal{R}' (\partial^i \mathcal{R}) (\partial_i \chi) \right. \\ & \left. + \frac{a^2}{2} \epsilon_1 \epsilon_2' \mathcal{R}^2 \mathcal{R}' + \frac{\epsilon_1}{2} (\partial^i \mathcal{R}) (\partial_i \chi) (\partial^2 \chi) + \frac{\epsilon_1}{4} (\partial^2 \mathcal{R}) (\partial \chi)^2 \right]. \end{aligned} \quad (67)$$

The three point correlation function of the curvature perturbation can be expressed in terms of the Fourier modes as follows:

$$\begin{aligned} \langle \hat{\mathcal{R}}(\eta, \mathbf{x}) \hat{\mathcal{R}}(\eta, \mathbf{x}) \hat{\mathcal{R}}(\eta, \mathbf{x}) \rangle = & \int \frac{d^3\mathbf{k}_1}{(2\pi)^{3/2}} \int \frac{d^3\mathbf{k}_2}{(2\pi)^{3/2}} \int \frac{d^3\mathbf{k}_3}{(2\pi)^{3/2}} \\ & \times \langle \hat{\mathcal{R}}_{\mathbf{k}_1}(\eta) \hat{\mathcal{R}}_{\mathbf{k}_2}(\eta) \hat{\mathcal{R}}_{\mathbf{k}_3}(\eta) \rangle e^{i(\mathbf{k}_1 + \mathbf{k}_2 + \mathbf{k}_3) \cdot \mathbf{x}}. \end{aligned} \quad (68)$$

At the leading order in the perturbations, one then finds that the three point correlation in Fourier space is described by the integral [24, 27, 28]

$$\begin{aligned} & \langle \hat{\mathcal{R}}_{\mathbf{k}_1}(\eta_e) \hat{\mathcal{R}}_{\mathbf{k}_2}(\eta_e) \hat{\mathcal{R}}_{\mathbf{k}_3}(\eta_e) \rangle \\ = & -i \int_{\eta_i}^{\eta_e} d\tau \left\langle \left[\hat{\mathcal{R}}_{\mathbf{k}_1}(\eta_e) \hat{\mathcal{R}}_{\mathbf{k}_2}(\eta_e) \hat{\mathcal{R}}_{\mathbf{k}_3}(\eta_e), \hat{H}_{\text{int}}(\tau) \right] \right\rangle, \end{aligned} \quad (69)$$

where \hat{H}_{int} is the operator corresponding to the interaction Hamiltonian (67), while η_i is the time at which the initial conditions are imposed on the modes when they are well inside the Hubble radius, and η_e denotes a very late time, say, close to when inflation ends. Moreover, while the square brackets imply the commutation of the operators, the angular brackets denote the fact that the correlations are evaluated in the initial vacuum state (viz. the Bunch-Davies vacuum in the situation of our interest).

The scalar bi-spectrum $\mathcal{B}_s(\mathbf{k}_1, \mathbf{k}_2, \mathbf{k}_3)$ is related to the three point correlation function of the Fourier modes of the curvature perturbation, evaluated at the end of inflation, say, η_e , as follows [1]:

$$\langle \hat{\mathcal{R}}_{\mathbf{k}_1}(\eta_e) \hat{\mathcal{R}}_{\mathbf{k}_2}(\eta_e) \hat{\mathcal{R}}_{\mathbf{k}_3}(\eta_e) \rangle = (2\pi)^3 \mathcal{B}_s(\mathbf{k}_1, \mathbf{k}_2, \mathbf{k}_3) \delta^{(3)}(\mathbf{k}_1 + \mathbf{k}_2 + \mathbf{k}_3). \quad (70)$$

For convenience, we shall set

$$\mathcal{B}_s(\mathbf{k}_1, \mathbf{k}_2, \mathbf{k}_3) = (2\pi)^{-9/2} G(\mathbf{k}_1, \mathbf{k}_2, \mathbf{k}_3) \quad (71)$$

and, it is useful to note that, the two quantities \mathcal{B}_s and G are of dimension -6 . We can arrive at the quantity $G(\mathbf{k}_1, \mathbf{k}_2, \mathbf{k}_3)$ from the expressions (69) and (67) for the three point function in Fourier space and the interaction Hamiltonian H_{int} , respectively. Upon using the decomposition (21), as well as the Wick's theorem, which applies to the correlation functions of free quantum fields, we find that $G(\mathbf{k}_1, \mathbf{k}_2, \mathbf{k}_3)$ can be written as

$$\begin{aligned} G(\mathbf{k}_1, \mathbf{k}_2, \mathbf{k}_3) &\equiv \sum_{C=1}^7 G_C(\mathbf{k}_1, \mathbf{k}_2, \mathbf{k}_3) \\ &\equiv M_{\text{Pl}}^2 \sum_{C=1}^6 \left\{ [f_{k_1}(\eta_e) f_{k_2}(\eta_e) f_{k_3}(\eta_e)] \mathcal{G}_C(\mathbf{k}_1, \mathbf{k}_2, \mathbf{k}_3) \right. \\ &\quad \left. + [f_{k_1}^*(\eta_e) f_{k_2}^*(\eta_e) f_{k_3}^*(\eta_e)] \mathcal{G}_C^*(\mathbf{k}_1, \mathbf{k}_2, \mathbf{k}_3) \right\} \\ &\quad + G_7(\mathbf{k}_1, \mathbf{k}_2, \mathbf{k}_3). \end{aligned} \quad (72)$$

The quantities $\mathcal{G}_C(\mathbf{k}_1, \mathbf{k}_2, \mathbf{k}_3)$ with $C = (1, 6)$, which are of dimension $-7/2$, correspond to the six terms in the interaction Hamiltonian (67), and are described by the integrals [24, 25, 27]

$$\mathcal{G}_1(\mathbf{k}_1, \mathbf{k}_2, \mathbf{k}_3) = 2i \int_{\eta_i}^{\eta_e} d\tau a^2 \epsilon_1^2 (f_{k_1}^* f_{k_2}^* f_{k_3}^* + \text{two permutations}), \quad (73)$$

$$\begin{aligned} \mathcal{G}_2(\mathbf{k}_1, \mathbf{k}_2, \mathbf{k}_3) &= -2i (\mathbf{k}_1 \cdot \mathbf{k}_2 + \text{two permutations}) \\ &\quad \times \int_{\eta_i}^{\eta_e} d\tau a^2 \epsilon_1^2 f_{k_1}^* f_{k_2}^* f_{k_3}^*, \end{aligned} \quad (74)$$

$$\begin{aligned} \mathcal{G}_3(\mathbf{k}_1, \mathbf{k}_2, \mathbf{k}_3) &= -2i \int_{\eta_i}^{\eta_e} d\tau a^2 \epsilon_1^2 \left[\left(\frac{\mathbf{k}_1 \cdot \mathbf{k}_2}{k_2^2} \right) f_{k_1}^* f_{k_2}^* f_{k_3}^* \right. \\ &\quad \left. + \text{five permutations} \right], \end{aligned} \quad (75)$$

$$\mathcal{G}_4(\mathbf{k}_1, \mathbf{k}_2, \mathbf{k}_3) = i \int_{\eta_i}^{\eta_e} d\tau a^2 \epsilon_1 \epsilon_2' (f_{k_1}^* f_{k_2}^* f_{k_3}^* + \text{two permutations}), \quad (76)$$

$$\begin{aligned} \mathcal{G}_5(\mathbf{k}_1, \mathbf{k}_2, \mathbf{k}_3) &= \frac{i}{2} \int_{\eta_i}^{\eta_e} d\tau a^2 \epsilon_1^3 \left[\left(\frac{\mathbf{k}_1 \cdot \mathbf{k}_2}{k_2^2} \right) f_{k_1}^* f_{k_2}^* f_{k_3}^* \right. \\ &\quad \left. + \text{five permutations} \right], \end{aligned} \quad (77)$$

$$\begin{aligned} \mathcal{G}_6(\mathbf{k}_1, \mathbf{k}_2, \mathbf{k}_3) &= \frac{i}{2} \int_{\eta_i}^{\eta_e} d\tau a^2 \epsilon_1^3 \left\{ \left[\frac{k_1^2 (\mathbf{k}_2 \cdot \mathbf{k}_3)}{k_2^2 k_3^2} \right] f_{k_1}^* f_{k_2}^* f_{k_3}^* \right. \\ &\quad \left. + \text{two permutations} \right\}. \end{aligned} \quad (78)$$

The additional, seventh term $G_7(\mathbf{k}_1, \mathbf{k}_2, \mathbf{k}_3)$ arises due to the field redefinition (66), and its contribution to $G(\mathbf{k}_1, \mathbf{k}_2, \mathbf{k}_3)$ is found to be given by [24, 27, 28]

$$G_7(\mathbf{k}_1, \mathbf{k}_2, \mathbf{k}_3) = \frac{\epsilon_2(\eta_e)}{2} (|f_{k_2}(\eta_e)|^2 |f_{k_3}(\eta_e)|^2 + \text{two permutations}). \quad (79)$$

Note that, whereas the first three integrals \mathcal{G}_1 , \mathcal{G}_2 and \mathcal{G}_3 involve ϵ_1^2 , the next three, viz. \mathcal{G}_4 , \mathcal{G}_5 and \mathcal{G}_6 , depend on either $\epsilon_1 \epsilon_2'$ or ϵ_1^3 . And, evidently, the term G_7 is proportional to ϵ_2 . During slow roll, the parameter ϵ_1 is almost constant and is typically of the order of 10^{-2} or so, while the second and higher slow roll corrections are even smaller than ϵ_1 . Therefore, in a slow roll inflationary scenario driven by the canonical scalar field, it is found that the first three terms G_1 , G_2 and G_3 (that involve the integrals \mathcal{G}_1 , \mathcal{G}_2 and \mathcal{G}_3) and the term G_7 , which arises due to the field redefinition, that contribute the most to the bi-spectrum [24, 27, 28]. However, when there are deviations from slow roll, it has been noticed that the contribution due to the term G_4 proves to be the largest to the bi-spectrum as the corresponding integral \mathcal{G}_4 contains the quantity $\epsilon_1 \epsilon_2'$ [25].

3.3. The non-Gaussianity parameter f_{NL}

The observationally relevant dimensionless non-Gaussianity parameter f_{NL} that we had discussed about in the introductory section is related to the three point correlation function of the curvature perturbation as follows. It is introduced through the equation [24, 25]

$$\mathcal{R}(\eta, \mathbf{x}) = \mathcal{R}^{\text{G}}(\eta, \mathbf{x}) - \frac{3 f_{\text{NL}}}{5} [\mathcal{R}^{\text{G}}(\eta, \mathbf{x})]^2, \quad (80)$$

where \mathcal{R}^{G} denotes the Gaussian quantity, and the factor of $3/5$ arises due to the relation between the Bardeen potential and the curvature perturbation during the matter dominated epoch. In Fourier space, the above equation can be written as

$$\mathcal{R}_{\mathbf{k}} = \mathcal{R}_{\mathbf{k}}^{\text{G}} - \frac{3 f_{\text{NL}}}{5} \int \frac{d^3 \mathbf{p}}{(2\pi)^{3/2}} \mathcal{R}_{\mathbf{p}}^{\text{G}} \mathcal{R}_{\mathbf{k}-\mathbf{p}}^{\text{G}}. \quad (81)$$

Upon using this relation, the Wick's theorem, which applies to the correlation functions of free quantum fields or, equivalently, to Gaussian random fluctuations, and the definition (24) of the power spectrum, one can arrive at the three point correlation of the curvature perturbation in Fourier space in terms of the parameter f_{NL} . It is found to be

$$\begin{aligned} \langle \hat{\mathcal{R}}_{\mathbf{k}_1} \hat{\mathcal{R}}_{\mathbf{k}_2} \hat{\mathcal{R}}_{\mathbf{k}_3} \rangle &= - \frac{3 f_{\text{NL}}}{10} (2\pi)^4 (2\pi)^{-3/2} \frac{1}{k_1^3 k_2^3 k_3^3} \delta^{(3)}(\mathbf{k}_1 + \mathbf{k}_2 + \mathbf{k}_3) \\ &\quad \times [k_1^3 \mathcal{P}_{\text{s}}(k_2) \mathcal{P}_{\text{s}}(k_3) + \text{two permutations}]. \end{aligned} \quad (82)$$

Using this expression for the three point function and the definition (70) of the bi-spectrum, we can then arrive at the following relation between the non-Gaussianity parameter f_{NL} and the bi-spectrum $\mathcal{B}_{\text{s}}(\mathbf{k}_1, \mathbf{k}_2, \mathbf{k}_3)$:

$$\begin{aligned} f_{\text{NL}} &= - \frac{10}{3} (2\pi)^{-4} (2\pi)^{9/2} k_1^3 k_2^3 k_3^3 \mathcal{B}_{\text{s}}(\mathbf{k}_1, \mathbf{k}_2, \mathbf{k}_3) \\ &\quad \times [k_1^3 \mathcal{P}_{\text{s}}(k_2) \mathcal{P}_{\text{s}}(k_3) + \text{two permutations}]^{-1} \\ &= - \frac{10}{3} (2\pi)^{-4} k_1^3 k_2^3 k_3^3 G(\mathbf{k}_1, \mathbf{k}_2, \mathbf{k}_3) \\ &\quad \times [k_1^3 \mathcal{P}_{\text{s}}(k_2) \mathcal{P}_{\text{s}}(k_3) + \text{two permutations}]^{-1}. \end{aligned} \quad (83)$$

In this paper, we shall restrict our attention to evaluating the bi-spectrum in the Starobinsky model in the equilateral limit (i.e. when $\mathbf{k}_1 = \mathbf{k}_2 = \mathbf{k}_3$). In such a case, the above expression for f_{NL} simplifies to

$$f_{\text{NL}}^{\text{eq}} = -\frac{10}{9} (2\pi)^{-4} \frac{k^6 G(k)}{\mathcal{P}_s^2(k)}, \quad (84)$$

with $G(k)$ given by [cf. Eq (72)]

$$\begin{aligned} G(k) &\equiv \sum_{C=1}^7 G_C(k) \\ &= M_{\text{Pl}}^2 \sum_{C=1}^6 [f_k^3(\eta_e) \mathcal{G}_C(k) + f_k^{*3}(\eta_e) \mathcal{G}_C^*(k)] + G_7(k). \end{aligned} \quad (85)$$

Using this expression and the dimensions of the quantities involved, which we had pointed out before, it is straightforward to check that f_{NL} is indeed a dimensionless quantity. Further, in the Starobinsky model, due to the difference in the dynamics before and after the transition, the integrals in Eqs. (73)–(78) need to be carried out separately on either side of the transition. Therefore, we can write

$$\begin{aligned} G(k) &= M_{\text{Pl}}^2 \sum_{C=1}^6 \left\{ f_k^3(\eta_e) [\mathcal{G}_C^+(k) + \mathcal{G}_C^-(k)] + f_k^{*3}(\eta_e) [\mathcal{G}_C^{+*}(k) + \mathcal{G}_C^{-*}(k)] \right\} \\ &\quad + G_7(k) \\ &= M_{\text{Pl}}^2 \sum_{C=1}^6 [f_k^3(\eta_e) \mathcal{G}_C^+(k) + f_k^{*3}(\eta_e) \mathcal{G}_C^{+*}(k)] \\ &\quad + M_{\text{Pl}}^2 \sum_{C=1}^6 [f_k^3(\eta_e) \mathcal{G}_C^-(k) + f_k^{*3}(\eta_e) \mathcal{G}_C^{-*}(k)] + G_7(k) \\ &= \sum_{C=1}^6 [G_C^+(k) + G_C^-(k)] + G_7(k), \end{aligned} \quad (86)$$

where, as we had mentioned earlier, the plus and the minus signs in the super-scripts refer to the quantities before and after the transition, respectively. In the following section, we shall first evaluate the contribution to the bi-spectrum due to the supposedly dominant term G_4 in the Starobinsky model. And, in the subsequent section, we shall evaluate all the remaining contributions as well. As we have pointed out before, remarkably, we are able to evaluate the bi-spectrum in the equilateral limit completely analytically without any further assumptions or approximations. We shall then discuss the range of values for the parameters of the Starobinsky model for which the non-Gaussianity parameter f_{NL} can be large.

4. The dominant contribution to the bi-spectrum in the Starobinsky model

In this section, we shall evaluate the contribution due to the term G_4 to the bi-spectrum in the Starobinsky model in the equilateral limit.

To begin with, recall that, in the Starobinsky model, the second roll parameter ϵ_2 is constant before the field reaches the discontinuity at ϕ_0 when $\eta = \eta_0 = -(a_0 H_0)^{-1} = k_0^{-1}$. As a result, the integral \mathcal{G}_4 which involves ϵ'_2 [cf. Eq. (76)] vanishes before η_0 and, hence, we are left with only the following contribution after the transition:

$$\mathcal{G}_4(\mathbf{k}_1, \mathbf{k}_2, \mathbf{k}_3) = i \int_{-k_0^{-1}}^0 d\tau a^2 \epsilon_{1-} \epsilon'_{2-} (f_{k_1}^* f_{k_2}^* f_{k_3}^* + \text{two permutations}). \quad (87)$$

Also, post-transition, the mode v_k and the quantity z are given by Eqs. (29) and (30), respectively. Since $f_k = v_k/z$, one obtains that

$$f_k^-(\eta) = \frac{i H_0 \alpha_k}{2 M_{\text{Pl}} \sqrt{k^3 \epsilon_{1-}}} (1 + i k \eta) e^{-i k \eta} - \frac{i H_0 \beta_k}{2 M_{\text{Pl}} \sqrt{k^3 \epsilon_{1-}}} (1 - i k \eta) e^{i k \eta}, \quad (88)$$

while the corresponding derivative with respect to the conformal time coordinate is given by

$$\begin{aligned} f_k'^-(\eta) = & \frac{i H_0 \alpha_k}{2 M_{\text{Pl}} \sqrt{k^3 \epsilon_{1-}}} \left[-\mathcal{H} \epsilon_{1-} (1 + i k \eta) - \frac{\mathcal{H} \epsilon_{2-}}{2} (1 + i k \eta) + k^2 \eta \right] e^{-i k \eta} \\ & - \frac{i H_0 \beta_k}{2 M_{\text{Pl}} \sqrt{k^3 \epsilon_{1-}}} \left[-\mathcal{H} \epsilon_{1-} (1 - i k \eta) - \frac{\mathcal{H} \epsilon_{2-}}{2} (1 - i k \eta) + k^2 \eta \right] e^{i k \eta}. \end{aligned} \quad (89)$$

In this expression, one can ignore the first term in the square bracket since it is proportional to the first slow roll parameter which, as demonstrated before, always remains small even when the field is crossing the discontinuity in the slope of the potential. However, we should stress here that, in doing so, we are in fact ignoring contributions to G_4 that are possibly of the same order as the sub-dominant terms, such as G_1 , G_2 , G_3 and G_7 . We shall comment more on this point in the next section.

We find that, upon using the expressions (14) and (19) for ϵ_1 and $\dot{\epsilon}_2$ after the transition, in the equilateral limit, we can write \mathcal{G}_4 as follows:

$$\begin{aligned} \mathcal{G}_4(k) = & \frac{81 \Delta A k_0^3 H_0^3}{2 \sqrt{2 k^9} M_{\text{Pl}}^2 A_-^2} \left[\alpha_k^{*3} I_4(k) - \beta_k^{*3} I_4^*(k) - \alpha_k^{*2} \beta_k^* J_4(k) \right. \\ & \left. + \alpha_k^* \beta_k^{*2} J_4^*(k) \right]. \end{aligned} \quad (90)$$

The quantities I_4 and J_4 in the above expression are described by the integrals

$$\begin{aligned} I_4(k) = & \int_{-k_0^{-1}}^0 \frac{d\tau \tau}{(1 - \rho^3 \tau^3)^4} (1 - i k \tau)^2 \left[k^2 + 3 \rho^3 (1 - i k \tau) \tau \right. \\ & \left. - k^2 \rho^3 \tau^3 \right] e^{3 i k \tau}, \end{aligned} \quad (91)$$

$$\begin{aligned} J_4(k) = & \int_{-k_0^{-1}}^0 \frac{d\tau \tau}{(1 - \rho^3 \tau^3)^4} (1 - i k \tau) \left[3 k^2 + 9 \rho^3 \tau + i k^3 \tau + 6 \rho^3 k^2 \tau^3 \right. \\ & \left. - i k^3 \rho^3 \tau^4 \right] e^{i k \tau}, \end{aligned} \quad (92)$$

where the quantity ρ is defined by the following expression

$$\rho^3 \equiv -\frac{\Delta A}{A_-} k_0^3. \quad (93)$$

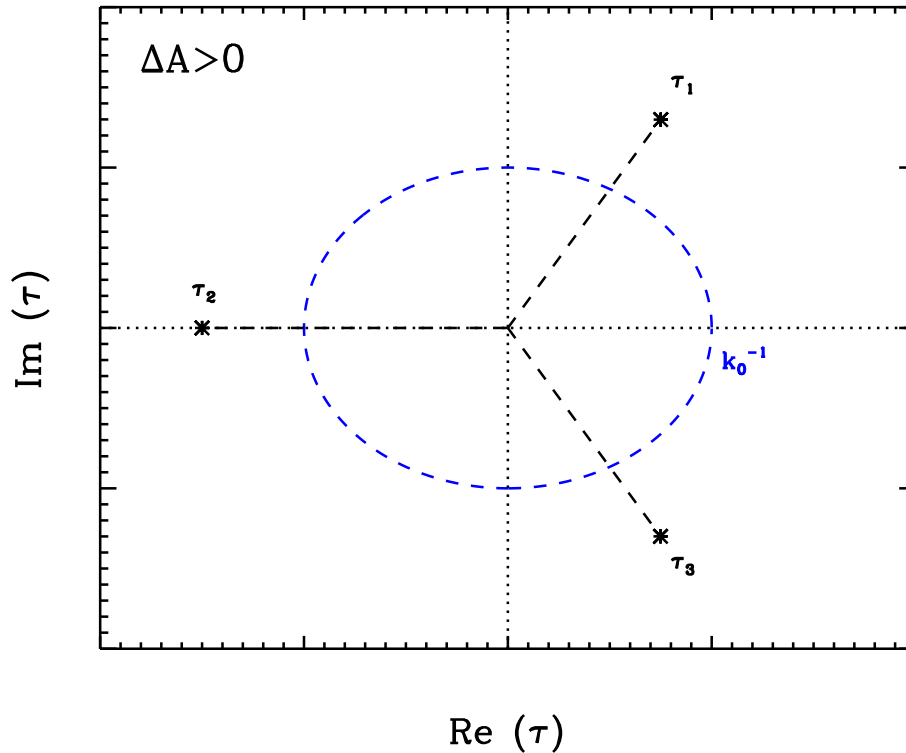


Figure 4. The three poles corresponding to the factor $(1 - \rho^3 \tau^3)^{-1}$ that appears in the integrals I_4 and J_4 [cf. Eqs. (91) and (92)] are marked with black asterisks in the complex τ -plane for the case wherein $\Delta A > 0$. Evidently, they will all fall on a circle of radius $|\rho|^{-1} = (A_-/|\Delta A|) k_0^{-1}$ which is centered at the origin [cf. Eq. (93)]. Note that, in the integrals I_4 and J_4 , the path of integration runs from $-k_0^{-1}$ to zero along the negative τ -axis. Amongst the three poles, viz. τ_1 , τ_2 and τ_3 [in this context, see Eq. (143) below], only τ_2 lies on the axis. The dashed blue curve represents a circle of radius k_0^{-1} about the origin. However, since $|\Delta A|/A_- < 1$ when $\Delta A > 0$, all the poles, including τ_2 , lie outside the blue curve. Therefore, no pole falls on the path of integration.

A concern could arise that, in the above integrals, one may encounter poles corresponding to the factor $(1 - \rho^3 \tau^3)^{-1}$ along the path of integration, viz. from $-k_0^{-1}$ to zero on the negative τ -axis. It is easy to establish that this does not occur. Since τ is negative over the region of interest, when $\Delta A < 0$, $\rho^3 > 0$, so that $\rho^3 \tau^3 < 0$. So, $(1 - \rho^3 \tau^3) > 0$ for all $\tau < 0$ and, hence, no pole occurs on the negative τ axis in such a case. [The poles when $\Delta A < 0$ are given by Eq. (144), and their actual locations in the complex τ -plane can be found represented in Fig. 7.] Whereas, when $\Delta A > 0$, $\rho^3 < 0$, and $\rho^3 \tau^3 > 0$ for $\tau < 0$. It is then clear that, under such conditions, a pole will indeed arise on the negative τ -axis. However, as we have illustrated in Fig. 4, the pole on the axis of integration only occurs at $\tau < -k_0^{-1}$, which lies beyond the lower limit of the integrals. Therefore, we encounter no poles on the path of integration.

As no poles arise, we find that the integrals I_4 and J_4 can be evaluated easily, and

we obtain that

$$I_4(k) = \frac{1}{3} - \frac{1}{3} \left[\frac{1 + i k/k_0}{1 + (\rho/k_0)^3} \right]^3 e^{-3 i k/k_0}, \quad (94)$$

$$J_4(k) = 1 - \frac{(1 - i k/k_0) (1 + i k/k_0)^2}{[1 + (\rho/k_0)^3]^3} e^{-i k/k_0}. \quad (95)$$

Upon substituting the above results for the integrals I_4 and J_4 in Eq. (90), we obtain that

$$\begin{aligned} \mathcal{G}_4(k) = & \frac{81 \Delta A k_0^3 H_0^3}{2 \sqrt{2} k^9 M_{\text{Pl}}^2 A_-^2} \left\{ \frac{\alpha_k^{*3}}{3} - \alpha_k^{*2} \tilde{\beta}_k^* e^{-2 i k/k_0} - \frac{[1 + (i k/k_0)]^3}{3 [1 + (\rho/k_0)^3]^3} e^{-3 i k/k_0} \right. \\ & \left. + \alpha^* \tilde{\beta}_k^{*2} e^{-4 i k/k_0} - \frac{\tilde{\beta}_k^{*3}}{3} e^{-6 i k/k_0} \right\}, \end{aligned} \quad (96)$$

where, for convenience, we have introduced the quantity

$$\tilde{\beta}_k \equiv \beta_k e^{-2 i k/k_0}. \quad (97)$$

As we shall see, working in terms of $\tilde{\beta}_k$ allows us to isolate exponential factors easily.

We next need to evaluate the quantity $G_4(k)$. According to our prior discussions [see in particular Eqs. (86)], this quantity is given by

$$G_4(k) = M_{\text{Pl}}^2 [f_k^3(\eta_e) \mathcal{G}_4(k) + f_k^{*3}(\eta_e) \mathcal{G}_4^*(k)]. \quad (98)$$

Towards the end of inflation, i.e. as $\eta \rightarrow 0$, the mode f_k reduces to

$$f_k(\eta_e) = \frac{i H_0}{2 M_{\text{Pl}} \sqrt{k^3 \epsilon_{1-}(\eta_e)}} (\alpha_k - \beta_k), \quad (99)$$

where $\epsilon_{1-}(\eta_e)$ denotes the value of the first slow roll parameter at late times. On using this expression and the relation (96) for \mathcal{G}_4 , we find that we can write G_4 as

$$\begin{aligned} k^6 G_4(k) = & \frac{81}{8 \sqrt{2} \epsilon_{1-}^3(\eta_e)} \left(\frac{k_0}{k} \right)^3 \frac{\Delta A H_0^6}{A_-^2 M_{\text{Pl}}^3} \left[\mathcal{A}_1(k) \sin \left(\frac{k}{k_0} \right) \right. \\ & \left. + \mathcal{A}_2(k) \cos \left(\frac{k}{k_0} \right) + \mathcal{A}_3(k) \sin \left(\frac{3k}{k_0} \right) + \mathcal{A}_4(k) \cos \left(\frac{3k}{k_0} \right) \right], \end{aligned} \quad (100)$$

where the four coefficients \mathcal{A}_1 , \mathcal{A}_2 , \mathcal{A}_3 and \mathcal{A}_4 are found to be

$$\begin{aligned} \mathcal{A}_1(k) = & \frac{3 A_-^3 \Delta A}{4 A_+^5} \left(1 + \frac{k^2}{k_0^2} \right)^2 \left[9 A_- \left(1 + \frac{k^2}{k_0^2} \right) \right. \\ & \left. + A_+ \left(-9 - \frac{9 k^2}{k_0^2} + \frac{2 k^4}{k_0^4} \right) \right] \left(\frac{k}{k_0} \right)^{-6}, \end{aligned} \quad (101)$$

$$\begin{aligned} \mathcal{A}_2(k) = & - \frac{3 A_-^3 \Delta A}{4 A_+^5} \left(1 + \frac{k^2}{k_0^2} \right)^2 \left[9 A_- \left(1 + \frac{k^2}{k_0^2} \right) \right. \\ & \left. - A_+ \left(9 + \frac{11 k^2}{k_0^2} \right) \right] \left(\frac{k}{k_0} \right)^{-5}, \end{aligned} \quad (102)$$

$$\mathcal{A}_3(k) = - \frac{A_-^3}{12 A_+^5} \left[27 \Delta A^2 \left(1 - \frac{k^2}{k_0^2} \right) - 27 \Delta A (5 A_- - 7 A_+) \frac{k^4}{k_0^4} \right]$$

$$- (9A_- - 11A_+)^2 \frac{k^6}{k_0^6} + 6A_+ (-3A_- + 5A_+) \frac{k^8}{k_0^8} \left] \left(\frac{k}{k_0} \right)^{-6}, \quad (103)$$

$$\begin{aligned} \mathcal{A}_4(k) = & \frac{A_-^3}{12 A_+^5} \left[-27 A_-^2 \left(-3 + \frac{k^2}{k_0^2} \right) \left(1 + \frac{k^2}{k_0^2} \right)^2 + 18 A_- A_+ \left(1 + \frac{k^2}{k_0^2} \right) \right. \\ & \times \left(-9 - \frac{7k^2}{k_0^2} + \frac{6k^4}{k_0^4} \right) + A_+^2 \left(81 + \frac{153k^2}{k_0^2} - \frac{9k^4}{k_0^4} - \frac{93k^6}{k_0^6} \right. \\ & \left. \left. + \frac{4k^8}{k_0^8} \right) \right] \left(\frac{k}{k_0} \right)^{-5}. \end{aligned} \quad (104)$$

Let us now understand the behavior of G_4 at large and small scales. Experience with the slow roll results suggest that, far from k_0 , on either side, one can expect $k^6 G_4$ to turn scale invariant. As $k/k_0 \rightarrow 0$, we find that

$$\lim_{k/k_0 \rightarrow 0} k^6 G_4(k) = \frac{27}{8 \sqrt{2 \epsilon_{1-}^3(\eta_e)}} \frac{\Delta A A_-^3 H_0^6}{A_+^5 M_{\text{Pl}}^3} \quad (105)$$

and, in the limit $k/k_0 \rightarrow \infty$, one arrives at the result

$$\lim_{k/k_0 \rightarrow \infty} k^6 G_4(k) = \frac{27}{8 \sqrt{2 \epsilon_{1-}^3(\eta_e)}} \frac{H_0^6 \Delta A A_-}{A_+^3 M_{\text{Pl}}^3} \cos \left(\frac{3k}{k_0} \right). \quad (106)$$

In Fig 5, we have plotted the absolute value of the quantity $k^6 G_4$ given by the expression (100). Clearly, while the quantity is strictly scale invariant for $k \ll k_0$, the scale invariant amplitude is modulated by superimposed oscillations for $k \gg k_0$.

It is interesting to note that, while the power spectrum had depended on trigonometric functions involving $2k/k_0$ [cf. Eq. (39)], the bi-spectrum depends on trigonometric functions involving $3k/k_0$. Definitely, these behavior can be attributed to the fact that the power spectrum and the bi-spectrum depend on the second and the third powers of the curvature perturbation, respectively. In fact, that such a behavior can broadly be expected to occur has been pointed out previously in the literature while investigating a model that, in some aspects, is similar to the Starobinsky model [28]. The model considered earlier contains a discontinuity in the potential itself rather than in the derivative of the potential. Despite this difference, the slow roll parameters seem to behave just as in the Starobinsky model, with the first slow roll parameter remaining small through the transition as the field crosses the discontinuity, whereas ϵ_2 and $\dot{\epsilon}_2$ grow large for a short period around the time of the transition. Since the background behavior is rather similar, it is possible for the two cases to be meaningfully compared. We find that, in order to evaluate the f_{NL} in the model, the earlier work [28] simply represents ϵ'_2 as a Dirac delta function at the transition which, then, permits an easy integration of the dominant contribution. However, such an approach cannot seem to reproduce the detailed pattern that we have obtained in our calculation here, and one arrives at only a rough oscillatory behavior on the small scales (in this context, see Eq. (6.32) of Ref. [28]). Moreover, the method does not seem to allow the calculation of the other, sub-dominant, contributions, as we are able to carry out in the case of the Starobinsky model (see our discussion in the following section). With regards to the

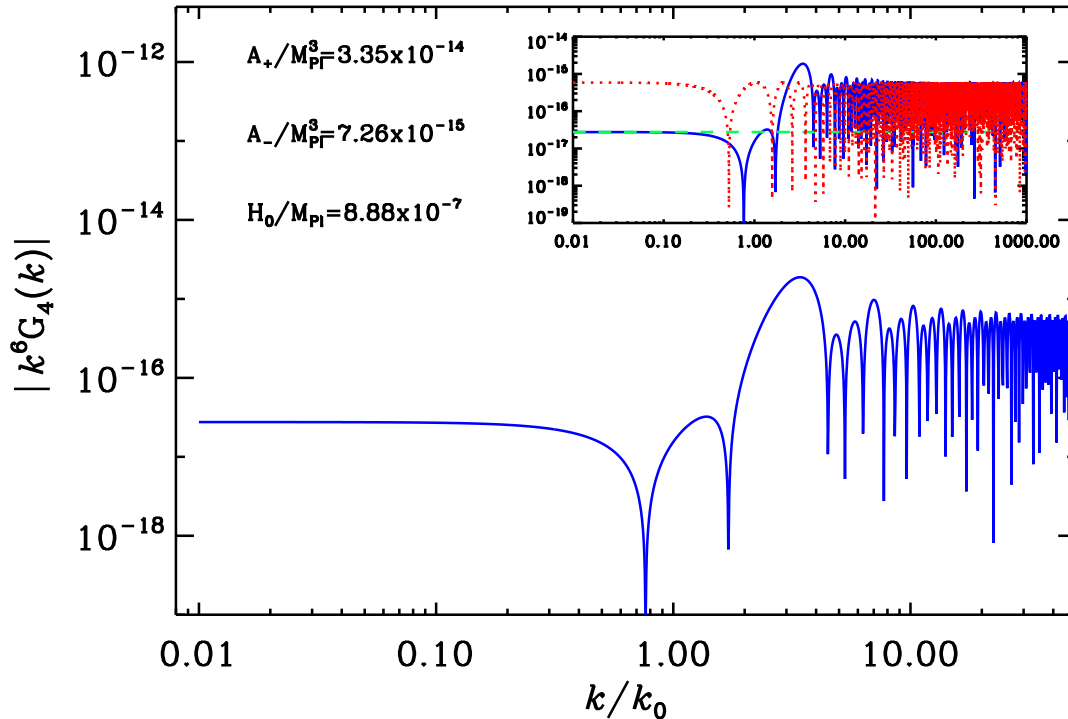


Figure 5. The absolute value of the quantity $k^6 G_4$, as given by Eq. (100), has been plotted as a function of k/k_0 (the blue curve). We have worked with the same of values of A_+ , A_- and H_0 as in the earlier figures. We should stress the fact that, as in the case of the power spectrum, the quantity $k^6 G_4$ depends on the wavenumber only through the ratio k/k_0 . The green and the red curves in the inset represent the asymptotic behavior for $k \ll k_0$ and $k \gg k_0$, respectively.

overall amplitude of the effect, it is not straightforward to compare the results, since the models are not exactly similar. However, the order of magnitude of f_{NL} is found to be in agreement with what we obtain (see Sec. 6). This leads us to conclude that our results are broadly consistent with those of Ref. [28].

5. The sub-dominant contributions to the bi-spectrum

In this section, we shall arrive at analytic expressions for the other, sub-dominant contributions to the bi-spectrum in the equilateral limit. Unlike the dominant term G_4 wherein no contribution arose before the transition (due to the vanishing $\dot{\epsilon}_2$), the other five terms involving integrals—viz. G_1 , G_2 , G_3 , G_5 and G_6 —contribute before as well as after the transition. As one would expect, the calculation of the contribution until the transition to fast roll largely follows the computations in the slow roll case. In contrast, the computation of the contribution post-transition proves to be more involved, but, as we shall see, tractable. The last term G_7 is, obviously, straightforward to evaluate

since it does not involve any integrals, and only requires the amplitude of the curvature perturbation at late times.

5.1. The contribution due to the second term

We shall first evaluate the contribution due to the second term in the interaction Hamiltonian (67), viz. the quantity G_2 arising due to the integral \mathcal{G}_2 [cf. Eq. (74)], as it involves simpler integrals.

5.1.1. Before the transition Since ϵ_1 remains a constant before the transition, the integral (74) can be written as

$$\begin{aligned} \mathcal{G}_2^+(\mathbf{k}_1, \mathbf{k}_2, \mathbf{k}_3) = & -2i (\mathbf{k}_1 \cdot \mathbf{k}_2 + \text{two permutations}) \epsilon_{1+}^2 \\ & \times \int_{-(1-i\gamma)\infty}^{-k_0^{-1}} d\tau a^2 f_{k_1}^* f_{k_2}^* f_{k_3}^*, \end{aligned} \quad (107)$$

where the γ which appears in the lower limit is an infinitesimal positive quantity that has been introduced by hand, as is done in the standard slow roll case [24, 27]. The procedure can also be viewed as though the integration contour has been rotated by a small angle γ in the complex τ plane. The inclusion of γ ensures the selection of the correct choice for the perturbative vacuum. Also, algebraically, its introduction allows us to avoid the increasingly rapid oscillations at very early times (i.e. as $\eta \rightarrow -\infty$), as it acts as an exponential cut-off that leads to the rapid convergence of the integral.

Note that, before the transition, the mode v_k and the quantity z are given by Eqs. (27) and (30), so that we have

$$f_k^+(\eta) = \frac{i H_0}{2 M_{\text{Pl}} \sqrt{k^3 \epsilon_{1+}}} (1 + i k \eta) e^{-i k \eta}, \quad (108)$$

Upon substituting this mode in the above expression for \mathcal{G}_2^+ , one finds that the resulting integral can be easily evaluated even in the most generic case of $\mathbf{k}_1 \neq \mathbf{k}_2 \neq \mathbf{k}_3$. We obtain the contribution until the transition to be

$$\begin{aligned} \mathcal{G}_2^+(\mathbf{k}_1, \mathbf{k}_2, \mathbf{k}_3) = & \frac{H_0}{4 M_{\text{Pl}}^3} \sqrt{\frac{\epsilon_{1+}}{(k_1 k_2 k_3)^3}} (\mathbf{k}_1 \cdot \mathbf{k}_2 + \mathbf{k}_1 \cdot \mathbf{k}_3 + \mathbf{k}_2 \cdot \mathbf{k}_3) e^{-i k_{\text{T}}/k_0} \\ & \times \left[k_0 - \frac{k_1 k_2 k_3}{k_{\text{T}} k_0} + \frac{i k_1 k_2 k_3}{k_{\text{T}}^2} + \frac{i}{k_{\text{T}}} (k_1 k_2 + k_2 k_3 + k_1 k_3) \right], \end{aligned} \quad (109)$$

where $k_{\text{T}} \equiv k_1 + k_2 + k_3$. It can be easily checked that this expression reduces to the standard slow roll result as $k_0 \rightarrow \infty$ [24, 27], which is basically equivalent to assuming that the transition to fast roll does not take place at all. On restricting to the equilateral case, the above expression simplifies to

$$\mathcal{G}_2^+(k) = \frac{3 H_0 k^2 k_0}{4 M_{\text{Pl}}^3} \sqrt{\frac{\epsilon_{1+}}{k^9}} \left(1 + \frac{10 i k}{9 k_0} - \frac{k^2}{3 k_0^2} \right) e^{-3 i k/k_0}. \quad (110)$$

With the help of the above \mathcal{G}_2^+ , we are now in a position to calculate G_2^+ , which is given by

$$\begin{aligned} G_2^+(k) &= M_{\text{Pl}}^2 \left[f_k^3(\eta_e) \mathcal{G}_2^+(k) + f_k^{*3}(\eta_e) \mathcal{G}_2^{*+}(k) \right] \\ &= \frac{-iH_0^3}{8M_{\text{Pl}}\sqrt{k^9\epsilon_{1-}^3(\eta_e)}} \left[(\alpha_k - \beta_k)^3 \mathcal{G}_2^+(k) - (\alpha_k^* - \beta_k^*)^3 \mathcal{G}_2^{*+}(k) \right]. \end{aligned} \quad (111)$$

Upon using the expressions (37) and (38) for α_k and β_k , straightforward manipulations allow us to write G_2^+ as follows:

$$\begin{aligned} k^6 G_2^+(k) &= \frac{1}{16\sqrt{2\epsilon_{1-}^3(\eta_e)}} \frac{k_0}{k} \frac{A_+ H_0^2}{M_{\text{Pl}}^5} \\ &\times \left\{ 3\Re \left[\left(\alpha_k^2 \tilde{\beta}_k + \alpha_k^* \tilde{\beta}_k^{*2} \right) \left(1 - \frac{k^2}{3k_0^2} \right) \right. \right. \\ &+ \frac{10ik}{9k_0} \left(\alpha_k^2 \tilde{\beta}_k - \alpha_k^* \tilde{\beta}_k^{*2} \right) \left. \right] \sin \left(\frac{k}{k_0} \right) \\ &- 3\Im \left[\left(\alpha_k^2 \tilde{\beta}_k + \alpha_k^* \tilde{\beta}_k^{*2} \right) \left(1 - \frac{k^2}{3k_0^2} \right) \right. \\ &+ \frac{10ik}{9k_0} \left(\alpha_k^2 \tilde{\beta}_k - \alpha_k^* \tilde{\beta}_k^{*2} \right) \left. \right] \cos \left(\frac{k}{k_0} \right) \\ &- \Re \left[\left(\alpha_k^3 + \tilde{\beta}_k^{*3} \right) \left(1 - \frac{k^2}{3k_0^2} \right) + \frac{10ik}{9k_0} \left(\alpha_k^3 - \tilde{\beta}_k^{*3} \right) \right] \sin \left(\frac{3k}{k_0} \right) \\ &\left. + \Im \left[\left(\alpha_k^3 + \tilde{\beta}_k^{*3} \right) \left(1 - \frac{k^2}{3k_0^2} \right) + \frac{10ik}{9k_0} \left(\alpha_k^3 - \tilde{\beta}_k^{*3} \right) \right] \cos \left(\frac{3k}{k_0} \right) \right\}, \end{aligned} \quad (112)$$

where \Re and \Im denote the real and the imaginary parts of the arguments. Notice that the above expression contains trigonometric functions of arguments k/k_0 and $3k/k_0$, as the contribution due to the fourth term had. Therefore, this expression can be expected to lead to a similar (but, in some ways, different!) oscillatory pattern as the dominant contribution.

Let us now understand the asymptotic forms of $k^6 G_2^+$. As $k/k_0 \rightarrow 0$, we find that it goes to a constant given by

$$\lim_{k/k_0 \rightarrow 0} k^6 G_2^+(k) = -\frac{17}{144\sqrt{2\epsilon_{1-}^3(\eta_e)}} \frac{A_-^3 H_0^2}{M_{\text{Pl}}^5 A_+^2}. \quad (113)$$

While, in the limit $k/k_0 \rightarrow \infty$, one obtains the following behavior

$$\begin{aligned} \lim_{k/k_0 \rightarrow \infty} k^6 G_2^+(k) &= \frac{1}{16\sqrt{2\epsilon_{1-}^3(\eta_e)}} \frac{A_+ H_0^2}{M_{\text{Pl}}^5} \left[\frac{3}{2} \left(1 - \frac{A_-}{A_+} \right) \cos \left(\frac{k}{k_0} \right) \right. \\ &\left. + \frac{1}{3} \frac{k}{k_0} \sin \left(\frac{3k}{k_0} \right) + \left(\frac{47}{18} - \frac{3A_-}{2A_+} \right) \cos \left(\frac{3k}{k_0} \right) \right]. \end{aligned} \quad (114)$$

It should be pointed out that the second term grows with k as $(k/k_0) \sin(3k/k_0)$. In other words, $k^6 G_2^+$ diverges linearly at large k . Interestingly, as we shall illustrate, this diverging term will be canceled by a similar term but with the opposite sign that arises

due to the contribution post-transition, ensuring that the complete $k^6 G_2$ remains finite at large k .

5.1.2. After the transition Let us now turn to the evaluation of the contribution \mathcal{G}_2^- after the transition. The calculation proceeds in a manner very similar to the computation of \mathcal{G}_4^- . But, in contrast to \mathcal{G}_4^- , for evaluating \mathcal{G}_2^- , we only require the behavior of the first slow roll parameter after the transition, which is given by Eq. (14). Upon substituting the modes (88) after the transition in Eq. (74) and, after some manipulations, one obtains that

$$\mathcal{G}_2^-(k) = \frac{3 H_0 k^2}{4 M_{\text{Pl}}^3 k^{9/2}} \left[\alpha_k^{*3} I_2(k) - \beta_k^{*3} I_2^*(k) - \alpha_k^{*2} \beta_k^* J_2(k) + \alpha_k^* \beta_k^{*2} J_2^*(k) \right], \quad (115)$$

where I_2 and J_2 are described by the integrals

$$I_2(k) = \frac{A_-}{\sqrt{18} H_0^2 M_{\text{Pl}}} \int_{-k_0^{-1}}^{\eta_e} \frac{d\tau}{\tau^2} (1 - \rho^3 \tau^3) (1 - i k \tau)^3 e^{3 i k \tau}, \quad (116)$$

$$J_2(k) = \frac{3 A_-}{\sqrt{18} H_0^2 M_{\text{Pl}}} \int_{-k_0^{-1}}^{\eta_e} \frac{d\tau}{\tau^2} (1 - \rho^3 \tau^3) (1 - i k \tau)^2 (1 + i k \tau) e^{i k \tau}, \quad (117)$$

with ρ^3 given by Eq. (93). It is clear that the structure of these integrals is very similar to that of I_4 and J_4 [cf. Eqs. (91) and (92)]. However, in contrast, the poles in I_2 and J_2 are located at the origin and, hence, they do not fall on the integration path. Due to this reason, the two integrals I_2 and J_2 can be performed easily, and the results can be written in the following form:

$$I_2(k) = \frac{A_- k_0}{\sqrt{18} H_0^2 M_{\text{Pl}}} \left[\mathcal{I}_2^a(k) + \mathcal{I}_2^b(k) e^{-3 i k/k_0} \right], \quad (118)$$

$$J_2(k) = \frac{3 A_- k_0}{\sqrt{18} H_0^2 M_{\text{Pl}}} \left[\mathcal{J}_2^a(k) + \mathcal{J}_2^b(k) e^{-i k/k_0} \right], \quad (119)$$

where the scale dependent quantities \mathcal{I}_2^a , \mathcal{I}_2^b , \mathcal{J}_2^a and \mathcal{J}_2^b are given by

$$\mathcal{I}_2^a(k) = -\frac{1}{k_0 \eta_e} + \frac{k}{81 k_0} \left(90 i + \frac{53 \Delta A k_0^3}{A_- k^3} \right), \quad (120)$$

$$\begin{aligned} \mathcal{I}_2^b(k) = & -1 - \frac{k}{81 k_0} \left(90 i + \frac{53 \Delta A k_0^3}{A_- k^3} \right) - \frac{53 i \Delta A k_0}{27 A_- k} \\ & + \frac{k^2}{3 k_0^2} \left(1 - \frac{\Delta A}{A_-} \right) + \frac{13 i \Delta A k}{9 A_- k_0} + \frac{22 \Delta A}{9 A_-}, \end{aligned} \quad (121)$$

$$\mathcal{J}_2^a(k) = -\frac{1}{k_0 \eta_e} - \frac{k}{k_0} \left(2 i + \frac{27 \Delta A k_0^3}{A_- k^3} \right), \quad (122)$$

$$\begin{aligned} \mathcal{J}_2^b(k) = & -1 + \frac{k}{k_0} \left(2 i + \frac{27 \Delta A k_0^3}{A_- k^3} \right) - \frac{k^2}{k_0^2} + \frac{27 i \Delta A k_0}{A_- k} \\ & - \frac{14 \Delta A}{A_-} - \frac{5 i \Delta A k}{A_- k_0} + \frac{\Delta A k^2}{A_- k_0^2}. \end{aligned} \quad (123)$$

Note that the coefficients \mathcal{I}_2^a and \mathcal{J}_2^a actually diverge in the limit $\eta_e \rightarrow 0$. This implies that I_2 and J_2 will diverge too, but, as we shall soon demonstrate, the corresponding contribution to \mathcal{G}_2^- remains perfectly finite. It is also worth remarking that the coefficients \mathcal{I}_2^a , \mathcal{I}_2^b , \mathcal{J}_2^a and \mathcal{J}_2^b depend on the wavenumber only through the ratio k/k_0 , as expected. Using the above expressions, one obtains that

$$\begin{aligned} \mathcal{G}_2^-(k) = & \frac{A_- k^2 k_0}{4 \sqrt{2} k^9 M_{\text{Pl}}^4 H_0} \left[\mathcal{I}_2^a(k) \alpha_k^{*3} - 3 \mathcal{J}_2^a(k) \alpha_k^{*2} \tilde{\beta}_k^* e^{-2ik/k_0} \right. \\ & \left. + \mathcal{K}_2(k) e^{-3ik/k_0} + 3 \mathcal{J}_2^{a*}(k) \alpha_k^* \tilde{\beta}_k^{*2} e^{-4ik/k_0} - \mathcal{I}_2^{a*}(k) \tilde{\beta}_k^{*3} e^{-6ik/k_0} \right], \end{aligned} \quad (124)$$

where the new coefficient \mathcal{K}_2 is given by

$$\mathcal{K}_2(k) \equiv \mathcal{I}_2^b(k) \alpha_k^{*3} - \mathcal{I}_2^{b*}(k) \tilde{\beta}_k^{*3} + 3 \alpha_k^* \tilde{\beta}_k^* \left[\mathcal{J}_2^{b*}(k) \tilde{\beta}_k^* - \mathcal{J}_2^b(k) \alpha_k^* \right]. \quad (125)$$

We can now evaluate the resulting G_2^- . The remarkable fact is that, all the terms proportional to $1/\eta_e$ cancel out and, therefore, the final result for G_2^- turns out to be finite in the limit $\eta_e \rightarrow 0$. We find that G_2^- can be expressed as

$$\begin{aligned} k^6 G_2^-(k) = & \frac{-i}{32 \sqrt{2} \epsilon_{1-}^3(\eta_e)} \frac{k_0}{k} \frac{A_- H_0^2}{M_{\text{Pl}}^5} \left([\mathcal{I}_2^a(k) - \mathcal{I}_2^{a*}(k)] \left(\alpha_k^3 \alpha_k^{*3} - \tilde{\beta}_k^3 \tilde{\beta}_k^{*3} \right) \right. \\ & + 9 [\mathcal{J}_2^a(k) - \mathcal{J}_2^{a*}(k)] \alpha_k \alpha_k^* \tilde{\beta}_k \tilde{\beta}_k^* \left(\alpha_k \alpha_k^* - \tilde{\beta}_k \tilde{\beta}_k^* \right) \\ & + 6i \Re \left[\mathcal{K}_2(k) \alpha_k \tilde{\beta}_k^2 + \mathcal{K}_2^*(k) \alpha_k^{*2} \tilde{\beta}_k^* \right] \sin \left(\frac{k}{k_0} \right) \\ & + 6i \Im \left[\mathcal{K}_2(k) \alpha_k \tilde{\beta}_k^2 + \mathcal{K}_2^*(k) \alpha_k^{*2} \tilde{\beta}_k^* \right] \cos \left(\frac{k}{k_0} \right) \\ & - 6i \Re \left\{ [\mathcal{I}_2^{a*}(k) - \mathcal{J}_2^a(k)] \alpha_k \tilde{\beta}_k^* \left(\alpha_k^2 \alpha_k^{*2} - \tilde{\beta}_k^2 \tilde{\beta}_k^{*2} \right) \right\} \sin \left(\frac{2k}{k_0} \right) \\ & + 6i \Im \left\{ [\mathcal{I}_2^{a*}(k) - \mathcal{J}_2^a(k)] \alpha_k \tilde{\beta}_k^* \left(\alpha_k^2 \alpha_k^{*2} - \tilde{\beta}_k^2 \tilde{\beta}_k^{*2} \right) \right\} \cos \left(\frac{2k}{k_0} \right) \\ & - 2i \Re \left[\mathcal{K}_2(k) \alpha_k^3 + \mathcal{K}_2^*(k) \tilde{\beta}_k^{*3} \right] \sin \left(\frac{3k}{k_0} \right) \\ & + 2i \Im \left[\mathcal{K}_2(k) \alpha_k^3 + \mathcal{K}_2^*(k) \tilde{\beta}_k^{*3} \right] \cos \left(\frac{3k}{k_0} \right) \\ & + 6i \Re \left\{ [\mathcal{I}_2^a(k) - \mathcal{J}_2^a(k)] \alpha_k^{*2} \tilde{\beta}_k^2 \left(\alpha_k \alpha_k^* - \tilde{\beta}_k \tilde{\beta}_k^* \right) \right\} \sin \left(\frac{4k}{k_0} \right) \\ & \left. + 6i \Im \left\{ [\mathcal{I}_2^a(k) - \mathcal{J}_2^a(k)] \alpha_k^{*2} \tilde{\beta}_k^2 \left(\alpha_k \alpha_k^* - \tilde{\beta}_k \tilde{\beta}_k^* \right) \right\} \cos \left(\frac{4k}{k_0} \right) \right). \end{aligned} \quad (126)$$

Let us now study the asymptotic behavior of G_2^- . In the limit $k/k_0 \rightarrow 0$, we find that $k^6 G_2^-$ goes to a constant given by

$$\lim_{k/k_0 \rightarrow 0} k^6 G_2^-(k) = \frac{3}{16 \sqrt{2} \epsilon_{1-}^3(\eta_e)} \frac{A_-^5 H_0^2}{M_{\text{Pl}}^5 A_+^4}. \quad (127)$$

Whereas, as $k/k_0 \rightarrow \infty$, it has the following behavior

$$\lim_{k/k_0 \rightarrow \infty} k^6 G_2^-(k) = \frac{1}{16\sqrt{2\epsilon_{1-}^3(\eta_e)}} \frac{A_+ H_0^2}{M_{\text{Pl}}^5} \left[\frac{10A_-}{9A_+} - \frac{3}{2} \left(1 - \frac{A_-}{A_+} \right) \cos\left(\frac{k}{k_0}\right) - \frac{k}{3k_0} \sin\left(\frac{3k}{k_0}\right) - \left(\frac{107}{18} - \frac{29A_-}{6A_+} \right) \cos\left(\frac{3k}{k_0}\right) \right]. \quad (128)$$

As we had mentioned earlier, $k^6 G_2^-$ too diverges at large k . Upon comparing with Eq. (114), it is clear that the divergence involving the $\sin(3k/k_0)$ term in the above expression is of the same form, but with an opposite sign. Therefore, the total contribution due to the second term, viz. $G_2(k) = G_2^+(k) + G_2^-(k)$ remains finite even at large k . We find that, as $k/k_0 \rightarrow 0$, $k^6 G_2$ turns strictly scale invariant with the amplitude

$$\lim_{k/k_0 \rightarrow 0} k^6 G_2(k) = \frac{1}{16\sqrt{2\epsilon_{1-}^3(\eta_e)}} \frac{A_-^3 H_0^2}{M_{\text{Pl}}^5 A_+^2} \left(-\frac{17}{9} + \frac{3A_-^2}{A_+^2} \right). \quad (129)$$

In the limit of large k/k_0 , the diverging terms cancel exactly and we are left with the following finite expression:

$$\lim_{k/k_0 \rightarrow \infty} k^6 G_2(k) = \frac{1}{16\sqrt{2\epsilon_{1-}^3(\eta_e)}} \frac{A_+ H_0^2}{M_{\text{Pl}}^5} \left[\frac{10A_-}{9A_+} - \frac{10}{3} \left(1 - \frac{A_-}{A_+} \right) \cos\left(\frac{3k}{k_0}\right) \right], \quad (130)$$

which is scale invariant with superimposed oscillations. Notice that the superimposed oscillations again involve a cosine function with the argument $3k/k_0$. These asymptotic behavior are also evident from Fig. 6, wherein we have plotted the absolute value of the quantity $k^6 G_2$.

5.2. The contributions due to the first and the third terms

Barring the \mathbf{k} dependent factors, the contributions \mathcal{G}_1 and \mathcal{G}_3 due to the first and the third terms in the interaction Hamiltonian (67) involve similar integrals [cf. (73) and (75)]. One finds that, their contributions can be combined and evaluated together in the equilateral limit. As in the case of the second term, we shall first evaluate the contribution before the transition and then turn our attention to the calculation of the contribution after the transition.

5.2.1. Before the transition To begin with, note that, before the transition, the mode f_k is given by Eq. (108), while its derivative can be computed to be

$$f_k^{+'}(\eta) = \frac{i H_0}{2 M_{\text{Pl}} \sqrt{k^3 \epsilon_{1+}}} \left[-\mathcal{H} \left(\epsilon_{1+} + \frac{\epsilon_{2+}}{2} \right) (1 + i k \eta) + k^2 \eta \right] e^{-i k \eta}. \quad (131)$$

As is usually done while working in the slow roll approximation, we shall ignore the first term within the square brackets involving ϵ_{1+} and ϵ_{2+} . Upon using the mode (108) and its derivative above in the integrals (73) and (75), and upon modifying the lower

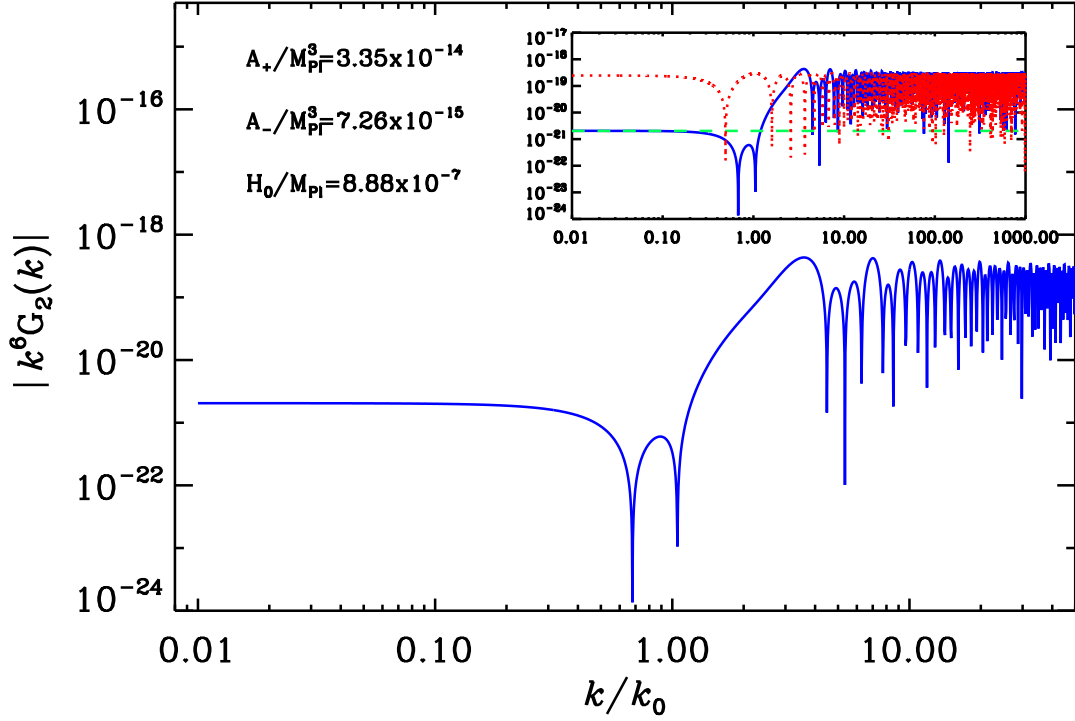


Figure 6. The absolute value of the quantity $k^6 G_2$ has been plotted as a function of k/k_0 (the blue curve). In plotting this figure, we have worked with the same values of the parameters that we had considered in the previous figures. As in the last plot, the green and the red curves in the inset represent the limiting forms for $k \ll k_0$ and $k \gg k_0$, respectively [see Eqs. (129) and (130)].

limit of the integrals as in Eq. (107), we find that the integrals can be evaluated easily without actually having to take the equilateral limit. We obtain that

$$\mathcal{G}_1^+(\mathbf{k}_1, \mathbf{k}_2, \mathbf{k}_3) = -\frac{H_0}{4 M_{\text{Pl}}^3} \sqrt{\frac{\epsilon_{1+}}{(k_1 k_2 k_3)^3}} e^{-i k_T/k_0} \left[\frac{k_2^2 k_3^2}{i k_T} \left(1 + \frac{k_1}{k_T} + \frac{i k_1}{k_0} \right) + \text{two permutations} \right] \quad (132)$$

and

$$\mathcal{G}_3^+(\mathbf{k}_1, \mathbf{k}_2, \mathbf{k}_3) = \frac{H_0}{4 M_{\text{Pl}}^3} \sqrt{\frac{\epsilon_{1+}}{(k_1 k_2 k_3)^3}} e^{-i k_T/k_0} \left[\frac{\mathbf{k}_1 \cdot \mathbf{k}_2}{k_2^2} \frac{k_2^2 k_3^2}{i k_T} \left(1 + \frac{k_1}{k_T} + \frac{i k_1}{k_0} \right) + \text{five permutations} \right], \quad (133)$$

which reduce to the standard slow roll results as $k_0 \rightarrow \infty$ [24, 27]. In the equilateral limit, the above expressions simplify to

$$\mathcal{G}_1^+(k) = \frac{i H_0 k^3}{4 M_{\text{Pl}}^3} \sqrt{\frac{\epsilon_{1+}}{k^9}} \left(\frac{4}{3} + \frac{i k}{k_0} \right) e^{-3 i k/k_0}, \quad (134)$$

$$\mathcal{G}_3^+(k) = -\frac{2i H_0 k^3}{4 M_{\text{Pl}}^3} \sqrt{\frac{\epsilon_{1+}}{k^9}} \left(\frac{4}{3} + \frac{ik}{k_0} \right) e^{-3ik/k_0}, \quad (135)$$

so that we have

$$\mathcal{G}_1^+(k) + \mathcal{G}_3^+(k) = -\frac{i H_0 k^3}{4 M_{\text{Pl}}^3} \sqrt{\frac{\epsilon_{1+}}{k^9}} \left(\frac{4}{3} + \frac{ik}{k_0} \right) e^{-3ik/k_0}. \quad (136)$$

The corresponding $G_1^+ + G_3^+$ is given by Eq. (86) which involves the mode function at late times [cf. Eq. (99)], and thereby the Bogoliubov coefficients. Upon using the expressions (37) and (38) for α_k and β_k , we find that we can write

$$\begin{aligned} k^6 [G_1^+(k) + G_3^+(k)] = & -\frac{1}{48\sqrt{2\epsilon_{1-}^3(\eta_e)}} \frac{A_+ H_0^2}{M_{\text{Pl}}^5} \\ & \times \left\{ -3\Im \left[\left(\frac{4}{3} + \frac{ik}{k_0} \right) (\alpha_k^2 \tilde{\beta}_k + \alpha_k \tilde{\beta}_k^2) \right] \sin \left(\frac{k}{k_0} \right) \right. \\ & - 3\Re \left[\left(\frac{4}{3} + \frac{ik}{k_0} \right) (\alpha_k^2 \tilde{\beta}_k - \alpha_k \tilde{\beta}_k^2) \right] \cos \left(\frac{k}{k_0} \right) \\ & + \Im \left[\left(\frac{4}{3} + \frac{ik}{k_0} \right) (\alpha_k^3 + \tilde{\beta}_k^3) \right] \sin \left(\frac{3k}{k_0} \right) \\ & \left. + \Re \left[\left(\frac{4}{3} + \frac{ik}{k_0} \right) (\alpha_k^3 - \tilde{\beta}_k^3) \right] \cos \left(\frac{3k}{k_0} \right) \right\}. \quad (137) \end{aligned}$$

We again encounter the by-now usual structure containing sine and cosine functions with arguments k/k_0 and $3k/k_0$. As we had carried out earlier, it is interesting to study the asymptotic behavior of the above expression at small and large scales. In the limit of small k/k_0 , one has

$$\lim_{k/k_0 \rightarrow 0} k^6 [G_1^+(k) + G_3^+(k)] = -\frac{1}{36\sqrt{2\epsilon_{1-}^3(\eta_e)}} \frac{A_+^3 H_0^2}{M_{\text{Pl}}^5 A_+^2}, \quad (138)$$

while in the limit of large k/k_0 , one obtains

$$\begin{aligned} \lim_{k/k_0 \rightarrow \infty} k^6 [G_1^+(k) + G_3^+(k)] = & -\frac{1}{48\sqrt{2\epsilon_{1-}^3(\eta_e)}} \frac{A_+ H_0^2}{M_{\text{Pl}}^5} \left[\frac{9}{2} \left(1 - \frac{A_-}{A_+} \right) \right. \\ & \times \cos \left(\frac{k}{k_0} \right) + \frac{k}{k_0} \sin \left(\frac{3k}{k_0} \right) \\ & \left. + \left(\frac{35}{6} - \frac{9A_-}{2A_+} \right) \cos \left(\frac{3k}{k_0} \right) \right]. \quad (139) \end{aligned}$$

It should be mentioned here that, as in the case of $k^6 G_2^+$, the above asymptotic form too diverges linearly at large k . Again, as in the earlier case, the contribution post-transition will cancel this divergent term leading to an overall finite $k^6 (G_1 + G_3)$.

5.2.2. After the transition We shall now evaluate the contribution due to first and the third terms arising from the post-transition phase. As the calculation proves to be somewhat heavy and lengthy (but manageable), we shall relegate some of the details of the calculation to an appendix. The starting point is similar to what we have already

encountered in the case of the first sub-dominant term: upon substituting the mode (88) and its derivative (89) in the integrals (73) and (74), we find that, we can write

$$\begin{aligned} \mathcal{G}_1^-(k) + \mathcal{G}_3^-(k) = & \frac{3H_0}{4M_{\text{Pl}}^3 k^{9/2}} \left[\alpha_k^{*3} I_{13}(k) - \beta_k^{*3} I_{13}^*(k) - \alpha_k^{*2} \beta_k^* J_{13}(k) \right. \\ & \left. + \alpha_k^* \beta_k^{*2} J_{13}^*(k) \right], \end{aligned} \quad (140)$$

where I_{13} and J_{13} are described by the integrals

$$\begin{aligned} I_{13}(k) = & \frac{A_-}{\sqrt{18} H_0^2 M_{\text{Pl}}} \int_{-k_0^{-1}}^{\eta_e} \frac{d\tau}{1 - \rho^3 \tau^3} (1 - ik\tau) \left[3\rho^3 \tau (1 - ik\tau) \right. \\ & \left. + k^2 (1 - \rho^3 \tau^3) \right]^2 e^{3ik\tau}, \end{aligned} \quad (141)$$

$$\begin{aligned} J_{13}(k) = & \frac{A_-}{\sqrt{18} H_0^2 M_{\text{Pl}}} \int_{-k_0^{-1}}^{\eta_e} \frac{d\tau}{1 - \rho^3 \tau^3} \left[3\rho^3 \tau (1 - ik\tau) + k^2 (1 - \rho^3 \tau^3) \right] \\ & \times \left[9 (1 - ik\tau) (1 + ik\tau) \rho^3 \tau + k^2 (1 - \rho^3 \tau^3) (3 - ik\tau) \right] e^{ik\tau}. \end{aligned} \quad (142)$$

In arriving at the above expressions, we have again ignored the term involving ϵ_{1-} within the square brackets in Eq. (89), just as we had done while evaluating the dominant contribution G_4 . We had earlier mentioned that, in the case of G_4 , the neglected terms can be expected to be of the same order as the contributions due to G_1 , G_2 , G_3 and G_7 . The terms that we shall ignore here are possibly of the same order as the contributions due to G_5 and G_6 .

Let us now analyze these integrals in some detail. Firstly, a concern could arise that these integrals may contain a pole—due to the $(1 - \rho^3 \tau^3)^{-1}$ term—along the path of integration, which runs along the real axis from $-k_0^{-1}$ to η_e , with the latter approaching zero from the negative direction. Actually, the integrals I_4 and J_4 [cf. Eqs. (91) and (92)] that we had to carry out earlier in the calculation of G_4 had also contained the same term, and we had discussed the issue of the poles in some detail then. In the case $\Delta A > 0$, the three poles corresponding to $(1 - \rho^3 \tau^3)^{-1}$ are actually located at

$$\tau_1 = \frac{e^{i\pi/3}}{|\rho|}, \quad \tau_2 = \frac{e^{i\pi}}{|\rho|}, \quad \tau_3 = \frac{e^{5i\pi/3}}{|\rho|}, \quad (143)$$

in the complex τ plane. In fact, we had illustrated the positions of these poles for a situation wherein $\Delta A > 0$ in Fig. 4. Whereas, when $\Delta A < 0$, the poles are found to be at

$$\tau_1 = \frac{1}{|\rho|}, \quad \tau_2 = \frac{e^{2i\pi/3}}{|\rho|}, \quad \tau_3 = \frac{e^{4i\pi/3}}{|\rho|}, \quad (144)$$

and their location is illustrated in Fig. 7. It should be clear from these two figures that no poles arise on the path of the integration.

Secondly, in order to compute the integrals, it is convenient to write the term containing the poles as follows:

$$\frac{1}{1 - \rho^3 \tau^3} = -\frac{1}{\rho^3} \frac{1}{\tau^3 - 1/\rho^3} = -\frac{1}{\rho^3} \frac{1}{(\tau - \tau_1)(\tau - \tau_2)(\tau - \tau_3)}$$

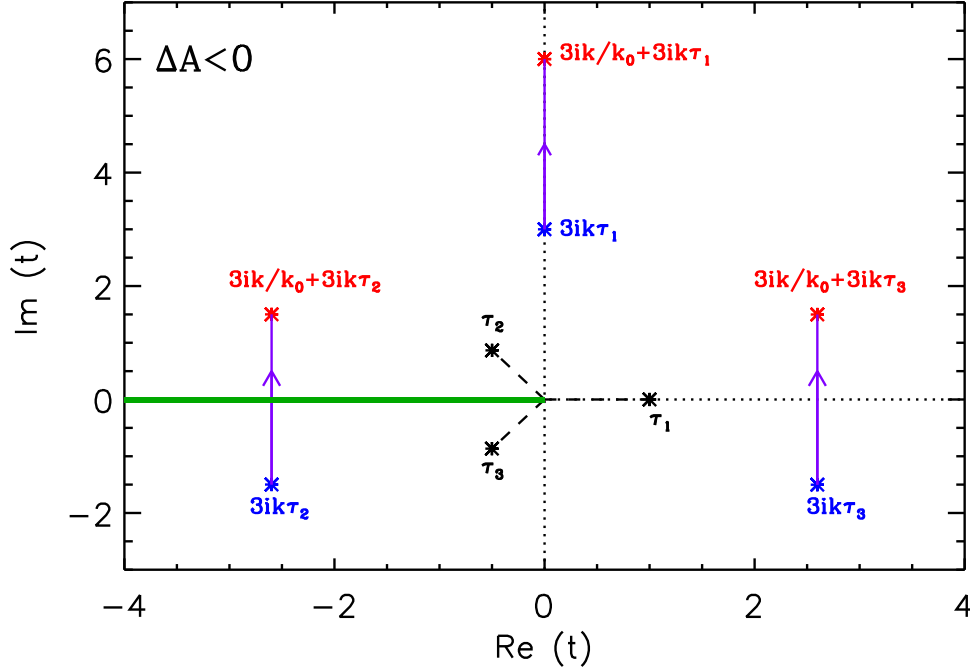


Figure 7. The poles corresponding to the $(1 - \rho^3 \tau^3)^{-1}$ term that appears in the integrals I_{13} and J_{13} [cf. Eqs. (141) and (142)]. We should mention here that, we had encountered the same term in the integrals I_4 and J_4 as well and, in Fig. 4, we had illustrated the positions of the poles when $\Delta A > 0$. The location of the three poles τ_1 , τ_2 and τ_3 in the complex τ -plane, for a case wherein $\Delta A < 0$, have been marked in the above figure with black asterisks [in this context, see Eq. (144)]. The solid blue line segments denote the three new integration paths corresponding to τ_1 , τ_2 and τ_3 in the complex t_n plane, with t_n being related to τ_n through Eq. (151). The solid green line running along the negative real axis represents the branch cut associated with the function $E_1(z)$.

$$= -\frac{|\rho|^2}{\rho^3} \left(\frac{b_1}{\tau - \tau_1} + \frac{b_2}{\tau - \tau_2} + \frac{b_3}{\tau - \tau_3} \right), \quad (145)$$

where b_1 , b_2 and b_3 are given by

$$b_1 = \frac{1}{|\rho|^2 (\tau_1 - \tau_2) (\tau_1 - \tau_3)} = \frac{1}{3}, \quad (146)$$

$$b_2 = -\frac{1}{|\rho|^2 (\tau_1 - \tau_2) (\tau_2 - \tau_3)} = -\frac{1}{6} (1 - i\sqrt{3}), \quad (147)$$

$$b_3 = \frac{1}{|\rho|^2 (\tau_1 - \tau_3) (\tau_2 - \tau_3)} = -\frac{1}{6} (1 + i\sqrt{3}) = b_2^*. \quad (148)$$

These expressions are valid when $\Delta A < 0$. If $\Delta A > 0$, then one has $b_1 = -[(1 + i\sqrt{3})/6]$, $b_2 = (1/3)$ and $b_3 = -[(1 - i\sqrt{3})/6]$, i.e. simply a permutation of the previous values.

Lastly, the numerators of the integrals I_{13} and J_{13} are polynomials in τ of order

seven. As a consequence, one can write

$$I_{13}(k) = -\frac{A_- |\rho|^2}{\sqrt{18} H_0^2 M_{\text{Pl}} \rho^3} \sum_{n=1}^3 b_n \int_{-k_0^{-1}}^{\eta_e} d\tau \frac{P_1(\tau)}{\tau - \tau_n} e^{3ik\tau}, \quad (149)$$

where $P_1(\tau)$ is the seventh order polynomial given by

$$P_1(\tau) \equiv (1 - ik\tau) [3\rho^3 \tau (1 - ik\tau) + k^2 (1 - \rho^3 \tau^3)]^2. \quad (150)$$

Let us now perform the following change of variable from τ to t_n :

$$t_n \equiv -3ik(\tau - \tau_n). \quad (151)$$

It should be stressed here that, because the change of the variable depends on τ_n , it is different for the three integrals in the above expression for I_{13} . The change of the variable leads to

$$I_{13}(k) = -\frac{A_- |\rho|^2}{\sqrt{18} H_0^2 M_{\text{Pl}} \rho^3} \sum_{n=1}^3 b_n e^{3ik\tau_n} \times \int_{3ik/k_0 + 3ik\tau_n}^{-3ik\eta_e + 3ik\tau_n} \frac{dt_n}{t_n} e^{-t_n} P_1\left(\frac{-t_n}{3ik} + \tau_n\right). \quad (152)$$

We find that this integral can be evaluated by initially expressing P_1 as a polynomial in t_n , and then carrying out the integral term by term. Since the computation proves to be somewhat longwinded, as we had mentioned before, we shall relegate the details of the calculation to an appendix (see Appendix A.1), and simply quote the final result here. We obtain that

$$I_{13}(k) = -\frac{A_- |\rho|^2 k^4}{\sqrt{18} H_0^2 M_{\text{Pl}} \rho^3} [\mathcal{I}_{13}^a(k) + \mathcal{I}_{13}^b(k) e^{-3ik/k_0}], \quad (153)$$

where the scale dependent quantities \mathcal{I}_{13}^a and \mathcal{I}_{13}^b can be expressed as

$$\mathcal{I}_{13}^a(k) = -\sum_{n=1}^3 b_n \left[c_{n0} \mathcal{E}_1(3ik\tau_n) + \sum_{m=1}^7 c_{nm} (m-1)! e_{m-1}(3ik\tau_n) \right], \quad (154)$$

$$\begin{aligned} \mathcal{I}_{13}^b(k) = & \sum_{n=1}^3 b_n \left[c_{n0} \mathcal{E}_1\left(\frac{3ik}{k_0} + 3ik\tau_n\right) \right. \\ & \left. + \sum_{m=1}^7 c_{nm} (m-1)! e_{m-1}\left(\frac{3ik}{k_0} + 3ik\tau_n\right) \right], \end{aligned} \quad (155)$$

with the coefficients c_{nm} being given by Eqs. (A.2)–(A.9). In these expressions, $e_n(z)$ denotes the exponential sum function (A.14), while $\mathcal{E}_1(z) \equiv e^z E_1(z)$, with $E_1(z)$ being the exponential integral function (A.15). Despite the fact that the calculation is more involved, it is clear that the structure of I_{13} resembles that of I_2 .

However, there is one particular point that we have overlooked in the above considerations. When one performs the change of variable from τ to $t_n = -3ik(\tau - \tau_n)$, one basically modifies the contour along which the integrations are performed. Since the change in the variable from τ to t_n involves τ_n , the modified path evidently depends on τ_n . The effect of multiplying by $3ik$ is to rotate the path by an angle of $\pi/2$ in

the anti-clockwise direction. Therefore, the contours start from $3ik\tau_n$ (corresponding to $\tau = 0$) and run vertically until $3ik/k_0$ has been added to $3ik\tau_n$. The three new integration paths corresponding to τ_1 , τ_2 and τ_3 are displayed (as the solid blue line segments) in the complex t_n plane in Fig. 7. Note that the function $E_1(z)$ has a branch cut running from $-\infty$ to 0 (represented as the solid green line in the figure). While the paths associated with t_1 and t_3 are further away, there seems to be the possibility that the path corresponding to t_2 may cross the branch cut. It is clear from the figure that this will occur if the imaginary part of t_2 corresponding to $\tau = -k_0^{-1}$ is positive, i.e. when

$$\Im[t_2(\tau = -k_0^{-1})] = \frac{3k}{k_0} \left[1 - \frac{1}{2} \left(\frac{A_-}{|\Delta A|} \right)^{1/3} \right] > 0. \quad (156)$$

For $\Delta A < 0$, this condition implies that $A_+/A_- > 9/8 = 1.125$. If this condition is satisfied, then one crosses the branch cut of the function $E_1(z)$ and, in such a case, one must add a suitable contribution to the integral I_{13} . We find that the additional contribution amounts to redefining the above \mathcal{I}_{13}^a by

$$\begin{aligned} \mathcal{I}_{13}^a(k) = & - \sum_{n=1}^3 b_n \left[c_{n0} \mathcal{E}_1(3ik\tau_n) + \sum_{m=1}^7 c_{nm} (m-1)! e_{m-1}(3ik\tau_n) \right] \\ & + (2i\pi) b_2 c_{20} e^{3ik\tau_2}. \end{aligned} \quad (157)$$

It is important to point out here that whether the additional term arises or not depends only on the ratio A_+/A_- and not on the wavenumber k .

We now need to calculate the integral J_{13} , which, as in the case of I_{13} , can be expressed as

$$J_{13}(k) = - \frac{A_- |\rho|^2}{\sqrt{18} H_0^2 M_{\text{Pl}} \rho^3} \sum_{n=1}^3 b_n \int_{-k_0^{-1}}^{\eta_e} d\tau \frac{P_2(\tau)}{\tau - \tau_n} e^{ik\tau}, \quad (158)$$

where $P_2(\tau)$ is a seventh order polynomial given by

$$\begin{aligned} P_2(\tau) \equiv & [3\rho^3 \tau (1 - ik\tau) + k^2 (1 - \rho^3 \tau^3)] \\ & \times [9 (1 - ik\tau) (1 + ik\tau) \rho^3 \tau + k^2 (1 - \rho^3 \tau^3) (3 - ik\tau)]. \end{aligned} \quad (159)$$

To evaluate the above integral, we can now apply the same strategy that we have followed above for I_{13} (for details, see Appendix A.1). We obtain that

$$J_{13}(k) = - \frac{A_- |\rho|^2 k^4}{\sqrt{18} H_0^2 M_{\text{Pl}} \rho^3} [\mathcal{J}_{13}^a(k) + \mathcal{J}_{13}^b(k) e^{-ik/k_0}], \quad (160)$$

where \mathcal{J}_{13}^a and \mathcal{J}_{13}^b can be written as

$$\mathcal{J}_{13}^a(k) = - \sum_{n=1}^3 b_n \left[d_{n0} \mathcal{E}_1(ik\tau_n) + \sum_{m=1}^7 d_{nm} (m-1)! e_{m-1}(ik\tau_n) \right], \quad (161)$$

$$\begin{aligned} \mathcal{J}_{13}^b(k) = & \sum_{n=1}^3 b_n \left[d_{n0} \mathcal{E}_1 \left(\frac{ik}{k_0} + ik\tau_n \right) \right. \\ & \left. + \sum_{m=1}^7 d_{nm} (m-1)! e_{m-1} \left(\frac{ik}{k_0} + ik\tau_n \right) \right], \end{aligned} \quad (162)$$

while the coefficients d_{nm} are given by Eqs. (A.20)–(A.27). Just as the structure of I_{13} had resembled I_2 , evidently, the form of J_{13} resembles that of J_2 . We again encounter here the issue regarding the path associated with t_2 crossing the branch cut of the exponential integral function $E_1(z)$. It is straightforward to show that the previous arguments apply for the present case as well. As a result, when $A_+/A_- > 9/8$, instead of \mathcal{J}_{13}^a above, one has

$$\begin{aligned} \mathcal{J}_{13}^a(k) = & - \sum_{n=1}^3 b_n \left[d_{n0} \mathcal{E}_1(ik\tau_n) + \sum_{m=1}^7 d_{nm} (m-1)! e_{m-1}(ik\tau_n) \right] \\ & + (2i\pi) b_2 d_{20} e^{ik\tau_2}. \end{aligned} \quad (163)$$

The above expressions for I_{13} and J_{13} then determine $\mathcal{G}_1^- + \mathcal{G}_3^-$ [cf. Eq. (140)], which in turn can be used to arrive at the corresponding $G_1^- + G_3^-$. We find that the calculation proceeds in exactly the same fashion as in the evaluation G_2^- , because, as we have already pointed out, the final expressions for the integrals I_{13} and J_{13} are very similar to that of I_2 and J_2 . As a consequence, one can write

$$\begin{aligned} k^6 [G_1^-(k) + G_3^-(k)] = & \frac{i}{32\sqrt{2\epsilon_{1-}^3(\eta_e)}} \frac{A_- |\rho|^2 H_0^2 k}{M_{\text{Pl}}^5 \rho^3} \\ & \times \left([\mathcal{I}_{13}^a(k) - \mathcal{I}_{13}^{a*}(k)] \left(\alpha_k^3 \alpha_k^{*3} - \tilde{\beta}_k^3 \tilde{\beta}_k^{*3} \right) \right. \\ & + 3 [\mathcal{J}_{13}^a(k) - \mathcal{J}_{13}^{a*}(k)] \alpha_k \alpha_k^* \tilde{\beta}_k \tilde{\beta}_k^* \left(\alpha_k \alpha_k^* - \tilde{\beta}_k \tilde{\beta}_k^* \right) \\ & + 6i \Re \left[\mathcal{K}_{13}(k) \alpha_k \tilde{\beta}_k^2 + \mathcal{K}_{13}^*(k) \alpha_k^{*2} \tilde{\beta}_k^* \right] \sin \left(\frac{k}{k_0} \right) \\ & + 6i \Im \left[\mathcal{K}_{13}(k) \alpha_k \tilde{\beta}_k^2 + \mathcal{K}_{13}^*(k) \alpha_k^{*2} \tilde{\beta}_k^* \right] \cos \left(\frac{k}{k_0} \right) \\ & - 2\Re \left\{ [3\mathcal{I}_{13}^{a*}(k) - \mathcal{J}_{13}^a(k)] \alpha_k \tilde{\beta}_k^* \right. \\ & \times \left. \left(\alpha_k^2 \alpha_k^{*2} - \tilde{\beta}_k^2 \tilde{\beta}_k^{*2} \right) \right\} \sin \left(\frac{2k}{k_0} \right) \\ & + 2i\Im \left\{ [3\mathcal{I}_{13}^{a*}(k) - \mathcal{J}_{13}^a(k)] \alpha_k \tilde{\beta}_k^* \right. \\ & \times \left. \left(\alpha_k^2 \alpha_k^{*2} - \tilde{\beta}_k^2 \tilde{\beta}_k^{*2} \right) \right\} \cos \left(\frac{2k}{k_0} \right) \\ & - 2i\Re \left[\mathcal{K}_{13}(k) \alpha_k^3 + \mathcal{K}_{13}^*(k) \tilde{\beta}_k^{*3} \right] \sin \left(\frac{3k}{k_0} \right) \\ & + 2i\Im \left[\mathcal{K}_{13}(k) \alpha_k^3 + \mathcal{K}_{13}^*(k) \tilde{\beta}_k^{*3} \right] \cos \left(\frac{3k}{k_0} \right) \\ & + 2i\Re \left\{ [3\mathcal{I}_{13}^a(k) - \mathcal{J}_{13}^a(k)] \alpha_k^{*2} \tilde{\beta}_k^2 \right. \\ & \times \left. \left(\alpha_k \alpha_k^* - \tilde{\beta}_k \tilde{\beta}_k^* \right) \right\} \sin \left(\frac{4k}{k_0} \right) \\ & + 2i\Im \left\{ [3\mathcal{I}_{13}^a(k) - \mathcal{J}_{13}^a(k)] \alpha_k^{*2} \tilde{\beta}_k^2 \right. \end{aligned}$$

$$\times \left(\alpha_k \alpha_k^* - \tilde{\beta}_k \tilde{\beta}_k^* \right) \left\} \cos \left(\frac{4k}{k_0} \right) \right), \quad (164)$$

where the coefficient \mathcal{K}_{13} has been defined to be

$$\mathcal{K}_{13} \equiv \mathcal{I}_{13}^b(k) \alpha_k^{*3} - \mathcal{I}_{13}^{b*}(k) \tilde{\beta}_k^{*3} + \alpha_k^* \tilde{\beta}_k^* \left[\mathcal{J}_{13}^{b*}(k) \tilde{\beta}_k^* - \mathcal{J}_{13}^b(k) \alpha_k^* \right]. \quad (165)$$

Obviously, in the calculation of the quantity $G_1^- + G_3^-$, the coefficient \mathcal{K}_{13} plays the same role that \mathcal{K}_2 had played in the evaluation of G_2^- . Therefore, it does not come as a surprise that the structure of \mathcal{K}_{13} is identical to that of \mathcal{K}_2 . Moreover, the expression of $G_1^- + G_3^-$ itself bears a lot of resemblance to G_2^- with, in particular, the ‘harmonics’ k/k_0 , $2k/k_0$, $3k/k_0$ and $4k/k_0$, all being present.

Let us now calculate the limiting forms of the above expression for small and large k/k_0 . As $k/k_0 \rightarrow 0$, we find that $G_1^- + G_3^-$ behaves as follows:

$$\begin{aligned} \lim_{k/k_0 \rightarrow 0} k^6 [G_1^-(k) + G_3^-(k)] &= - \frac{1}{320 \sqrt{2 \epsilon_{1-}^3(\eta_e)}} \frac{A_-^3 H_0^2}{M_{\text{Pl}}^5 A_+^2} \left(\frac{k}{k_0} \right)^2 \\ &\times \left(15 + \frac{2A_-}{A_+} + \frac{3A_-^2}{A_+^2} \right), \end{aligned} \quad (166)$$

i.e. it goes to zero quadratically for small wavenumbers. Therefore, in this limit, it is the term before the transition that dominates and, hence, the complete contribution due to the first and the third terms reduces to

$$\begin{aligned} \lim_{k/k_0 \rightarrow 0} k^6 [G_1(k) + G_3(k)] &= \lim_{k/k_0 \rightarrow 0} k^6 [G_1^+(k) + G_3^+(k)] \\ &= - \frac{1}{36 \sqrt{2 \epsilon_{1-}^3(\eta_e)}} \frac{A_-^3 H_0^2}{M_{\text{Pl}}^5 A_+^2}. \end{aligned} \quad (167)$$

In the limit $k/k_0 \rightarrow \infty$, one finds that

$$\begin{aligned} \lim_{k/k_0 \rightarrow \infty} k^6 [G_1^-(k) + G_3^-(k)] &= - \frac{1}{36 \sqrt{2 \epsilon_{1-}^3(\eta_e)}} \frac{A_- H_0^2}{M_{\text{Pl}}^5} \left\{ 1 \right. \\ &+ \frac{27 \Delta A}{8 A_-} \cos \left(\frac{k}{k_0} \right) - \frac{36 A_+}{48 A_-} \frac{k}{k_0} \sin \left(\frac{3k}{k_0} \right) \\ &+ \frac{1}{8} \left[\frac{\Delta A}{A_-} \left(50 + 27 \frac{\Delta A}{A_+} \right) - 8 - 27 \frac{\Delta A}{A_+} \right] \\ &\left. \times \cos \left(\frac{3k}{k_0} \right) \right\}. \end{aligned} \quad (168)$$

As usual, only trigonometric functions with the argument $3k/k_0$ remain in the final expression of the limit. Also, note that the coefficient of the $\sin(3k/k_0)$ term diverges linearly at large k , exactly as the contribution before the transition had [cf. Eq. (139)], albeit with an opposite sign. Hence, the complete contribution remains finite and, we find that, in the limit $k/k_0 \rightarrow \infty$, $G_1 + G_3$ goes to

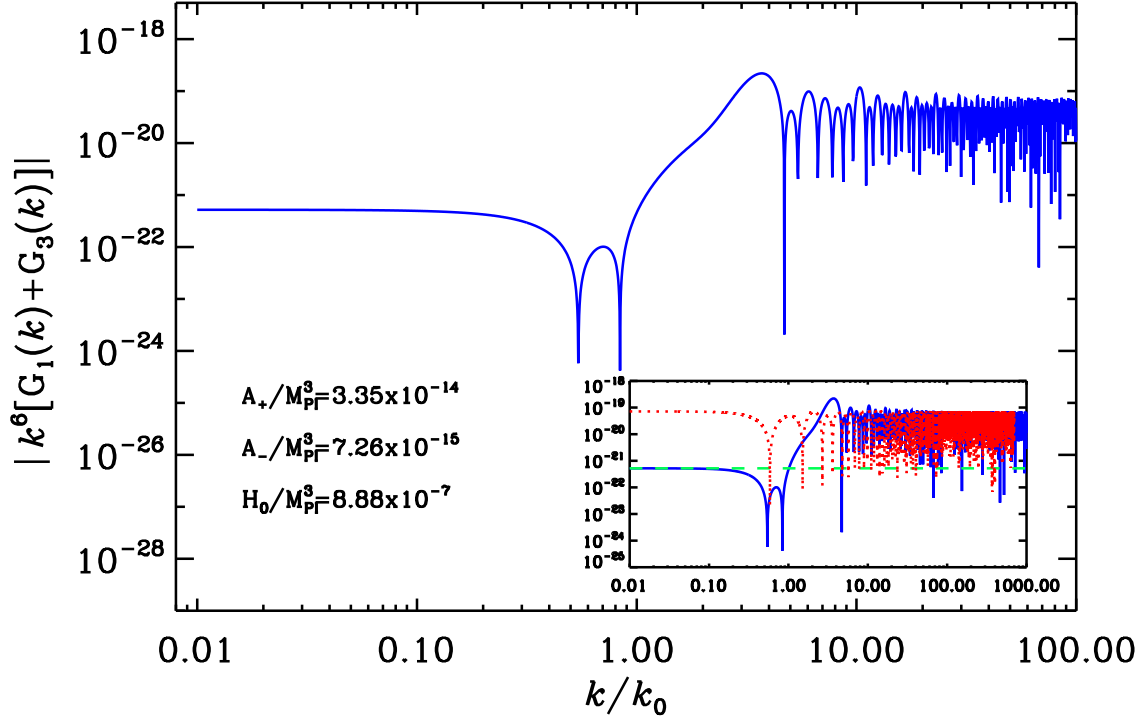


Figure 8. The absolute value of the quantity $k^6 (G_1 + G_3)$ has been plotted as a function of k/k_0 (the blue curve). We have again worked with the same values of the parameters as in the earlier figures. As in the plots before, the green and the red curves in the inset denote the asymptotic forms.

$$\begin{aligned}
 \lim_{k/k_0 \rightarrow \infty} k^6 [G_1(k) + G_3(k)] = & -\frac{1}{36 \sqrt{2 \epsilon_{1-}^3(\eta_e)}} \frac{A_- H_0^2}{M_{\text{Pl}}^5} \left(1 + \left(-1 \right. \right. \\
 & - \frac{27}{8} \left(\frac{A_-}{A_+} - 1 \right) + \left(1 - \frac{A_+}{A_-} \right) \left[\frac{50}{8} \right. \\
 & \left. \left. + \frac{27}{8} \left(\frac{A_-}{A_+} - 1 \right) \right] + \frac{A_+}{A_-} \left(\frac{35}{8} - \frac{27}{8} \frac{A_-}{A_+} \right) \right) \\
 & \times \cos \left(\frac{3k}{k_0} \right), \tag{169}
 \end{aligned}$$

As before, at large wavenumbers, we obtain a scale invariant amplitude which is modulated by super-imposed oscillations of the form $\cos(3k/k_0)$. In Fig. 8, we have plotted the absolute value of the quantity $[k^6 (G_1 + G_3)]$. The figure clearly reflects the limiting forms that we have obtained above.

5.3. The contribution due to the fifth and the sixth terms

Let us now turn to the evaluation of the contribution due to the remaining two terms in the interaction Hamiltonian (67), viz. the fifth and the sixth. As in the case of \mathcal{G}_1 and \mathcal{G}_3 , we find that, the terms \mathcal{G}_5 and \mathcal{G}_6 too contain the same types of integrals. Hence, in the equilateral limit, they can be evaluated together.

5.3.1. Before the transition Since ϵ_1 is a constant before the transition, the integrals encountered in \mathcal{G}_5 and \mathcal{G}_6 prove to be exactly of the same form as in the cases of \mathcal{G}_1 and \mathcal{G}_3 . Therefore, they can be evaluated in the same fashion and, in the most generic situation of $\mathbf{k}_1 \neq \mathbf{k}_2 \neq \mathbf{k}_3$, one obtains that

$$\begin{aligned} \mathcal{G}_5^+(\mathbf{k}_1, \mathbf{k}_2, \mathbf{k}_3) &= \frac{iH_0}{16M_{\text{Pl}}^3 k_T} \sqrt{\frac{\epsilon_{1+}^3}{(k_1 k_2 k_3)^3}} e^{-ik_T/k_0} \left[(\mathbf{k}_1 \cdot \mathbf{k}_2) k_3^2 \right. \\ &\quad \left. \times \left(1 + \frac{k_1}{k_T} + \frac{i k_1}{k_0} \right) + \text{five permutations} \right] \end{aligned} \quad (170)$$

and

$$\begin{aligned} \mathcal{G}_6^+(\mathbf{k}_1, \mathbf{k}_2, \mathbf{k}_3) &= \frac{iH_0}{16M_{\text{Pl}}^3 k_T} \sqrt{\frac{\epsilon_{1+}^3}{(k_1 k_2 k_3)^3}} e^{-ik_T/k_0} \left[k_1^2 (\mathbf{k}_2 \cdot \mathbf{k}_3) \right. \\ &\quad \left. \times \left(1 + \frac{k_1}{k_T} + \frac{i k_1}{k_0} \right) + \text{two permutations} \right]. \end{aligned} \quad (171)$$

In the equilateral limit, we find that

$$\begin{aligned} \mathcal{G}_5^+(k) + \mathcal{G}_6^+(k) &= \frac{3 i H_0 k^3}{16 M_{\text{Pl}}^3} \sqrt{\frac{\epsilon_{1+}^3}{k^9}} \left(\frac{4}{3} + \frac{i k}{k_0} \right) e^{-3 i k/k_0} \\ &= -\frac{3 \epsilon_{1+}}{4} [\mathcal{G}_1^+(k) + \mathcal{G}_3^+(k)]. \end{aligned} \quad (172)$$

From the last equality, we can then immediately conclude that $G_5^+(k) + G_6^+(k) = -3 \epsilon_{1+} [G_1^+(k) + G_3^+(k)] / 4$. As a consequence, the asymptotic behavior of $G_5^+ + G_6^+$ can be arrived at from the forms of $G_1^+ + G_3^+$ we had obtained earlier. As $k/k_0 \rightarrow 0$, one has

$$\begin{aligned} \lim_{k/k_0 \rightarrow 0} k^6 [G_5^+(k) + G_6^+(k)] &= \frac{\epsilon_{1+}}{48 \sqrt{2 \epsilon_{1-}^3(\eta_e)}} \frac{A_-^3 H_0^2}{M_{\text{Pl}}^5 A_+^2} \\ &= \frac{1}{864 \sqrt{2 \epsilon_{1-}^3(\eta_e)}} \frac{A_-^3}{M_{\text{Pl}}^7 H_0^2}, \end{aligned} \quad (173)$$

while, as $k/k_0 \rightarrow \infty$, one obtains

$$\begin{aligned} \lim_{k/k_0 \rightarrow \infty} k^6 [G_5^+(k) + G_6^+(k)] &= \frac{1}{1152 \sqrt{2 \epsilon_{1-}^3(\eta_e)}} \frac{A_+^3}{M_{\text{Pl}}^7 H_0^2} \\ &\quad \times \left[\frac{9}{2} \left(1 - \frac{A_-}{A_+} \right) \cos \left(\frac{k}{k_0} \right) \right. \\ &\quad \left. + \frac{k}{k_0} \sin \left(\frac{3k}{k_0} \right) \right] \end{aligned}$$

$$+ \left(\frac{35}{6} - \frac{9 A_-}{2 A_+} \right) \cos \left(\frac{3 k}{k_0} \right) \Big]. \quad (174)$$

Note that, while $k^6 (G_5^+ + G_6^+)$ goes to a constant at small k/k_0 , it diverges linearly (modulated by oscillations) at large k/k_0 , as in the case of $k^6 (G_1^+ + G_3^+)$. Also, as we shall illustrate, just as in the earlier cases, the diverging term will be exactly canceled by a corresponding term that arises post-transition.

5.3.2. After the transition The next step is to perform the calculation after the transition. The calculation proceeds exactly as in the case of $\mathcal{G}_1^- + \mathcal{G}_3^-$. We find that, we can write

$$\begin{aligned} \mathcal{G}_5^-(k) + \mathcal{G}_6^-(k) = & - \frac{9 H_0}{16 M_{\text{Pl}}^3 k^{9/2}} \left[\alpha_k^{*3} I_{56}(k) - \beta_k^{*3} I_{56}^*(k) - \alpha_k^{*2} \beta_k^* J_{56}(k) \right. \\ & \left. + \alpha_k^* \beta_k^{*2} J_{56}^*(k) \right], \end{aligned} \quad (175)$$

where I_{56} and J_{56} are described by the integrals

$$\begin{aligned} I_{56}(k) = & \frac{A_-^3}{54 \sqrt{2} H_0^6 M_{\text{Pl}}^3} \int_{-k_0^{-1}}^{\eta_e} d\tau (1 - \rho^3 \tau^3) (1 - i k \tau) \\ & \times [3 \rho^3 \tau (1 - i k \tau) + k^2 (1 - \rho^3 \tau^3)]^2 e^{3 i k \tau}, \end{aligned} \quad (176)$$

$$\begin{aligned} J_{56}(k) = & \frac{A_-^3}{54 \sqrt{2} H_0^6 M_{\text{Pl}}^3} \int_{-k_0^{-1}}^{\eta_e} d\tau (1 - \rho^3 \tau^3) [3 \rho^3 \tau (1 - i k \tau) \\ & + k^2 (1 - \rho^3 \tau^3)] \left[9 (1 - i k \tau) (1 + i k \tau) \rho^3 \tau \right. \\ & \left. + k^2 (1 - \rho^3 \tau^3) (3 - i k \tau) \right] e^{i k \tau}. \end{aligned} \quad (177)$$

These integrals are very similar to the ones considered before but, crucially, they do not contain any poles. This makes their explicit calculation considerably easier. Upon following the same strategy that we had adopted in the cases of I_{13} and J_{13} , one obtains that

$$I_{56}(k) = \frac{A_-^3 k^3}{54 \sqrt{2} H_0^6 M_{\text{Pl}}^3} [\mathcal{I}_{56}^a(k) + \mathcal{I}_{56}^b(k) e^{-3 i k/k_0}]. \quad (178)$$

with

$$\mathcal{I}_{56}^a(k) = - \sum_{n=0}^{10} \left(\frac{i}{3} \right)^{n+1} n! f_n, \quad (179)$$

$$\mathcal{I}_{56}^b(k) = \sum_{n=0}^{10} \left(\frac{i}{3} \right)^{n+1} n! f_n e_n \left(\frac{3 i k}{k_0} \right), \quad (180)$$

where the coefficients f_n are given by Eqs. (A.30)–(A.40), while $e_n(z)$ is the exponential sum function (A.14). Similarly, we find that J_{56} can be obtained to be

$$J_{56}(k) = \frac{A_-^3 k^3}{54 \sqrt{2} H_0^6 M_{\text{Pl}}^3} [\mathcal{J}_{56}^a(k) + \mathcal{J}_{56}^b(k) e^{-i k/k_0}] \quad (181)$$

with

$$\mathcal{J}_{56}^a(k) = - \sum_{n=0}^{10} i^{n+1} n! g_n, \quad (182)$$

$$\mathcal{J}_{56}^b(k) = \sum_{n=0}^{10} i^{n+1} n! g_n e_n \left(\frac{i k}{k_0} \right), \quad (183)$$

and the coefficients g_n being given by Eqs. (A.41)–(A.51).

At this stage, the calculation of $G_5^- + G_6^-$ progresses as before and the final expression reads

$$\begin{aligned} k^6 [G_5^-(k) + G_6^-(k)] &= \frac{i}{768 \sqrt{2\epsilon_{1-}^3(\eta_e)}} \frac{A_-^3}{M_{\text{Pl}}^7 H_0^2} \\ &\times \left([\mathcal{I}_{56}^a(k) - \mathcal{I}_{56}^{a*}(k)] \left(\alpha_k^3 \alpha_k^{*3} - \tilde{\beta}_k^3 \tilde{\beta}_k^{*3} \right) \right. \\ &+ 3 [\mathcal{J}_{56}^a(k) - \mathcal{J}_{56}^{a*}(k)] \alpha_k \alpha_k^* \tilde{\beta}_k \tilde{\beta}_k^* \left(\alpha_k \alpha_k^* - \tilde{\beta}_k \tilde{\beta}_k^* \right) \\ &+ 6 i \Re \left[\mathcal{K}_{56}(k) \alpha_k \tilde{\beta}_k^2 + \mathcal{K}_{56}^*(k) \alpha_k^{*2} \tilde{\beta}_k^* \right] \sin \left(\frac{k}{k_0} \right) \\ &+ 6 i \Im \left[\mathcal{K}_{56}(k) \alpha_k \tilde{\beta}_k^2 + \mathcal{K}_{56}^*(k) \alpha_k^{*2} \tilde{\beta}_k^* \right] \cos \left(\frac{k}{k_0} \right) \\ &- 2 i \Re \left\{ [3 \mathcal{I}_{56}^{a*}(k) - \mathcal{J}_{56}^a(k)] \right. \\ &\quad \times \alpha_k \tilde{\beta}_k^* \left(\alpha_k^2 \alpha_k^{*2} - \tilde{\beta}_k^2 \tilde{\beta}_k^{*2} \right) \left. \right\} \sin \left(\frac{2k}{k_0} \right) \\ &+ 2 i \Im \left\{ [3 \mathcal{I}_{56}^{a*}(k) - \mathcal{J}_{56}^a(k)] \right. \\ &\quad \times \alpha_k \tilde{\beta}_k^* \left(\alpha_k^2 \alpha_k^{*2} - \tilde{\beta}_k^2 \tilde{\beta}_k^{*2} \right) \left. \right\} \cos \left(\frac{2k}{k_0} \right) \\ &- 2 i \Re \left[\mathcal{K}_{56}(k) \alpha_k^3 + \mathcal{K}_{56}^*(k) \tilde{\beta}_k^{*3} \right] \sin \left(\frac{3k}{k_0} \right) \\ &+ 2 i \Im \left[\mathcal{K}_{56}(k) \alpha_k^3 + \mathcal{K}_{56}^*(k) \tilde{\beta}_k^{*3} \right] \cos \left(\frac{3k}{k_0} \right) \\ &+ 2 i \Re \left\{ [3 \mathcal{I}_{56}^a(k) - \mathcal{J}_{56}^a(k)] \alpha_k^{*2} \tilde{\beta}_k^2 \left(\alpha_k \alpha_k^* - \tilde{\beta}_k \tilde{\beta}_k^* \right) \right\} \\ &\quad \times \sin \left(\frac{4k}{k_0} \right) \\ &+ 2 i \Im \left\{ [3 \mathcal{I}_{56}^a(k) - \mathcal{J}_{56}^a(k)] \alpha_k^{*2} \tilde{\beta}_k^2 \left(\alpha_k \alpha_k^* - \tilde{\beta}_k \tilde{\beta}_k^* \right) \right\} \\ &\quad \times \cos \left(\frac{4k}{k_0} \right) \left. \right), \quad (184) \end{aligned}$$

where the coefficient \mathcal{K}_{56} has been defined to be

$$\mathcal{K}_{56}(k) = \mathcal{I}_{56}^b(k) \alpha_k^{*3} - \mathcal{I}_{56}^{b*}(k) \tilde{\beta}_k^{*3} + \alpha_k^* \tilde{\beta}_k^* \left[\mathcal{J}_{56}^{b*}(k) \tilde{\beta}_k^* - \mathcal{J}_{56}^b(k) \alpha_k^* \right]. \quad (185)$$

Needless to add, the coefficient \mathcal{K}_{56} is similar to \mathcal{K}_2 and \mathcal{K}_{13} . Further, as far as the structure of $G_5^- + G_6^-$ is concerned, it again involves the various trigonometric functions

that we had observed in the earlier cases.

Let us now evaluate the asymptotic forms of the above expression. As $k/k_0 \rightarrow 0$, we find that

$$\begin{aligned} \lim_{k/k_0 \rightarrow 0} k^6 [G_5^-(k) + G_6^-(k)] &= \frac{1}{887040 \sqrt{2 \epsilon_{1-}^3(\eta_e)}} \frac{A_-^3}{H_0^2 M_{\text{Pl}}^7} \left(\frac{k}{k_0} \right)^2 \\ &\times \left(550 + \frac{600 A_-}{A_+} + \frac{675 A_-^2}{A_+^2} + \frac{194 A_-^3}{A_+^3} \right. \\ &\left. + \frac{291 A_-^4}{A_+^4} \right). \end{aligned} \quad (186)$$

In other words, this term vanishes quadratically for small wavenumbers, just as the contributions due to the first and the third terms, post-transition, had. So, in this limit, the total contribution due to the fifth and the sixth terms reduces to the strictly scale invariant value arising before the transition, i.e. we have

$$\begin{aligned} \lim_{k/k_0 \rightarrow 0} k^6 [G_5(k) + G_6(k)] &= \lim_{k/k_0 \rightarrow 0} k^6 [G_5^+(k) + G_6^+(k)] \\ &= \frac{1}{864 \sqrt{2 \epsilon_{1-}^3(\eta_e)}} \frac{A_-^3}{M_{\text{Pl}}^7 H_0^2}. \end{aligned} \quad (187)$$

In the limit $k/k_0 \rightarrow \infty$, we find that

$$\begin{aligned} \lim_{k/k_0 \rightarrow \infty} k^6 [G_5^-(k) + G_6^-(k)] &= \frac{1}{864 \sqrt{2 \epsilon_{1-}^3(\eta_e)}} \frac{A_-^3}{M_{\text{Pl}}^7 H_0^2} \left[1 \right. \\ &- \frac{27 A_+^3}{8 A_-^3} \left(1 - \frac{A_-}{A_+} \right) \cos \left(\frac{k}{k_0} \right) \\ &- \frac{3 A_+^3}{4 A_-^3} \frac{k}{k_0} \sin \left(\frac{3k}{k_0} \right) \\ &\left. - \frac{A_+^3}{8 A_-^3} \left(35 - \frac{27 A_-}{A_+} \right) \cos \left(\frac{3k}{k_0} \right) \right]. \end{aligned} \quad (188)$$

If we now combine the asymptotic forms before and after the transition, for large k/k_0 , we find that the terms proportional to k/k_0 cancel, and one is led to the expression

$$\lim_{k/k_0 \rightarrow \infty} k^6 [G_5(k) + G_6(k)] = \frac{1}{864 \sqrt{2 \epsilon_{1-}^3(\eta_e)}} \frac{A_-^3}{M_{\text{Pl}}^7 H_0^2}, \quad (189)$$

which is exactly the same as the scale invariant quantity that we had encountered in the limit of small k/k_0 . In particular, it is interesting to note that, in this case, no superimposed oscillations are present. These asymptotic behavior are evident in Fig. 9, wherein we have plotted the absolute value of $k^6 (G_5 + G_6)$.

5.4. The contribution due to the field redefinition

Let us now turn to the contribution G_7 due to the field redefinition (79) which in the equilateral limit simplifies to

$$G_7(k) = \frac{3 \epsilon_{2-}(\eta_e)}{2} |f_k^-(\eta_e)|^4 = 6 \epsilon_{1-}(\eta_e) |f_k^-(\eta_e)|^4, \quad (190)$$

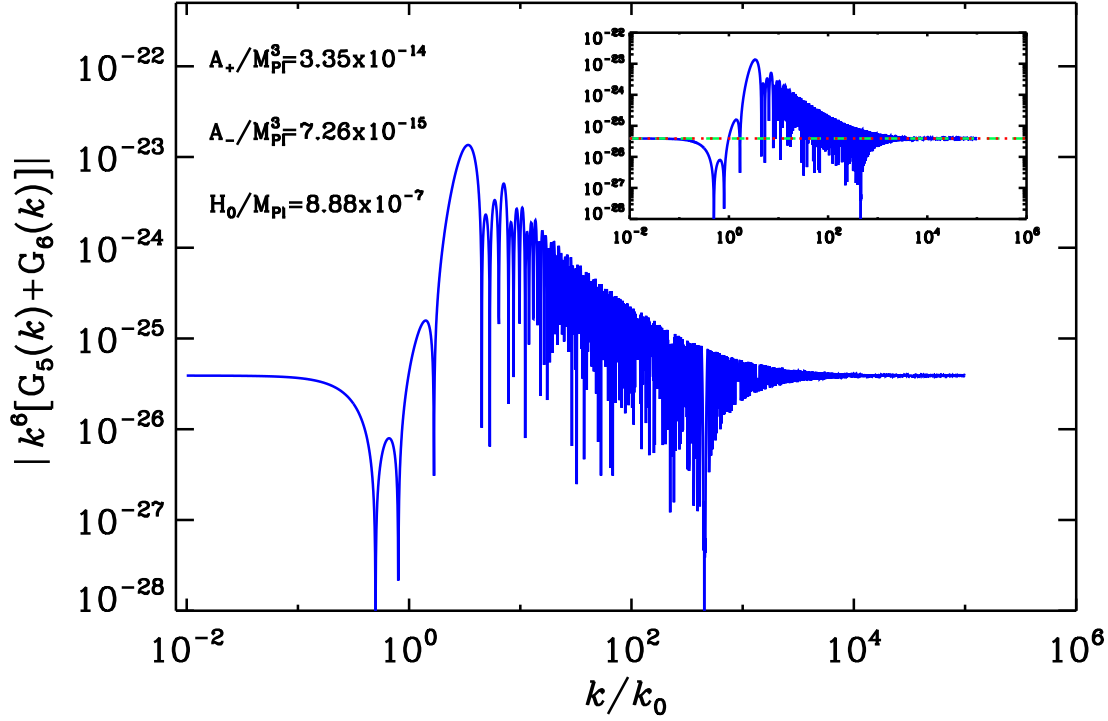


Figure 9. The absolute value of the quantity $k^6 (G_5 + G_6)$ (in blue) and the asymptotic behavior (in green and in red in the inset) has been plotted for the same set of parameters as in the previous figures. The inset highlights the fact that the quantity goes to the same scale invariant value at small and large wavenumbers.

where the last equality follows from the fact that, at late times, for the linear potential of our interest, $\epsilon_{2-} = 4\epsilon_{1-}$. Upon using the expression (99) for f_k^- at late times, we obtain that

$$k^6 G_7(k) = \frac{3 H_0^4}{8 M_{\text{Pl}}^4 \epsilon_{1-}(\eta_e)} |\alpha_k - \beta_k|^4. \quad (191)$$

Using the expressions (37) and (38) for α_k and β_k , we find that, we can write

$$\begin{aligned} k^6 G_7(k) = \frac{3 H_0^4}{8 M_{\text{Pl}}^4 \epsilon_{1-}(\eta_e)} & \left\{ \left(\alpha_k \alpha_k^* + \tilde{\beta}_k \tilde{\beta}_k^* \right)^2 + 2 \alpha_k \alpha_k^* \tilde{\beta}_k \tilde{\beta}_k^* \right. \\ & - 4 \Im \left[\left(\alpha_k \alpha_k^* + \tilde{\beta}_k \tilde{\beta}_k^* \right) \left(\alpha_k \tilde{\beta}_k^* \right) \right] \sin \left(\frac{2k}{k_0} \right) \\ & - 4 \Re \left[\left(\alpha_k \alpha_k^* + \tilde{\beta}_k \tilde{\beta}_k^* \right) \left(\alpha_k \tilde{\beta}_k^* \right) \right] \cos \left(\frac{2k}{k_0} \right) \\ & \left. + 2 \Im \left(\alpha_k^2 \tilde{\beta}_k^{*2} \right) \sin \left(\frac{4k}{k_0} \right) + 2 \Re \left(\alpha_k^2 \tilde{\beta}_k^{*2} \right) \cos \left(\frac{4k}{k_0} \right) \right\}. \quad (192) \end{aligned}$$

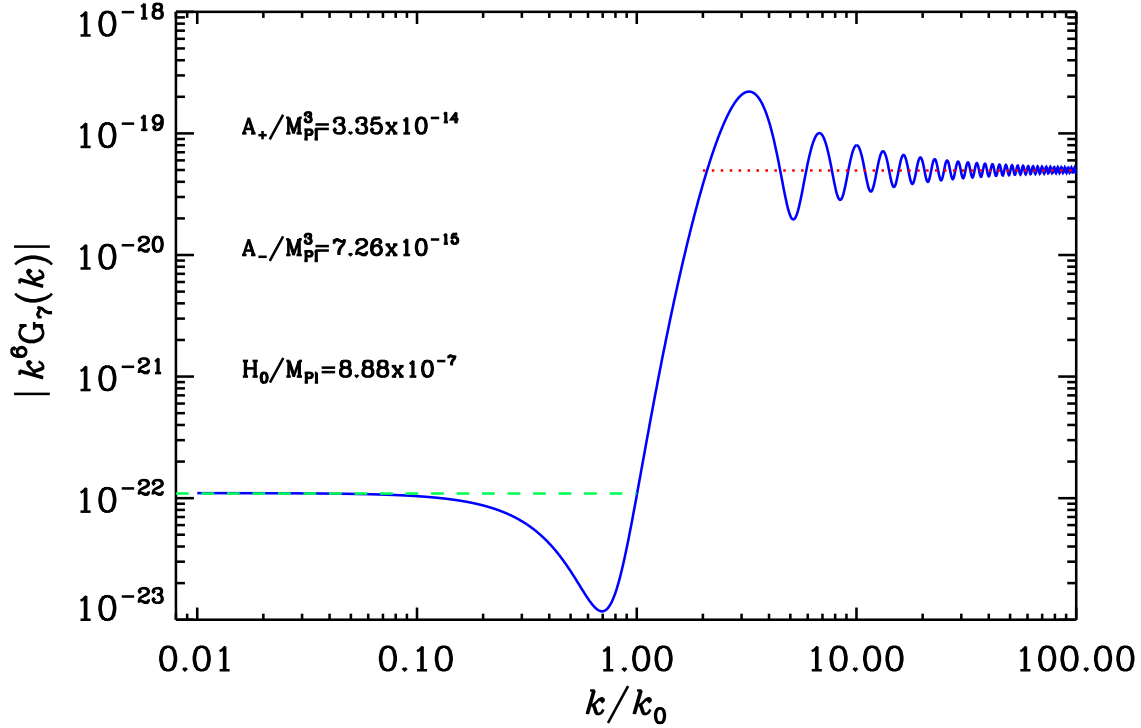


Figure 10. The absolute value of the quantity $k^6 G_7$ (in blue) and its asymptotic forms (in green and in red) have been plotted for the same set of parameters as in the previous figures.

Far away from the characteristic scale k_0 , this quantity turns strictly scale invariant, just as the power spectrum does. Its asymptotic forms are found to be

$$\lim_{k/k_0 \rightarrow 0} k^6 G_7(k) = \frac{3 A_-^4 H_0^4}{8 A_+^4 M_{\text{Pl}}^4 \epsilon_{1-}(\eta_e)} = \frac{27 A_-^2 H_0^8}{4 A_+^4 M_{\text{Pl}}^2} \quad (193)$$

and

$$\lim_{k/k_0 \rightarrow \infty} k^6 G_7(k) = \frac{3 H_0^4}{8 M_{\text{Pl}}^4 \epsilon_{1-}(\eta_e)} = \frac{27 H_0^8}{4 A_-^2 M_{\text{Pl}}^2}. \quad (194)$$

In Fig. 10, we have plotted the absolute value of the above expression for $k^6 G_7$. The figure clearly illustrates that the quantity turns scale invariant asymptotically.

This concludes our calculation of the complete bi-spectrum. With all the expressions at our disposal, we can now relate these results to the observable parameter f_{NL} , and also discuss the various possible conclusions and implications.

6. f_{NL} in the Starobinsky model

In this section, we shall discuss two issues. We shall firstly focus on whether the Starobinsky model can lead to as large a value for the non-Gaussianity parameter f_{NL} as

the currently quoted mean values. Recall that, as we had mentioned in the introduction, the recent CMB data constrains the parameter to be $f_{\text{NL}} = 32 \pm 21$ in the local limit. However, at this stage, it is important to stress that the local non-Gaussianity parameter is a priori different from a scale dependent f_{NL} in the equilateral case. In fact, the relevance of the constraints on the local parameter to the $f_{\text{NL}}^{\text{eq}}$ that we obtain below is not entirely clear. This point needs to be borne in mind when we compare the f_{NL} in the equilateral limit with the observational constraints quoted above. Then, in the second part of this section, we shall focus on an issue related to the hierarchy of the various contributions to the bi-spectrum.

6.1. Can $f_{\text{NL}}^{\text{eq}}$ be large in the Starobinsky model?

Let us now discuss as to how large can the non-Gaussianity parameter $f_{\text{NL}}^{\text{eq}}$ be in the Starobinsky model. Since it is the fourth term that seems to often provide the dominant contribution to the bi-spectrum (in this context, however, see, the following sub-section), the quantity $f_{\text{NL}}^{\text{eq}}$ can be evaluated based on this contribution. On substituting the expression (100) for $k^6 G_4$ in the definition (84) of f_{NL} in the equilateral limit, we obtain that

$$f_{\text{NL}}^{\text{eq}(4)} = -\frac{10}{9} \frac{81}{8(2\pi)^4 \sqrt{2\epsilon_{1-}^3(\eta_e)}} \left(\frac{k_0}{k}\right)^3 \frac{\Delta A H_0^6}{A_-^2 M_{\text{Pl}}^3} [\mathcal{P}_s(k)]^{-2} \\ \times \left[\mathcal{A}_1(k) \sin\left(\frac{k}{k_0}\right) + \mathcal{A}_2(k) \cos\left(\frac{k}{k_0}\right) + \mathcal{A}_3(k) \sin\left(\frac{3k}{k_0}\right) \right. \\ \left. + \mathcal{A}_4(k) \cos\left(\frac{3k}{k_0}\right) \right], \quad (195)$$

with the power spectrum \mathcal{P}_s being given by Eq. (39), whereas the coefficients \mathcal{A}_1 – \mathcal{A}_4 are given by Eqs. (101)–(104). Let us now consider the various qualitative aspects of this result^{||}. It is important to notice that, as already remarked in the section devoted to the calculation of G_4 , f_{NL} is not simply given by an expression proportional to $\sin(3k/k_0 + \varphi_0)$, φ_0 being a phase (in this context, see, Ref. [28]), but contains four different terms that oscillate with different frequencies. It is only in the limit $k/k_0 \rightarrow \infty$ that a simple behavior as the one previously mentioned is recovered. Moreover, interestingly, we find that the expression for $f_{\text{NL}}^{\text{eq}(4)}$ above depends on the slopes A_+ and A_- of the potential only through the ratio $R \equiv A_-/A_+$, and it does not depend on the parameter H_0 at all. As should be clear by now, both the power spectrum and the bi-spectrum [or, equivalently, $G_n(k)$] exhibit a step in the Starobinsky model. Note that, in all the earlier figures, we had worked with the parameters A_+ and A_- such that $R = 0.216 < 1$. As is obvious from the figures, the step always rises towards the larger wavenumbers in such a case. In contrast, one finds that the step in the power

^{||} As we were completing this manuscript, a preprint appeared, which deals with a similar but different model, and also evaluates the non-Gaussianities analytically [36]. We should emphasize that our effort is more complete, as we evaluate the complete bi-spectrum rather than just focus on the dominant contribution.

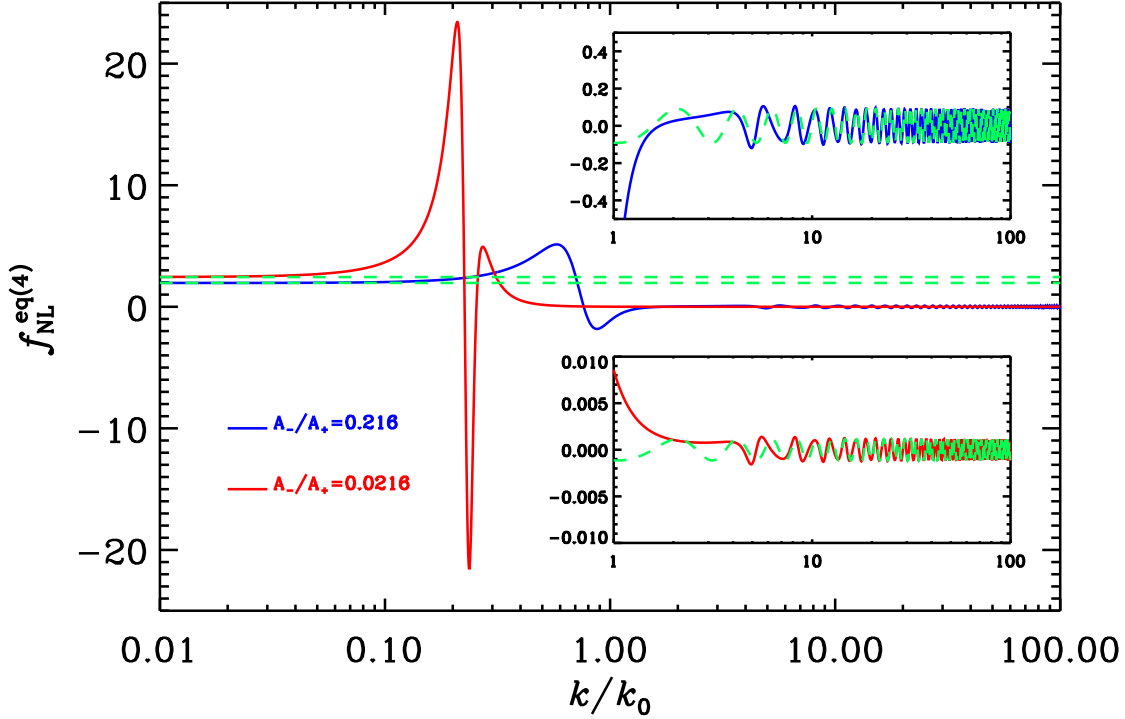


Figure 11. The non-Gaussianity parameter in the equilateral limit, i.e. $f_{\text{NL}}^{\text{eq}}$, due to the dominant term in the Starobinsky model. The blue curve corresponds to the values of the parameters that we had considered in the previous figures. The red curve corresponds a larger A_+ (we have set $A_+/M_{\text{Pl}}^3 = 3.35 \times 10^{-13}$), but with the remaining parameters being the same as for the blue curve. The dashed green lines represent the corresponding asymptotic values for small k/k_0 [given by Eq. (196)]. The insets exhibit the oscillations about zero, with the dashed green curves highlighting the behavior at large k/k_0 .

spectrum and the bi-spectrum reverse direction when $R > 1$, with the lower level of the step being located at large wavenumbers. The height of the step depends on the extent of the difference in the slopes of the potential on either side of the discontinuity. The further is R from unity, the larger proves to be height of the step. This property becomes explicit in the limit $k/k_0 \rightarrow 0$ wherein the dominant contribution to f_{NL} due to the term G_4 has the following simple form:

$$\lim_{k/k_0 \rightarrow 0} f_{\text{NL}}^{\text{eq}(4)} = \frac{5}{2} (1 - R). \quad (196)$$

In Fig. 11, we have plotted the expression (195) for $f_{\text{NL}}^{\text{eq}(4)}$ for two different values of the ratio of the slopes of the potential. And, Fig. 12 contains a two-dimensional contour plot $f_{\text{NL}}^{\text{eq}(4)}$ in the plane of R and k/k_0 . It is clear from these figures that, in the Starobinsky model, the non-Gaussianity parameter $f_{\text{NL}}^{\text{eq}}$ can be as large as the currently indicated mean value.

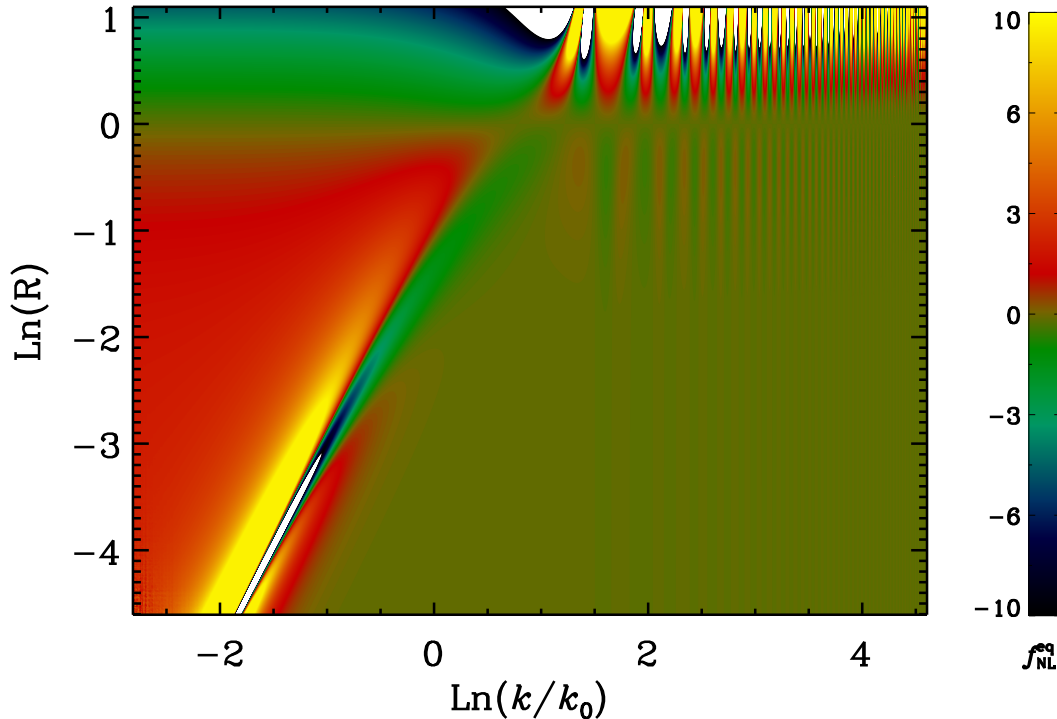


Figure 12. A two-dimensional contour plot of the non-Gaussianity parameter $f_{\text{NL}}^{\text{eq}}$ due to the dominant term in the Starobinsky model, plotted in the plane of k/k_0 and $R = A_-/A_+$. The white contours indicate regions wherein $f_{\text{NL}}^{\text{eq}}$ can be as large as 50. Note that, provided R is reasonably small, $f_{\text{NL}}^{\text{eq}}$ can be of the order of 25 or so, as is indicated by the currently observed mean value.

But, the question that immediately springs mind is whether $f_{\text{NL}}^{\text{eq}}$ can be large for values of the parameters of the Starobinsky model for which the power spectrum proves to be consistent with the data. In plotting all the figures, we have ensured that the parameters that we have been working with lead to the COBE normalization of the power spectrum at suitably small scales. Given a H_0 , COBE normalization restricts the parameter A_- to a fixed value [cf. Eq. (41)], while leaving the parameter A_+ or, equivalently, R , unconstrained. Though the actual power spectrum that arises in the Starobinsky model in itself has not been compared with the CMB data, comparisons of some variations thereof have been carried out. These variations have essentially involved introducing, by hand, an overall multiplicative factor to incorporate a suitable spectral tilt or a sharp cut-off at the lower wavenumbers (see the fourth reference in Refs. [8]). While the tilt ensures a good fit to the data at the higher multipoles, a sharp cut-off can improve the fit to the outliers at the lower multipoles that we had discussed in some detail in the introductory section. One finds that, in the presence of a suitable spectral tilt, the best fit value of R proves to be about $0.73^{+0.25}_{-0.14}$ (see the fourth reference in Refs. [8]; also, according to the article, the best fit value for k_0 is

$k_0 \simeq 3.1_{-2.8}^{+5.8} \times 10^{-4} \text{ Mpc}^{-1}$) and, therefore, the domain $R < 1$ is favored by the data. This implies that $R = 0.216$ is about 3.6σ from the mean value, whereas $R = 0.00216$ is further away, being at 5.21σ , from the mean value. Clearly, had these results been obtained for the exact case of the Starobinsky model (i.e. in the absence of the overall tilt that has been introduced by hand), low values of R , such as $R = 0.00216$, would be ruled out. In summary, as is evident from Fig. 11, the Starobinsky model can result in a power spectrum that remains reasonably consistent with the data while at the same time lead to an f_{NL} that is as large as a few, at most $\simeq \mathcal{O}(10)$. Indeed, it would be interesting to strengthen such a conclusion by carrying out an explicit comparison of the power spectrum in the Starobinsky model with the data and also studying the exact implications of an oscillatory, scale dependent, f_{NL} for the non-Gaussianities in the CMB.

Though the Starobinsky model, with parameters that are consistent with the data, in itself, may not lead to a large f_{NL} , we believe that the Starobinsky model with a much smaller R , and hence a rather large f_{NL} can be considered to effectively capture certain aspects of other models that are known to lead to a better fit to the data than the conventional, power law, primordial spectrum. An example of such a model would be the punctuated inflationary scenario [10]. In punctuated inflation, a step in the power spectrum arises exactly as in the Starobinsky model with $R < 1$. However, the step turns out to be sharper (than in the case of the best fit value of $R \simeq 0.73$), and the oscillations at the higher level of the step, before the spectrum turns scale invariant, are fewer. The Starobinsky model with a much smaller R can broadly be considered to mimic the sharper step that arises in punctuated inflation. Therefore, if one naively extends the results of the Starobinsky model to punctuated inflation, it suggests that there can exist scenarios which lead to a sharp step in the power spectrum (along with certain characteristic oscillations), an improved fit to the data as well as a reasonably large f_{NL} .

6.2. The hierarchy of contributions to the bi-spectrum

As we have argued before, prior experience suggests that, when departures from the slow roll arise, it is the fourth term in the interaction Hamiltonian (67) that leads to the most significant contribution to the bi-spectrum. However, such a conclusion has largely been based on numerical analysis, which typically involves working with specific values (or, at the most, a limited range of values) for the parameters of the model concerned. Since we have been able to arrive at analytic expressions for all the different contributions to the bi-spectrum for the Starobinsky model, it is interesting to investigate whether such a conclusion indeed applies for a wide range of the parameters of the model or if there exist certain values of the parameters for which other terms can possibly contribute as much as or even more than the fourth term.

Let us quickly recall some essential properties of the various contributions to the bi-spectrum, arising out of the interaction Hamiltonian and the field redefinition. While

the contributions due to the first, the second and the third terms in the interaction Hamiltonian involve ϵ_1^2 , the fourth term contains $\epsilon_1 \epsilon_2'$, whereas the fifth and the sixth terms depend on ϵ_1^3 [cf. Eqs. (73)–(78)]. Also, note that, apart from the difference in the dependence on the slow roll parameter ϵ_1 , the first, the third, the fifth and the sixth terms depend on the curvature perturbation and its derivative in the same fashion, viz. they depend linearly on the curvature perturbation and quadratically on its derivative. In contrast, the second term does not depend on the derivative of the curvature perturbation at all, while the fourth term depends linearly on the derivative and quadratically on the curvature perturbation itself. Further, the additional seventh term arising due to the field redefinition depends on the late time behavior of ϵ_2 and the fourth power of the curvature perturbation. In a slow roll inflationary scenario, one can anticipate that the first, the second, the third and the seventh terms lead to contributions of similar magnitudes to the bi-spectrum, while the contributions due to the fourth, the fifth and the sixth terms can be expected to be suitably suppressed in amplitude due to the presence of the additional slow roll parameter. In fact, these expectations are broadly corroborated by the results obtained [24, 27].

When there arise deviations from slow roll, as we have repeatedly mentioned, it is the fourth term that is expected to dominate, with the first, the second, the third and the seventh terms proving to be of roughly similar order, but smaller in amplitude than the fourth term. The contributions of the fifth and the sixth terms can be expected to be further smaller in amplitude. These expectations are confirmed by Fig. 13, wherein we have plotted the absolute values of all the contributions to the bi-spectrum in the equilateral limit that we have focused on. It is worth pointing out here that the slightly higher amplitude of the second term in contrast to the contributions due to the first and the third terms can be attributed to the fact that the second term does not involve any derivative of the curvature perturbation. We shall return to this point a little later in our discussion.

Since the hierarchy of the different contributions changes as one moves from the slow roll to a fast roll regime, it is interesting to identify the domain where the hierarchy shifts in the Starobinsky model. Recall that, a crucial assumption of the Starobinsky model is that it is the constant V_0 in the potential which is dominant near the discontinuity. Once this condition is satisfied, the departures from slow roll can essentially be described in terms of the ratio R . Upon plotting the various contributions for different R , we find that, deviations from the slow roll hierarchy begin to occur even for an $|R - 1|$ as small as 10^{-5} .

With the analytic results that we have at hand, it is also worthwhile to investigate whether the fourth term remains the dominant term for all values of the parameters of the Starobinsky model when deviations from slow roll occur or if there exist regimes where the hierarchy is mixed or even, possibly, absent. Motivated by such an aim, let us enquire if, say, the second term G_2 can probably be as large as the fourth term G_4 for any set or a range of parameters of the Starobinsky model. Let us consider, for instance,

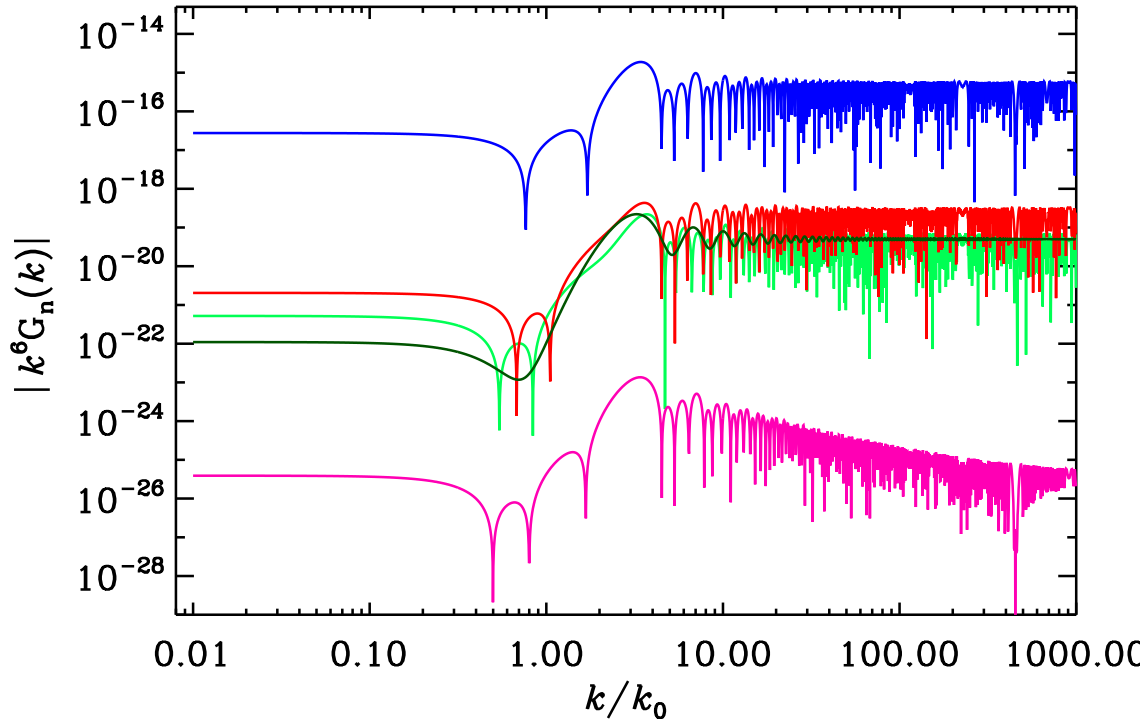


Figure 13. The contributions due to the different terms to the bi-spectrum—viz. k^6 times the absolute values of $G_1 + G_3$ (in light green), G_2 (in red), G_4 (in blue), $G_5 + G_6$ (in purple) and G_7 (in dark green)—that we had plotted in the earlier figures (i.e. in Figs. 8, 6, 5, 9 and 10, respectively) for the Starobinsky model, have been assembled here to illustrate the hierarchy in a fast roll regime. The hierarchy of the various contributions to the bi-spectrum is evident from the figure.

the ratio

$$Q(k) = \frac{G_2(k)}{G_4(k) \epsilon_{1+}} = \frac{f_{\text{NL}}^{\text{eq}(2)}(k)}{f_{\text{NL}}^{\text{eq}(4)}(k) \epsilon_{1+}}, \quad (197)$$

where $f_{\text{NL}}^{\text{eq}(2)}$ and $f_{\text{NL}}^{\text{eq}(4)}$ are the contributions to the non-Gaussianity parameter f_{NL} due to the terms G_2 and G_4 in the equilateral limit. As we have discussed, the first slow roll parameter before the transition, viz. ϵ_{1+} , is expected to be small. In plotting the earlier figures, we have worked with parameters such that $\epsilon_{1+} \simeq 10^{-4}$ (cf. Fig. 1). But, the various assumptions and the approximations of the Starobinsky model will remain valid even if ϵ_{1+} is larger, say, about 10^{-2} or so. If we choose $\epsilon_{1+} \simeq 10^{-2}$, we can have $G_2 \simeq G_4$, provided $Q \simeq 10^2$. Interestingly, we find that the quantity Q can be expressed completely in terms of R and, as in the case of all the other perturbed quantities, its dependence on the wavenumber arises only through the ratio k/k_0 . In Fig. 14, we have plotted the absolute value of the quantity Q as a function of k/k_0 for a few different values of the ratio R . It is clear from the figure that, there does exist ranges of parameters of the Starobinsky model for which $Q \simeq 10^2$ and, therefore, $G_2 \simeq G_4$, in

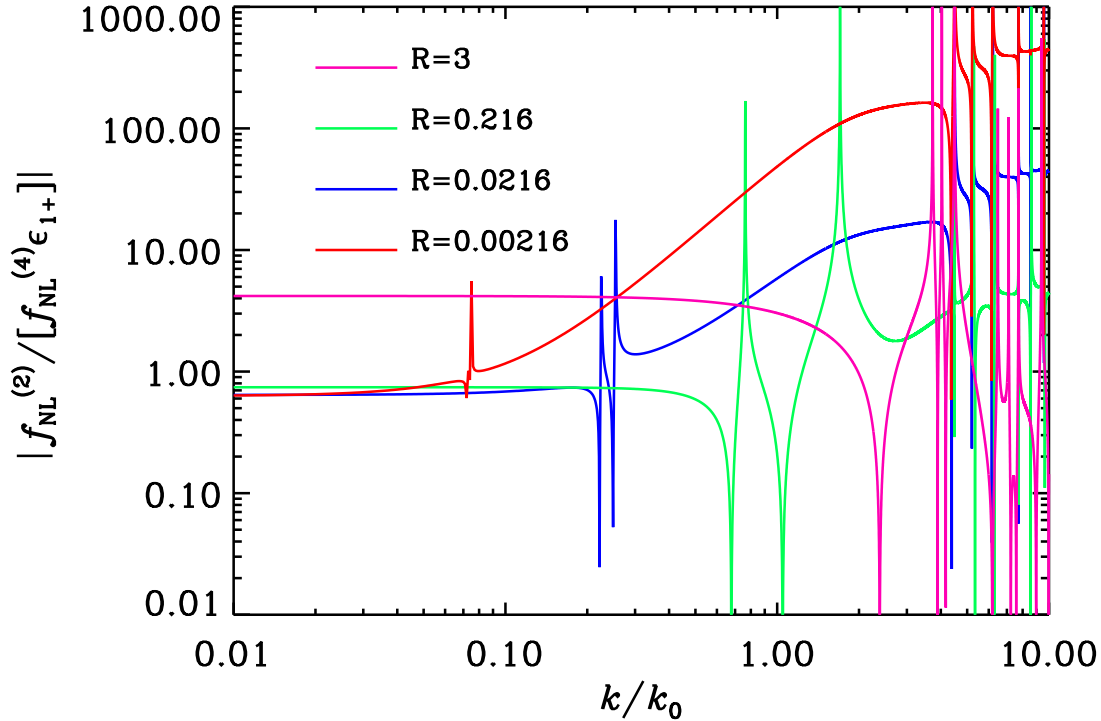


Figure 14. The absolute value of the quantity Q , which essentially reflects the amplitude of the contribution due to the second term G_2 in contrast to the fourth term G_4 , has been plotted as a function of k/k_0 for a few different values of the ratio $R = A_-/A_+$. We should stress again that Q depends only on R and k/k_0 . One finds that, deviations from slow roll begin to occur for $|R - 1|$ as small as 10^{-5} . The upward spikes correspond to the wavenumbers at which G_4 vanishes, so that the contribution due to G_2 turns dominant. Even apart from these specific locations, it is evident that Q can be as large as 10^2 in a domain which admits fast roll. Since ϵ_{1+} can be possibly as large as 10^{-2} with the assumptions and approximations of the Starobinsky model continuing to remain valid, this indicates that G_2 can be of the order of G_4 in a fast roll regime.

domains that could admit departures from slow roll (i.e. when R deviates sufficiently from unity). To our knowledge, this conclusion is new, since, in the literature, G_4 has always been considered to be the dominant term when deviations from slow roll occur. Moreover, we believe that this is the first time that this phenomenon has been explicitly illustrated. This suggests that, it is plausible that the hierarchy is different in different regions of the parameter space of a model. However, a cautionary remark needs to be added to arriving at such a conclusion. Recall that, in our evaluation of \mathcal{G}_4 , we had neglected certain terms in the quantity $f_k'^-$ [see our remarks that immediately follow Eq. (89)]. As a result, a concern could arise that, for the parameters discussed above, the neglected terms contribute sufficiently to restore the hierarchy wherein G_4 is the dominant term during fast roll. But, we have also analyzed the issue using a numerical

code [37] and our preliminary results seem to confirm the above conclusion, viz. that the neglected terms are not significant enough to restore the commonly expected fast roll hierarchy.

In order to reinforce and also to explicitly illustrate the above conclusion, it is important to arrive at a specific set of parameters of the Starobinsky model which allow fast roll as well as lead to G_2 and G_4 that are of the same order. But, in order to converge on a viable set of parameters, a few points concerning certain aspects of the Starobinsky model and the results that we have obtained requires some emphasis. In particular, as $k/k_0 \rightarrow 0$, we find that Q has the following simple form:

$$\lim_{k/k_0 \rightarrow 0} Q(k) = \frac{17 - 27 R^2}{27 - 27 R}. \quad (198)$$

In this limit, $Q \simeq 17/27 \simeq 0.63$ for small R , while $Q \simeq R$, when R is large. These behavior are clearly reflected in Fig. 14. So, if we require Q to be large, we can either work with a high enough R and focus on small wavenumbers, or choose an R that is suitably smaller than unity which permits sufficient deviation from slow roll and also possibly leads to $G_2 \simeq G_4$ at large wavenumbers. However, recall that the regime $R < 1$ seems to be favored by the CMB data. With these points in mind, let us now focus on arriving at a set of parameters in the $R < 1$ domain which leads to $Q \simeq 10^2$. Since, given a H_0 , A_- is already determined by COBE normalization, choosing an ϵ_{1+} fixes A_+ . We find that, if we work with the earlier values of H_0 and A_- (listed in the caption of Fig. 1), while set $\epsilon_{1+} \simeq 1/75 \simeq 0.013$, corresponding to $A_+/M_{\text{Pl}}^3 = 3.87 \times 10^{-13}$ and $R = 0.0188$, the hierarchy of the contributions is indeed different, with G_2 being of the same order as G_4 at large wavenumbers. This point is evident from Fig. 15 wherein we have plotted the various contributions G_n for these values of the parameters. Of course, such a low value of R lies about 5σ away from the best fit value of $R \simeq 0.73$ that we had mentioned earlier. Given that the Starobinsky model in itself has not been directly constrained (only certain variations around it have been tested precisely), this could indicate that the above choice of R is possibly not completely ruled out by the data. However, in the case of the Starobinsky model, it seems to us that, an altered hierarchy of the contributions to the bi-spectrum is systematically associated with regions of the parameter space that is not favored by the CMB data. If this is indeed true, this obviously tones down the importance of this modification to the hierarchy in the Starobinsky model. But, as we had discussed in the previous sub-section, the Starobinsky model with a smaller R may be considered to mimic other models that provide a good fit to the data. It is possible that one may encounter such altered hierarchies in these models.

Before we conclude, let us briefly touch upon the possible reasons for the variations to the hierarchy. We find that the understanding gained on the hierarchy of the different contributions to the bi-spectrum has been largely based on the behavior of the slow roll parameters. Needless to mention, in addition to the slow roll parameters, the various contributions involve the curvature perturbation and its derivative as well. In a slow roll inflationary scenario, the amplitude of the curvature perturbation evolves monotonically once it leaves the Hubble radius. In particular, while the amplitude of the mode f_k

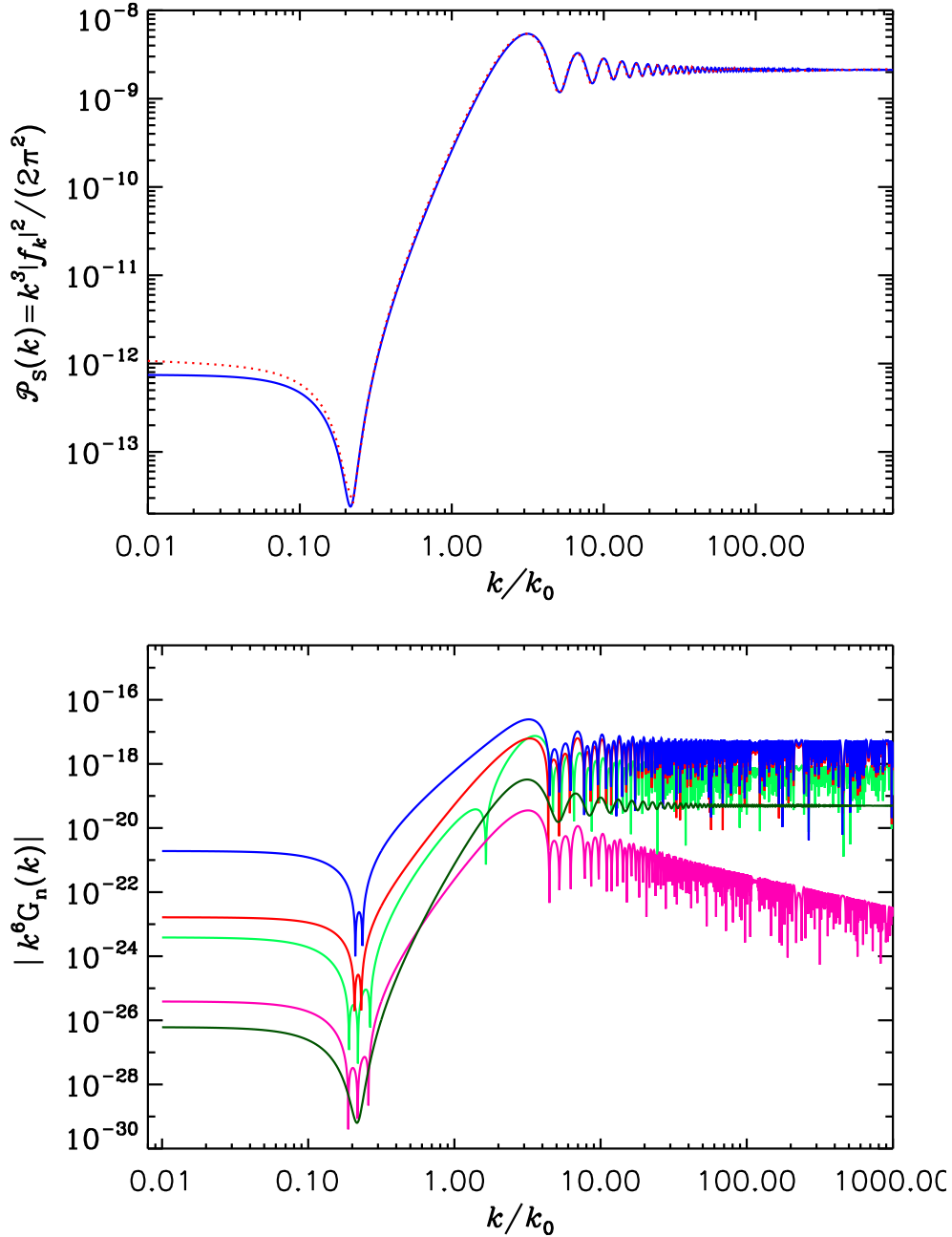


Figure 15. The power spectrum (on top) and the contributions due to the different terms to the bi-spectrum (below) for a case wherein $Q \simeq 10^2$. The power spectrum and the different contributions to the bi-spectrum have been plotted in the same fashion as in Figs. 3 and 13. In arriving at these plots, we have worked with the same values of H_0 and A_- as in Figs. 3 and 13, but we have set $A_+/M_{\text{Pl}}^3 = 3.87 \times 10^{-13}$, which corresponds to $R = 0.0188$. The match between the analytical and the numerical results in the case of the power spectrum is rather good, which indicates that the assumptions and approximations of the Starobinsky model are quite valid for the parameters that we are working with here. Interestingly, in contrast to Fig. 13, where G_4 was the dominant term, here we find that the contribution due to G_2 is of the same order as G_4 at large wavelengths.

quickly goes to a constant value, its time derivative f'_k dies down as e^{-2N} at super Hubble scales. Because of such a monotonic behavior of the curvature perturbation during slow roll, in such situations, the hierarchy is largely dependent on the slow parameters themselves. However, when departures from slow arise, it is known that the modes which leave the Hubble radius just before or during the periods of deviations from slow roll can evolve strongly around the time of Hubble exit. In fact, at super Hubble scales, the amplitude of these modes can be enhanced or suppressed compared to their amplitudes at Hubble exit (in this context, see, for instance, Refs. [30]). Therefore, it seems that, when departures from slow roll occur, the hierarchy can be different based on a mixture of the non-trivial evolution of the slow roll parameters and the curvature perturbation. We believe that this is an interesting aspect that demands further investigation.

7. Summary and outlook

As we had discussed in some detail in the introductory section, models that lead to features in the primordial spectrum gain importance due to the fact that certain features can lead to a better fit to the CMB data than the conventional, nearly scale invariant scalar power spectrum, as is generated by slow roll inflation. The generation of features in the primordial spectrum requires one or more periods of fast roll. While the scalar power spectrum and the bi-spectrum can be evaluated in a model independent fashion in the slow roll approximation, such a model independent approach seems difficult when departures from slow roll arise. This is essentially due to the fact that the deviations from slow roll can occur in a multitude of forms and it is impossible to describe all possible deviations in terms of a limited number of variables or parameters (for a broader effort, that attempts to capture a certain class of departures from slow roll, see Ref. [18]). In fact, in the literature, numerical computations are often resorted to in order to investigate scenarios involving fast roll.

In such a situation, the Starobinsky model provides a welcome relief as it allows the background as well as the scalar power spectrum to be evaluated analytically to a very good approximation, even though it contains departures from slow roll. In this work, we have shown that the scalar bi-spectrum can also be computed analytically. Simultaneously, we have also been working towards numerically computing the scalar bi-spectrum and the non-Gaussianity parameter f_{NL} in the Starobinsky model. Preliminary investigations indicate that the analytic expressions we have obtained match the numerical results quite well [37], which reflect the extent of the accuracy of the assumptions and approximations of the Starobinsky model.

Interestingly, we have found that, in the Starobinsky model, for certain values of the parameters, the non-Gaussianity parameter f_{NL} in the equilateral limit can be as large as indicated by the currently observed mean values, with the possible limitation that this occurs in a region of the parameter space that is not favored by the current CMB data. We had focused here on the equilateral limit and, clearly, it is imperative

that we extend the analysis to other configurations such as, say, the squeezed limit [38]. Further, there exist a few other models in the literature which allow the background and the perturbations to be evaluated analytically, and it is worthwhile to evaluate the bi-spectrum in these models too. We are currently investigating these issues.

Acknowledgments

JM and LS wish to thank the Harish-Chandra Research Institute, Allahabad, India, and the Institut d'Astrophysique de Paris, France, for hospitality, respectively, where part of this work was carried out. JM would like to thank Guillaume Faye for help on numerical issues. LS wishes to thank David Seery for discussions.

Appendix A. Evaluation of the integrals

This appendix contains some additional information pertaining to the evaluation of certain non-trivial integrals we had encountered in the text.

Appendix A.1. Evaluation of I_{13} and J_{13}

In this sub-section, we shall provide a few details regarding the evaluation of the integrals I_{13} and J_{13} .

Let us start with the expression (141) for I_{13} . As we had mentioned, the integral can be evaluated by writing P_1 as a polynomial in the variable t_n , and computing the integral term by term. If we write

$$P_1 \left(\frac{-t_n}{3ik} + \tau_n \right) = k^4 \sum_{m=0}^7 c_{nm} t_n^m, \quad (\text{A.1})$$

we find that the coefficients c_{nm} are given by

$$c_{n0} = -27i\varepsilon\delta^3 - 27\varepsilon\delta^2 e^{i\theta_n} + 9(i\varepsilon\delta + \delta^4) e^{2i\theta_n}, \quad (\text{A.2})$$

$$c_{n1} = -42i\varepsilon\delta^3 + (-27\varepsilon\delta^2 + 6i\delta^5) e^{i\theta_n} + (6i\varepsilon\delta + 27\delta^4) e^{2i\theta_n}, \quad (\text{A.3})$$

$$c_{n2} = -22i\varepsilon\delta^3 - \delta^6 - 9(\varepsilon\delta^2 - i\delta^5) e^{i\theta_n} + (i\varepsilon\delta + 22\delta^4) e^{2i\theta_n}, \quad (\text{A.4})$$

$$c_{n3} = -\frac{132}{27}i\varepsilon\delta^3 - \delta^6 + \left(-\varepsilon\delta^2 + \frac{44}{9}i\delta^5\right) e^{i\theta_n} + \frac{70}{9}\delta^4 e^{2i\theta_n}, \quad (\text{A.5})$$

$$c_{n4} = -\frac{33}{81}i\varepsilon\delta^3 - \frac{11}{27}\delta^6 + \frac{35}{27}i\delta^5 e^{i\theta_n} + \frac{35}{27}\delta^4 e^{2i\theta_n}, \quad (\text{A.6})$$

$$c_{n5} = -\frac{7}{81}\delta^6 + \frac{14}{81}i\delta^5 e^{i\theta_n} + \frac{7}{81}\delta^4 e^{2i\theta_n}, \quad (\text{A.7})$$

$$c_{n6} = -\frac{7}{729}\delta^6 + \frac{7}{729}i\delta^5 e^{i\theta_n} \quad (\text{A.8})$$

$$c_{n7} = -\frac{1}{2187}\delta^6, \quad (\text{A.9})$$

where $\delta \equiv (|\rho|/k) = (|\Delta A|/A_-)^{1/3} (k_0/k)$ and $\varepsilon = 1$ if $\Delta A < 0$ and $\varepsilon = -1$ if $\Delta A > 0$. (The quantity ε that we have introduced here should not be confused with the slow roll

parameters.) Moreover, when $\Delta A > 0$, then we have $\theta_1 = \pi/3$, $\theta_2 = \pi$, and $\theta_3 = 5\pi/3$. On the other hand, if $\Delta A < 0$, then we find that $\theta_1 = 0$, $\theta_2 = 2\pi/3$ and $\theta_3 = 4\pi/3$. Upon using the expression (A.1), I_{13} can be written as

$$I_{13}(k) = -\frac{A_- |\rho|^2 k^4}{\sqrt{18} H_0^2 M_{\text{Pl}} \rho^3} \sum_{n=1}^3 \sum_{m=0}^7 b_n c_{nm} e^{3ik\tau_n} \times \int_{3ik/k_0 + 3ik\tau_n}^{-3ik\eta_e + 3ik\tau_n} dt_n t_n^{m-1} e^{-t_n} \quad (\text{A.10})$$

which can be integrated to yield

$$I_{13}(k) = -\frac{A_- |\rho|^2 k^4}{\sqrt{18} H_0^2 M_{\text{Pl}} \rho^3} \sum_{n=1}^3 \sum_{m=0}^7 b_n c_{nm} e^{3ik\tau_n} \left[\Gamma\left(m, \frac{3ik}{k_0} + 3ik\tau_n\right) - \Gamma(m, -3ik\eta_e + 3ik\tau_n) \right], \quad (\text{A.11})$$

where $\Gamma(m, z)$ is the incomplete Gamma function (see, for example, Ref. [39])

$$\Gamma(m, z) \equiv \int_z^\infty dt e^{-t} t^{m-1}. \quad (\text{A.12})$$

If m is a non-vanishing integer, the incomplete Gamma function reduces to an elementary function [39], viz.

$$\Gamma(m, z) = (m-1)! e^{-z} e_{m-1}(z), \quad (\text{A.13})$$

where $e_n(z)$ is the exponential sum function defined as

$$e_n(z) \equiv \sum_{\ell=0}^n \frac{z^\ell}{\ell!}. \quad (\text{A.14})$$

However, if $m = 0$, then

$$\Gamma(0, z) \equiv E_1(z) = \int_z^\infty \frac{dt}{t} e^{-t}, \quad (\text{A.15})$$

where $E_1(z)$ is the exponential integral function [39]. For this reason, it is convenient to split the sum over m into two parts as follows:

$$I_{13}(k) = -\frac{A_- |\rho|^2 k^4}{\sqrt{18} H_0^2 M_{\text{Pl}} \rho^3} \sum_{n=1}^3 b_n e^{3ik\tau_n} \left\{ c_{n0} E_1\left(\frac{3ik}{k_0} + 3ik\tau_n\right) - c_{n0} E_1(3ik\tau_n) + \sum_{m=1}^7 c_{nm} \left[\Gamma\left(m, \frac{3ik}{k_0} + 3ik\tau_n\right) - \Gamma(m, 3ik\tau_n) \right] \right\}, \quad (\text{A.16})$$

where we have taken the limit $\eta_e \rightarrow 0$. In terms of the exponential sum function $e_n(z)$ and the exponential integral function $E_1(z)$, we can rewrite the above expression for I_{13} as

$$I_{13}(k) = -\frac{A_- |\rho|^2 k^4}{\sqrt{18} H_0^2 M_{\text{Pl}} \rho^3} \left\{ -\sum_{n=1}^3 b_n \left[c_{n0} e^{3ik\tau_n} E_1(3ik\tau_n) \right. \right.$$

$$\begin{aligned}
& + \sum_{m=1}^7 c_{nm} (m-1)! e_{m-1} (3 i k \tau_n) \Big] \\
& + e^{-3 i k / k_0} \sum_{n=1}^3 b_n \left[c_{n0} e^{3 i k / k_0 + 3 i k \tau_n} E_1 \left(\frac{3 i k}{k_0} + 3 i k \tau_n \right) \right. \\
& \left. + \sum_{m=1}^7 c_{nm} (m-1)! e_{m-1} \left(\frac{3 i k}{k_0} + 3 i k \tau_n \right) \right] \Big\} \quad (A.17)
\end{aligned}$$

which is the expression (153) we have quoted in the text.

Let us now turn to the evaluation of J_{13} described by the integral (158). In this case, we can perform the change of variable $t_n \equiv -i k (\tau - \tau_n)$, which leads to

$$\begin{aligned}
J_{13}(k) = & - \frac{A_- |\rho|^2}{\sqrt{18} H_0^2 M_{\text{Pl}} \rho^3} \sum_{n=1}^3 b_n e^{i k \tau_n} \\
& \times \int_{i k / k_0 + i k \tau_n}^{-i k \eta_e + i k \tau_n} \frac{dt_n}{t_n} e^{-t_n} P_2 \left(\frac{-t_n}{i k} + \tau_n \right). \quad (A.18)
\end{aligned}$$

We can write, as in the case of the function P_1 ,

$$P_2 \left(\frac{-t_n}{i k} + \tau_n \right) = k^4 \sum_{m=0}^7 d_{nm} t_n^m, \quad (A.19)$$

where the coefficients d_{nm} 's are given by

$$d_{n0} = -27 i \varepsilon \delta^3 + 27 \varepsilon \delta^2 e^{i \theta_n} + 27 (-i \varepsilon \delta + \delta^4) e^{2 i \theta_n}, \quad (A.20)$$

$$d_{n1} = 54 i \varepsilon \delta^3 + (99 \varepsilon \delta^2 + 54 i \delta^5) e^{i \theta_n} + (-18 i \varepsilon \delta + 81 \delta^4) e^{2 i \theta_n}, \quad (A.21)$$

$$d_{n2} = 162 i \varepsilon \delta^3 - 27 \delta^6 + (45 \varepsilon \delta^2 + 81 i \delta^5) e^{i \theta_n} + (9 i \varepsilon \delta - 54 \delta^4) e^{2 i \theta_n}, \quad (A.22)$$

$$d_{n3} = 60 i \varepsilon \delta^3 - 27 \delta^6 + (-27 \varepsilon \delta^2 - 36 i \delta^5) e^{i \theta_n} - 150 \delta^4 e^{2 i \theta_n}, \quad (A.23)$$

$$d_{n4} = -33 i \varepsilon \delta^3 + 9 \delta^6 - 75 i \delta^5 e^{i \theta_n} - 45 \delta^4 e^{2 i \theta_n}, \quad (A.24)$$

$$d_{n5} = 15 \delta^6 - 18 i \delta^5 e^{i \theta_n} + 21 \delta^4 e^{2 i \theta_n}, \quad (A.25)$$

$$d_{n6} = 3 \delta^6 + 7 i \delta^5 e^{i \theta_n}, \quad (A.26)$$

$$d_{n7} = -\delta^6. \quad (A.27)$$

It is clear that the coefficients d_{mn} and c_{mn} have a very similar structure. The integral $J_{13}(k)$ can then be rewritten as

$$\begin{aligned}
J_{13}(k) = & - \frac{A_- |\rho|^2 k^4}{\sqrt{18} H_0^2 M_{\text{Pl}} \rho^3} \sum_{n=1}^3 \sum_{m=0}^7 b_n d_{nm} e^{i k \tau_n} \\
& \times \int_{i k / k_0 + i k \tau_n}^{-i k \eta_e + i k \tau_n} dt_n t_n^{m-1} e^{-t_n}, \quad (A.28)
\end{aligned}$$

which can be integrated, as earlier, to yield

$$\begin{aligned}
J_{13}(k) = & - \frac{A_- |\rho|^2 k^4}{\sqrt{18} H_0^2 M_{\text{Pl}} \rho^3} \sum_{n=1}^3 \sum_{m=0}^7 b_n d_{nm} e^{i k \tau_n} \\
& \times \left[\Gamma \left(m, \frac{i k}{k_0} + i k \tau_n \right) - \Gamma \left(m, -i k \eta_e + i k \tau_n \right) \right]. \quad (A.29)
\end{aligned}$$

The rest of the calculation in arriving at the final expression (160) proceeds just as in the case of I_{13} .

Appendix A.2. The coefficients f_n and g_n

The coefficients f_n are given by

$$f_0 = 1, \tag{A.30}$$

$$f_1 = -i + \frac{6\rho^3}{k^3}, \tag{A.31}$$

$$f_2 = -\frac{12i\rho^3}{k^3} + \frac{9\rho^6}{k^6}, \tag{A.32}$$

$$f_3 = -\frac{9\rho^3}{k^3} - \frac{27i\rho^6}{k^6}, \tag{A.33}$$

$$f_4 = \frac{3i\rho^3}{k^3} - \frac{39\rho^6}{k^6}, \tag{A.34}$$

$$f_5 = \frac{33i\rho^6}{k^6} - \frac{9\rho^9}{k^9}, \tag{A.35}$$

$$f_6 = \frac{15\rho^6}{k^6} + \frac{27i\rho^9}{k^9}, \tag{A.36}$$

$$f_7 = -\frac{3i\rho^6}{k^6} + \frac{33\rho^9}{k^9}, \tag{A.37}$$

$$f_8 = -\frac{21i\rho^9}{k^9}, \tag{A.38}$$

$$f_9 = -\frac{7\rho^9}{k^9}, \tag{A.39}$$

$$f_{10} = \frac{i\rho^9}{k^9}, \tag{A.40}$$

while g_n are given by

$$g_0 = 3, \tag{A.41}$$

$$g_1 = -i + \frac{18\rho^3}{k^3}, \tag{A.42}$$

$$g_2 = -\frac{12i\rho^3}{k^3} + \frac{27\rho^6}{k^6}, \tag{A.43}$$

$$g_3 = -\frac{3\rho^3}{k^3} - \frac{27i\rho^6}{k^6}, \tag{A.44}$$

$$g_4 = \frac{3i\rho^3}{k^3} - \frac{9\rho^6}{k^6}, \tag{A.45}$$

$$g_5 = -\frac{3i\rho^6}{k^6} - \frac{27\rho^9}{k^9}, \tag{A.46}$$

$$g_6 = -\frac{3\rho^6}{k^6} + \frac{27i\rho^9}{k^9}, \tag{A.47}$$

$$g_7 = -\frac{3i\rho^6}{k^6} - \frac{9\rho^9}{k^9}, \tag{A.48}$$

$$g_8 = \frac{15i\rho^9}{k^9}, \tag{A.49}$$

$$g_9 = \frac{3\rho^9}{k^9}, \quad (\text{A.50})$$

$$g_{10} = \frac{i\rho^9}{k^9}. \quad (\text{A.51})$$

References

- [1] D. Larson *et al.*, *Astrophys. J. Suppl.* **192**, 16 (2011); E. Komatsu *et al.*, *Astrophys. J. Suppl.* **192**, 18 (2011).
- [2] H. V. Peiris *et al.*, *Astrophys. J. Suppl.* **148**, 213 (2003); M. Tristram *et al.*, *Astron. Astrophys.* **436**, 785 (2005); D. N. Spergel *et al.*, *Astrophys. J. Suppl.* **S170**, 377 (2007). M. R.olta *et al.*, *Astrophys. J. Suppl.* **180**, 296 (2009); J. Dunkley *et al.*, *Astrophys. J. Suppl.* **180**, 306 (2009); E. Komatsu *et al.*, *Astrophys. J. Suppl.* **180**, 330 (2009).
- [3] J. Martin and C. Ringeval, *JCAP* **0608**, 009 (2006).
- [4] L. Lorentz, J. Martin and C. Ringeval, *JCAP* **0804**, 001 (2008).
- [5] L. Lorentz, J. Martin and C. Ringeval, *Phys. Rev. D* **78**, 063543 (2008).
- [6] J. Martin and C. Ringeval, *Phys. Rev. D* **82**, 023511 (2010).
- [7] S. L. Bridle, A. M. Lewis, J. Weller and G. Efstathiou, *Mon. Not. Roy. Astron. Soc.* **342**, L72 (2003); P. Mukherjee and Y. Wang, *Astrophys. J.* **599**, 1 (2003); S. Hannestad, *JCAP* **0404**, 002 (2004); A. Shafieloo and T. Souradeep, *Phys. Rev. D* **70**, 043523 (2004); D. Tocchini-Valentini, Y. Hoffman and J. Silk, *Mon. Not. Roy. Astron. Soc.* **367**, 1095 (2006); A. Shafieloo, T. Souradeep, P. Manimaran, P. K. Panigrahi and R. Rangarajan, *Phys. Rev. D* **75**, 123502 (2007); A. Shafieloo and T. Souradeep, *Phys. Rev. D* **78**, 023511 (2008); R. Nagata and J. Yokoyama, *Phys. Rev. D* **79**, 043010 (2009); G. Nicholson and C. R. Contaldi, *JCAP* **0907**, 011 (2009).
- [8] J. Yokoyama, *Phys. Rev. D* **59**, 107303 (1999); B. Feng and X. Zhang, *Phys. Lett. B* **570**, 145 (2003); M. Kawasaki and F. Takahashi, *Phys. Lett. B* **570**, 151 (2003); R. Sinha and T. Souradeep, *Phys. Rev. D* **74**, 043518 (2006); M. J. Mortonson and W. Hu, *Phys. Rev. D* **80**, 027301 (2009).
- [9] J. M. Cline, P. Crotty and J. Lesgourgues, *JCAP* **0309**, 010 (2003); C. R. Contaldi, M. Peloso, L. Kofman and A. Linde, *JCAP* **0307**, 002 (2003); D. Boyanovsky, H. J. de Vega and N. G. Sanchez, *Phys. Rev. D* **74**, 123006 (2006); *Phys. Rev. D* **74**, 123007 (2006); B. A. Powell and W. H. Kinney, *Phys. Rev. D* **76**, 063512 (2007); C. Destri, H. J. de Vega and N. G. Sanchez, *Phys. Rev. D* **78**, 023013 (2008).
- [10] R. K. Jain, P. Chingangbam, J.-O. Gong, L. Sriramkumar and T. Souradeep, *JCAP* **0901**, 009 (2009); R. K. Jain, P. Chingangbam, L. Sriramkumar and T. Souradeep, *Phys. Rev. D* **82**, 023509 (2010).
- [11] L. Covi, J. Hamann, A. Melchiorri, A. Slosar and I. Sorbera, *Phys. Rev. D* **74**, 083509 (2006); J. Hamann, L. Covi, A. Melchiorri and A. Slosar, *Phys. Rev. D* **76**, 023503 (2007); M. Joy, V. Sahni and A. A. Starobinsky, *Phys. Rev. D* **77**, 023514 (2008); M. Joy, A. Shafieloo, V. Sahni and A. A. Starobinsky, *JCAP* **0906**, 028 (2009); M. J. Mortonson, C. Dvorkin, H. V. Peiris and W. Hu, *Phys. Rev. D* **79**, 103519 (2009); D. K. Hazra, M. Aich, R. K. Jain, L. Sriramkumar and T. Souradeep, *JCAP* **1010**, 008 (2010); M. Benetti, M. Lattanzi, E. Calabrese and A. Melchiorri, arXiv:1107.4992v1 [astro-ph.CO].
- [12] J. Martin and C. Ringeval, *Phys. Rev. D* **69**, 083515 (2004); *Phys. Rev. D* **69**, 127303 (2004); *JCAP* **0501**, 007 (2005); P. Hunt and S. Sarkar, *Phys. Rev. D* **70**, 103518 (2004); *Phys. Rev. D* **76**, 123504 (2007); M. Kawasaki, F. Takahashi and T. Takahashi, *Phys. Letts. B* **605**, 223 (2005); J.-O. Gong, *JCAP* **0507**, 015 (2005); M. Kawasaki and K. Miyamoto, arXiv:1010.3095v2 [astro-ph.CO]; A. Achucarro, J.-O. Gong, S. Hardeman, G. A. Palma and S. P. Patil, *JCAP* **1101**, 030 (2011); K. Kumazaki, S. Yokoyama and N. Sugiyama, arXiv:1105.2398v1 [astro-ph.CO]; C. Dvorkin and W. Hu, arXiv:1106.4016v1 [astro-ph.CO].

- [13] C. Pahud, M. Kamionkowski and A. R. Liddle, Phys. Rev. D **79**, 083503 (2009); R. Flauger, L. McAllister, E. Pajer, A. Westphal and G. Xu, JCAP **1006**, 009 (2010); M. Aich, D. K. Hazra, L. Sriramkumar and T. Souradeep, arXiv:1106.2798v1 [astro-ph.CO].
- [14] S. Dodelson, *Modern Cosmology* (Academic Press, San Diego, U.S.A., 2003); V. F. Mukhanov, *Physical Foundations of Cosmology* (Cambridge University Press, Cambridge, England, 2005); S. Weinberg, *Cosmology* (Oxford University Press, Oxford, England, 2008); R. Durrer, *The Cosmic Microwave Background* (Cambridge University Press, Cambridge, England, 2008); D. H. Lyth and A. R. Liddle, *The Primordial Density Perturbation* (Cambridge University Press, Cambridge, England, 2009). P. Peter and J-P. Uzan, *Primordial Cosmology* (Oxford University Press, Oxford, England, 2009).
- [15] J. E. Lidsey, A. Liddle, E. W. Kolb, E. J. Copeland, T. Barreiro and M. Abney, Rev. Mod. Phys. **69**, 373 (1997); A. Riotto, arXiv:hep-ph/0210162; W. H. Kinney, astro-ph/0301448; J. Martin, Lect. Notes Phys. **738**, 193 (2008); J. Martin, Lect. Notes Phys. **669**, 199 (2005); J. Martin, Braz. J. Phys. **34**, 1307 (2004); B. Bassett, S. Tsujikawa and D. Wands, Rev. Mod. Phys. **78**, 537 (2006); W. H. Kinney, arXiv:0902.1529 [astro-ph.CO]; L. Sriramkumar, Curr. Sci. **97**, 868 (2009); D. Baumann, arXiv:0907.5424v1 [hep-th].
- [16] A. A. Starobinsky, Sov. Phys. JETP Lett. **55**, 489 (1992).
- [17] H. M. Hodges, G. R. Blumenthal, L. A. Kofman and J. R. Primack, Nucl. Phys. B **335**, 197 (1990); V. F. Mukhanov and M. I. Zelnikov, Phys. Lett. B **263**, 169 (1991); D. Polarski and A. A. Starobinsky, Nucl. Phys. B **385**, 623 (1992); D. Polarski, Phys. Rev. D **49**, 6319 (1994); J. A. Adams, G. G. Ross and S. Sarkar, Nucl. Phys. B **503**, 405 (1997); J. Lesgourgues, Nucl. Phys. B **582**, 593 (2000); J. Barriga, E. Gaztanaga, M. Santos and S. Sarkar, Mon. Not. Roy. Astron. Soc. **324**, 977 (2001); Nucl. Phys. Proc. Suppl. **95**, 66 (2001); J. A. Adams, B. Cresswell, R. Easther, Phys. Rev. D **64**, 123514 (2001).
- [18] C. Dvorkin and W. Hu, Phys. Rev. D **81**, 023518 (2010); W. Hu, arXiv:1104.4500v1 [astro-ph.CO].
- [19] J. Martin, C. Ringeval and R. Trotta, Phys. Rev. D **83**, 063514 (2011).
- [20] E. Komatsu and D. N. Spergel, Phys. Rev. D **63**, 063002 (2001); E. Komatsu, D. N. Spergel and B. D. Wandelt, Astrophys. J. **634**, 14 (2005); D. Babich and M. Zaldarriaga, Phys. Rev. D **70**, 083005 (2004); M. Liguori, F. K. Hansen, E. Komatsu, S. Matarrese and A. Riotto, Phys. Rev. D **73**, 043505 (2006); C. Hikage, E. Komatsu and T. Matsubara, Astrophys. J. **653** (2006) 11 (2006); J. R. Fergusson and E. P. S. Shellard, Phys. Rev. D **76**, 083523 (2007); A. P. S. Yadav, E. Komatsu and B. D. Wandelt, Astrophys. J. **664**, 680 (2007); P. Creminelli, L. Senatore and M. Zaldarriaga, JCAP **0703**, 019 (2007); A. P. S. Yadav and B. D. Wandelt, Phys. Rev. Lett. **100**, 181301 (2008); C. Hikage, T. Matsubara, P. Coles, M. Liguori, F. K. Hansen and S. Matarrese, Mon. Not. Roy. Astron. Soc. **389**, 1439 (2008); O. Rudjord, F. K. Hansen, X. Lan, M. Liguori, D. Marinucci and S. Matarrese, Astrophys. J. **701**, 369 (2009); K. M. Smith, L. Senatore and M. Zaldarriaga, JCAP **0909**, 006 (2009); J. Smidt, A. Amblard, C. T. Byrnes, A. Cooray, A. Heavens and D. Munshi, Phys. Rev. D **81**, 123007 (2010); J. R. Fergusson, M. Liguori and E. P. S. Shellard, arXiv:1006.1642v1 [astro-ph.CO].
- [21] M. Liguori, E. Sefusatti, J. R. Fergusson and E. P. S. Shellard, Adv. Astron. **2010**, 980523 (2010); A. P. S. Yadav and B. D. Wandelt, arXiv:1006.0275v3 [astro-ph.CO]; E. Komatsu, Class. Quantum Grav. **27**, 124010 (2010).
- [22] See, <http://www.sciops.esa.int/PLANCK/>.
- [23] A. Gangui, F. Lucchin, S. Matarrese and S. Mollerach, Astrophys. J. **430**, 447 (1994); A. Gangui, Phys. Rev. D **50**, 3684 (1994); A. Gangui and J. Martin, Mon. Not. Roy. Astron. Soc. **313**, 323 (2000); A. Gangui, J. Martin and M. Sakellariadou, Phys. Rev. D **66**, 083502 (2002).
- [24] J. Maldacena, JHEP **0305**, 013 (2003).
- [25] X. Chen, R. Easther and E. A. Lim, JCAP **0706**, 023 (2007); JCAP **0804**, 010 (2008); S. Hotchkiss and S. Sarkar, JCAP **1005**, 024 (2010); S. Hannestad, T. Haugbolle, P. R. Jarnhus and M. S. Sloth, JCAP **1006**, 001 (2010); R. Flauger and E. Pajer, JCAP **1101**, 017 (2011); P. Adshead, W. Hu, C. Dvorkin and H. V. Peiris, arXiv:1102.3435v1 [astro-ph.CO]; X. Chen,

- arXiv:1104.1323v2 [hep-th].
- [26] A. Gangui, J. Martin and M. Sakellariadou, Phys. Rev. D **66**, 083502 (2002); R. Holman and A. J. Tolley, JCAP **0805**, 001 (2008); W. Xue and B. Chen, Phys. Rev. D **79**, 043518 (2009); P. D. Meerburg, J. P. van der Schaar and P. S. Corasaniti, JCAP **0905**, 018 (2009); X. Chen, JCAP **1012**, 003 (2010).
 - [27] D. Seery and J. E. Lidsey, JCAP **0506**, 003 (2005); X. Chen, Phys. Rev. D **72**, 123518 (2005); X. Chen, M.-x. Huang, S. Kachru and G. Shiu, JCAP **0701**, 002 (2007); D. Langlois, S. Renaux-Petel, D. A. Steer and T. Tanaka, Phys. Rev. Lett. **101**, 061301 (2008); Phys. Rev. D **78**, 063523 (2008).
 - [28] X. Chen, Adv. Astron. **2010**, 638979 (2010).
 - [29] Y. Takamizu, S. Mukohyama, M. Sasaki and Y. Tanaka, JCAP **1006**, 019 (2010).
 - [30] S. M. Leach and A. R. Liddle, Phys. Rev. D **63**, 043508 (2001); S. M. Leach, M. Sasaki, D. Wands and A. R. Liddle, *ibid.* **64**, 023512 (2001); R. K. Jain, P. Chingangbam and L. Sriramkumar, JCAP **0710**, 003 (2007).
 - [31] D. J. Schwarz, C. A. Terrero-Escalante and A. A. Garcia, Phys. Rev. D **66**, 023515 (2002).
 - [32] S. M. Leach, A. R. Liddle, J. Martin and D. J. Schwarz, Phys. Lett. B **517**, 243 (2001).
 - [33] R. Arnowitt, S. Deser and C. W. Misner, Phys. Rev. **117**, 1595 (1960).
 - [34] D. Lyth, Phys. Rev. D **31**, 1792 (1985).
 - [35] D. J. Schwarz and J. Martin, Phys. Rev. D **57**, 3302 (1998).
 - [36] F. Arroja, A. E. Romano and M. Sasaki, arXiv:1106.5384v1 [astro-ph.CO].
 - [37] D. K. Hazra, L. Sriramkumar and J. Martin, in preparation.
 - [38] J. Martin and L. Sriramkumar, in preparation.
 - [39] I. S. Gradshteyn and I. M. Ryzhik, *Table of Integrals, Series and Products* (Academic, New York, 1980).